TITLE:
Development of New Resonance Theory and Theoretical Evaluation of Metal-Ligand Binding Energy(Dissertation_全文)

AUTHOR(S):
Ikeda, Atsushi

CITATION:
Ikeda, Atsushi. Development of New Resonance Theory and Theoretical Evaluation of Metal-Ligand Binding Energy. 京都大学, 2008, 博士(工学)

ISSUE DATE:
2008-03-24

URL:
https://doi.org/10.14989/doctor.k13840

RIGHT:

京都大学学術情報リポジトリ
KURENAI 紅
Kyoto University Research Information Repository

Development of New Resonance Theory and Theoretical Evaluation of Metal-Ligand Binding Energy

Atsushi Ikeda

2008

Preface

Heitler and London applied quantum mechanics to dihydrogen molecule on 1927. Triggered by their monumental work, “Quantum Chemistry” has been developed as the fundamental theory to understand the chemistry. Nowadays, quantum chemistry and modern electronic structure theory based on the quantum chemistry are indispensable for all researchers and powerful tools for chemical research in various areas. However, we need further development of the quantum chemistry and the electronic structure theory. What type of development is required? Of course, it is quite important to develop an accurate electronic structure theory which can be applied to large-scale systems and variety of systems. Also, important is to develop a method to analyze electronic wave function in terms of *chemical* concepts. This is because chemists want to understand systems and molecules with chemical concepts; note that it is not easy to present such understanding directly from modern electronic structure calculations.

This thesis consists of two parts. In part I, the author wishes to focus on accurate calculation of the binding energy of transition metal complexes with large π-conjugate molecule. The electronic structure of transition metal complexes with large π-conjugate molecule is highly complicated and delocalized. Their interaction, bonding nature, and electronic structure are interesting research sunjects of modern theoretical chemistry. However, the computational approach is not easy. The present thesis provides reliable binding energies and bonding nature of these systems. Another important result is that the DFT method considerably underestimates binding energies. In part II, the author wishes to present the development of new resonance theory with which electronic wave function can be analyzed in detail. In the modern quantum

chemistry, the understanding of the nature of chemical bond based on the ionic and covalent interactions is difficult, although they are fundamental concepts in chemistry. In the present research, a novel evaluation method based on the second quantized expression of singlet coupling is developed and applied to various systems including solvated molecules.

These studies were carried out at Department of Molecular Engineering, Graduate School of Engineering, Kyoto University. The supervisor of the studies is Professor Shigeyoshi Sakaki. Firstly, the author would like to express his deepest appreciation to Prof. Shigeyoshi Sakaki for his careful discussion and warm encouragement. The studies in Part I was performed with his full cooperation. The author should express his deepest appreciation to Associate Professor Hirofumi Sato for his elegant and fruitful suggestions. Various discussions about theoretical chemistry and physical chemistry with him were exciting and meaningful experiences for the author. The achieving in Part II didn't come without the collaboration with him.

The author also expresses gratitude to Assistant Professor Yoshihide Nakao for his technical advice and valuable comments. The author is also grateful to Mr. Yu-ya Ohnishi and Mr. Daisuke Yokogawa. Scientific talks with them on various occasions were very enjoyable and fruitful. Acknowledgement is also made to all members of the research group of Prof. Shigeyoshi Sakaki. Especially, the informal seminars with them were great opportunities to learn many things for the author.

Finally, the author sincerely thanks his parents Takeyasu Ikeda and Toshimi Ikeda, and his wife Ai Ikeda for their understanding, encouragement, and support from all sides.

Contents

General Introduction

1 Overview of electronic structure theory

Now, the quantum chemistry is sophisticatedly developed and accurate electronic structure calculations based on the quantum chemistry are routinely carried out in various research areas. However, nobody thinks that the quantum chemistry has been completed. What progress is needed in the quantum chemistry nowadays? Before considering the answers, the history of the quantum chemistry is briefly overviewed here.

1.1 Resonance theory

The development of the quantum chemistry leading to the state-of-the-art electronic structure theory was triggered by the monumental work by Heitler and London, in which the covalent bond between hydrogen atoms was discussed by using quantum mechanics [1]. Based on their method, "resonance theory" was developed, which is the first comprehensive theory to understand the nature of chemical bond [2]. In the resonance theory, the electronic structures of molecules are discussed in terms of resonance between several resonance structures, which built up of atoms with linking each other through ionic and covalent types of interaction. For example, the electronic wave function of molecule AB is expressed by a superposition of ionic and covalent types of wave function as follows,

$$\Psi_{\mathrm{AB}} = C_1 \Psi_{\mathrm{A^-B^+}} + C_2 \Psi_{\mathrm{A\text{–}B}} + C_3 \Psi_{\mathrm{A^+B^-}}, \tag{1}$$

where C is the coefficient of each wave function. Chemist's traditional approach to molecule was based on the resonance theory. The resonance theory is still useful because it provides clear understanding of the bonding nature, reactivity, and character of molecules.

However, it should be noted that the resonance theory is not a practical ab-initio method. When we apply the resonance theory straightforwardly, the computational costs become prohibitively large. The concepts in resonance theory are very useful, however the calculation based on the resonance theory is very difficult.

1.2 The Hartree-Fock theory

The Hartree-Fock (HF) theory is the most basic ab-initio method to calculate electronic wave function of molecule.

In general, total Hamiltonian $\hat{H}$ under the Born-Oppenheimer approximation is defined as follows,

$$\hat{H} = \hat{T} + \hat{V}_{ne} + \hat{V}_{ee} + V_{nn}, \tag{2}$$

where $\hat{T}$ is the momentum operator of electron, $\hat{V}_{ne}$ is the nuclear attraction operator, $\hat{V}_{ee}$ is the electron repulsion operator and V_{nn} is the term corresponding to nuclear repulsion. Only $\hat{V}_{ee}$ is a two-electron operator and this term makes the Hamiltonian complicated. HF theory is based on one-electron model, in which $\hat{V}_{ee}$ is approximated by one-electron effective potential $\hat{V}^{HF}$ as follows,

$$\hat{H}_{HF} = \hat{T} + \hat{V}_{ne} + \hat{V}^{HF} + V_{nn}. \tag{3}$$

The effective potential $\hat{V}^{HF}$ is corresponding to coulomb and exchange term in $\hat{V}_{ee}$. The HF wave function which is a Slater determinant composed by orthonormal spin orbitals (Eq. 4), is obtained by the variational principal.

$$\Psi_{HF} = |\phi_1 \phi_2 \phi_3 \cdots| \tag{4}$$

Here, ϕ is a spin orbital.

Though the HF theory is based on rough (one-electron) approximation, it delivers > 99 % of the exact energy [3]. Furthermore, the computational costs of the HF theory become very low, due to the orthogonality of molecular orbitals (MOs). For these reasons, most of modern ab initio calculations are based on the HF theory.

However, it should be noted that the MOs calculated by the HF method are delocalized in whole molecule and then those MOs often don't provide local picture of molecule, such as the covalent and ionic bonds introduced in the resonance theory.

1.3 Post-Hartree-Fock theory and density functional theory

Although the HF theory delivers $>$ 99 % of the exact energy, the rest 1 % often becomes very important from the standpoint of chemistry. To calculate the rest 1 %, named correlation energy, various accurate theories have been developed.

One way to treat the correlation energy is post HF calculation. Møller-Pleset perturbation theory (MP) is one of the most useful methods [4], in which the difference between the Hamiltonian $\hat{H}$ (Eq. 2) and the sum of Fock operator $\hat{H}_{HF}$ (Eq. 3) is treated as a perturbation term. In the MP method, the wave function and the energy are represented by the perturbation expansion. The MP method works well when the zero-th order wave function (HF wave function) is good approximation of the real wave function. When the electronic structure of the system contains multi-reference character, the perturbation expansion shows poor convergence. Coupled-cluster theory (CC) is more sophisticated method to calculate the correlation energy, which is based on the cluster expansion of the wave function [5].

On the other hand, several multi-reference methods have been developed. When one slater determinant is not good approximation of the real wave function, the system has *multi-reference* character, in which it is necessary to represent the wave function by using multi-refference wave function. In such cases, MC-SCF calculation and their extensions are very powerful. These methods are very important in modern quantum chemistry. However, they are not related to central themes of this thesis and therefore, the details are omitted here.

Density functional theory (DFT) is completely different method from the post HF method. The DFT is based on the Hohenberg-Kohn theorem, which states that the ground-state electronic structure is completely determined by the electron density [6]. In other words, the total energy is defined by the functional of the electron density and the correlation energy is also defined by using the exchange-correlation functional. Various functionals have been devel-

Table 1: Comparison of theoretical and experimental reaction energies (kcal/mol). $< x >$ express the mean absolute deviations and σ mean the standard deviations.

Method	$< x > \pm \sigma$
HF	54.82 ± 59.83
MP2	11.86 ± 11.25
SVWN	26.28 ± 27.28
BLYP	9.95 ± 12.50
BPW91	9.35 ± 11.81
B3PW91	8.05 ± 10.00

ref. [13]

oped for the exchange-correlation terms. The simplest one is the LDA functional, such as SVWN, in which the electron distribution is assumed to be homogeneous [7, 8]. This approximation is very simple and provides large error in molecular systems. On the basis of this situation, the generalized gradient approximation was proposed and several functionals have been developed, for example BLYP, BPW91, and so on [9–11]. Another type of the functional is the hybrid one which is based on the adiabatic connection theorem, for example B3LYP, B3PW91 and so on [12]. In the case of hybrid functional, the HF exchange term is added to the functional.

In many cases, the accuracy of the DFT method is the same as to that of the MP2 method. Table 1 shows the result of the HF, MP2 and DFT methods for the reaction energies of 108 atomization reactions [13]. The results show the accuracy of the functional BLYP, BPW91 and B3PW91 is comparable to the MP2 results. Furthermore the computational cost of the DFT method is comparable to HF method.

2 The aims of part I in this thesis

In modern chemistry, large-scale molecules and their assemblies are considerably focused because they are expected to be new materials with interesting properties. Thus, the electronic structure calculations of these systems are very important. What types of theory are useful for these systems? One of the useful methods is the DFT. However, the DFT method is not perfect, which I wish to briefly discuss it here.

2.1 Weak point of the DFT method

Density functional theory (DFT) is believed to be very useful, in particular for large systems, nowadays. However, several weak points have been pointed out.

One of them is insufficient description of dispersion interaction [14–19]. Whereas it plays important roles in van der Waals complexes, crystal packing of organic molecules, and three dimensional structures of biological systems. Fig. 1 shows potential energy curves of argon dimer [18]. These results show the MP2 and CCSD(T) methods describe the formation of

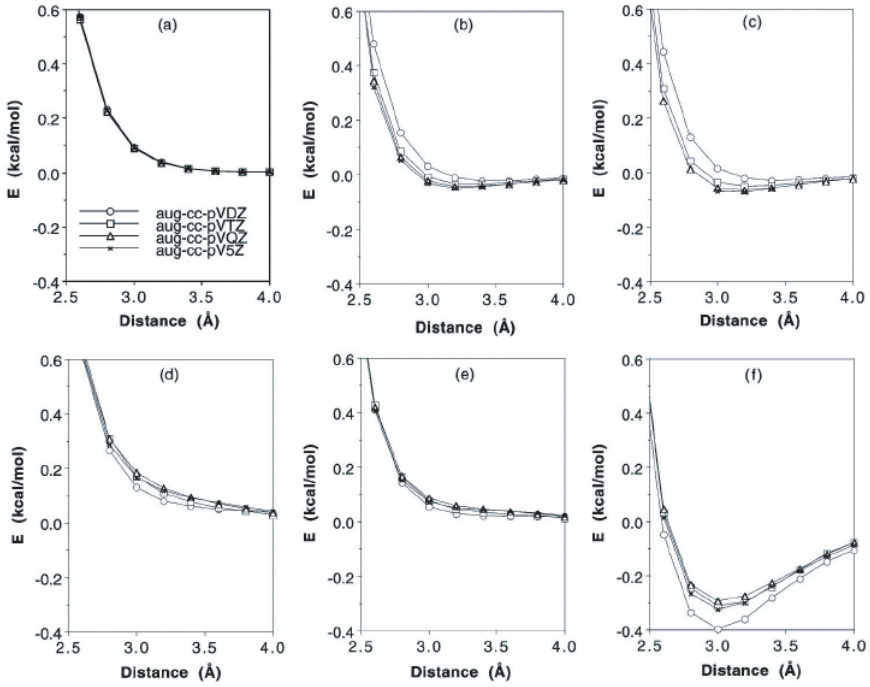

Figure 1: The (a)HF, (b)MP2, (c)CCSD(T), (d)BLYP, (e)B3LYP, and (f) B3PW91 calculated potential energy curves of argon dimer. Ref. [18]

van der Waals complex, but the BLYP and B3LYP functionals fail to reproduce the complex formation. The B3PW91 functional presents better result but it is not clear whether this functional correctly describes dispersion interaction or not. For example, it is known that PBEOP functional presents better result for this system as in the case of B3PW91, but recently it was reported that the successful behaviour is originated from the error in the functional [18]. Because the dispersion interaction often plays key role to determine the structure of molecular

Table 2: Values for the electronic static longitudinal polarrizability (α) and second hyper polarizability (γ). (a. u.)

Method	α	γ
MP2	917	336
HF	1327	200
SVWN	2039	584
SLYP	2046	576
BLYP	2041	585
BPW91	2036	590
B3LYP	1789	563

ref. [20]

assembly, this weak point is serious problem in the DFT method.

Another weak point is the incorrect evaluation of polarizabilities and hyperpolarizabilities of large π-conjugate molecules [20]. Table 2 shows polarizabilities and hyperpolarizabilities calculated by the HF, MP2 and DFT methods. The hybrid functional, namely B3LYP, presents slightly better result but the other functional overestimates these quantities. Because large π-conjugate molecules are expected to be the functional molecules, this weak point should be improved in the DFT method, too.

2.2 The binding energy and bonding nature of transition metal complexes of large π conjugated molecules

One of large-scale molecules is the transition metal complexes including large π-conjugate molecule [21]. However, in general, the electronic structure of transition metal complex is very complicated and that of large π-conjugate molecule is considerably delocalized. In such case, it is not clear whether the conventional DFT method provides reliable results or not.

In part I of this thesis, the author evaluated the binding energy of transition metal complexes of large π-conjugate molecule. The present thesis provided reliable binding energies and clarified that the DFT method considerably underestimates binding energies. The author also studied the bonding nature of these systems by using the population analysis based on the fragment MOs.

3 The aims of part II in this thesis

In the modern quantum chemistry, the theories provide accurate total energy of various systems. However, the total energy is often not enough to obtain chemical understanding of the systems. At the same time, it is very difficult to understand the meanings of huge amount of numbers describing the calculated wave functions. Thus, it is absolutely essential that the wave function is *analyzed* in terms of chemical concepts.

3.1 Wave function analysis

Mulliken population analysis and ab-initio bond order analysis

Many analysis methods of electronic wave function have been developed. Mulliken population analysis (MPA) is the most basic, in which partial atomic charges are calculated in ab-initio flame work [22]. In general, Mulliken population of atom A is defined as follows,

$$N_{\mathrm{A}} = \sum_{\mu \in \mathrm{A}} (\mathbf{PS})_{\mu\mu}. \tag{5}$$

Here, $\mathbf{S}$ is overlap matrix and $\mathbf{P}$ is defined as $(\mathbf{P})_{\mu\nu} = 2\sum_{i}^{occ} (\mathbf{C})_{\mu,i}(\mathbf{C})_{\nu,i}$, where $(\mathbf{C})_{\mu,i}$ is LCAO coefficient of molecular orbital i. It should be noted that another types of method to evaluate atomic population have been proposed by various researchers [23, 24].

One of such analysis methods is ab-initio bond order analysis in which a bond order between atoms is defined by using density matrix [25–28]. Ab-initio bond order between A and B atoms is defined as follows,

$$B_{\text{A-B}} = \sum_{\mu \in \mathrm{A}} \sum_{\nu \in \mathrm{B}} (\mathbf{PS})_{\mu\nu}(\mathbf{PS})_{\nu\mu}. \tag{6}$$

It should be also noted that the variations of ab-initio bond order analysis have been proposed [29].

Results of MPA and ab-initio bond order analysis for water molecule are shown in Fig. 2. Apparently, these analyses show the oxygen atom is negative, the hydrogen atoms are positive, and bonds are formed between oxygen, and hydrogen atoms.

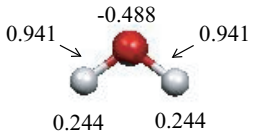

Figure 2: The calculated Mulliken charges and ab-initio bond orders of H_2O.

Energy decomposition analysis

Energy decomposition method is another type of analysis method. The most widely-used method is Morokuma-Kitaura decomposition scheme [30], in which intermolecular interaction energy calculated by the HF method is decomposed into the electrostatic, exchange repulsion, polarization, and charge transfer interaction energies. In the method, the Fock matrix is represented in the MO basis and the off-diagonal part of the matrix is re-defined so as to present those interaction energies. The method provides clear picture in several systems, but the application is limited to *intermolecular* interactions. Thus, the method cannot be applied to *intramolecular* interactions, for examples the chemical bond between atoms.

On the basis of this situation, energy partitioning analysis which decomposes total energy into one and two centers has been developed by several researchers [31–35]. In general, the total energy is defined, as follows,

$$\begin{aligned} E_{total} &= \sum_{A\neq B}\frac{Z_A Z_B}{R_{AB}} + \sum_{ab}(\mathbf{P})_{ab}\int \chi_b(r_1)\hat{T}\chi_a(r_1)dr_1 \\ &+ \sum_{A}\sum_{ab}(\mathbf{P})_{ab}\int \chi_b(r_1)\frac{-Z_A}{r_A}\chi_a(r_1)dr_1 \\ &+ \sum_{abcd}(\mathbf{\Omega})_{abcd}\int \chi_a(r_1)\chi_b(r_1)\frac{1}{r_{12}}\chi_c(r_2)\chi_d(r_2)dr_1dr_2, \end{aligned} \tag{7}$$

where Z_A and Z_B is nuclear charge and Ω is a second-order density matrix. This total energy is decomposed into one and two center energies in the manner similar to MPA.

3.2 Second quantization

Quantum chemistry can be formulated by using second quantization technique, which is very elegant in quantum mechanics of many-body systems. This provides the physical (and

chemical) meanings of operators and density matrix, which is nessesary to develop the wave function analysis.

In standard quantum mechanics (Schrödinger representation), observables are represented by operators. In second quantization framework, electronic states are also represented by operators.

Firstly, the creation and annihilation operators are defined as follows,

$$a_i^+|\phi_1\phi_2\phi_3\cdots\rangle = |\phi_1\phi_2\phi_3\cdots\phi_i\cdots\rangle, \quad (\text{creation}) \tag{8}$$

$$a_i^-|\phi_1\phi_2\phi_3\cdots\phi_i\cdots\rangle = |\phi_1\phi_2\phi_3\cdots\rangle. \quad (\text{annihilation}) \tag{9}$$

The operator a_i^+ creates electron in orbital i and the a_i^- annihilates electron in orbital i in an antisymmetrized wave function. In this framework, the electronic state is also defined by using operators, as follows,

$$|\phi_1\phi_2\phi_3\cdots\rangle = a_1^+a_2^+a_3^+\cdots|0\rangle, \tag{10}$$

where $|0\rangle$ is the vacuum state.

By using these operators, the electron number N in orbital i can be defined as follows,

$$N_i = \langle\Psi|a_i^+a_i^-|\Psi\rangle. \tag{11}$$

Reformulation of Mulliken population analysis

MPA can be formulated by using second quantization technique but a straightforward extension of Eq. 11 cannot reconstruct MPA due to nonorthogonality of AOs. For examples, the creation χ_μ^+ and annihilation χ_μ^- operators corresponding to AO μ are defined as follows,

$$a_i^+ = (\mathbf{C})_{\mu i}\chi_\mu^+, \quad (\text{creation}), \tag{12}$$

$$a_i^- = (\mathbf{C})_{\mu i}\chi_\mu^-, \quad (\text{annihilation}). \tag{13}$$

The expectation value of the occupation number evaluated from the pair of them (AO μ) is not equal to MPA value.

$$(\mathbf{PS})_{\mu\mu} \neq \langle\Psi|\chi_\mu^+\chi_\mu^-|\Psi\rangle \tag{14}$$

Futhermore the sum of expectation value is not equal to the total electron number N_e of the system,

$$N_e \neq \sum_{\mu} \langle \Psi | \chi_\mu^+ \chi_\mu^- | \Psi \rangle. \tag{15}$$

A theoretical background of MPA was clarified by Mayer's reformulation using mixed formalism of the second quantization [27]. In this reformulation, annihilation operator is defined by using biorthogonal orbital φ_μ which is defined in terms of biorthogonal relation between AOs.

$$\int \varphi_\mu(r) \chi_\nu(r) dr = 0, \quad (\mu \neq \nu) \tag{16}$$

In the mixed formalism, Mulliken population of atom A can be represented as

$$N_{\mathrm{A}} = \sum_{\mu \in \mathrm{A}} \langle \Psi | \chi_\mu^+ \varphi_\mu^- | \Psi \rangle. \tag{17}$$

3.3 Development and application of the new resonance theory

In part II of this thesis, a new analysis method of wave function based on resonance theory and it's applications are presented. Chemist's traditional approach to molecule is based on the resonance theory. The resonance theory is still useful because it provides clear understanding of the bonding nature, reactivity and character of molecules [36]. However, most of modern ab-initio calculation method are based on the MO theory. Because MO theory is quite different from the resonance theory, it is hard to extract the traditional picture of molecule from a MO wave function.

The method presented here, which is based on the second quantization of singlet-coupling, enables us to evaluate the weights of resonance structures from MO wave function. The evaluation is carried out through localization of molecular orbitals followed by algebraic calculation of density matrices. The theory is completely consistent with MPA. This method is applied to various systems including the solvated molecules. The calculated weights of covalent and ionic structures are in excellent agreement with our chemical intuition.

Bibliography

[1] Heitler, W.; London, F. *Z. Physik* **1927**, *44*, 619.

[2] Pauling, L. *The Nature of the Chemical Bond (1960) Cornell University Press*

[3] Jensen, F. *Introduction to Computational Chemistry (1999) John Wiley and Sons*

[4] Moller, C.; Plesset, M. S. *Phys. Rev.* **1934**, *46*, 618.

[5] (a) Cizek, J. *J. Chem. Phys.* **1966**, *45*, 4256.(b) Cizek, J. *Adv. Chem. Phys.* **1969**, *14*, 35.. (c) Cizek, J.; Paldus, J. *Int. J. Quantum Chem.* **1971**, *5*, 359.

[6] Hohenberg, P.; Kohn, W. *Phys. Rev. B* **1964**, *136*, 864.

[7] Slater, J. C. *Phys. Rev.* **1951**, *81*, 385.

[8] Vosko, S. J.; Wilk, L.; Nusair, M. *Can. J. Phys.* **1980**, *58*, 1200.

[9] (a) Becke, A. D. *J. Chem. Phys.* **1986**, *84*, 4524.(b) Becke, A. D. *Phys. Rev. A* **1988**, *38*, 3098.

[10] (a) Perdew, J. P.*Phys. Rev. Lett.* **1985**, *55*, 1665.(b) Perdew, J. P. *Phys. Rev. B* **1986**, *33*, 8800.(c) Perdew, J. P.; Wang, Y. *Phys. Rev. B* **1992**, *45*, 13244.

[11] (a) Colle, R.; Salvetti, O. *Theoret. Chim. Acta* **1975**, *37*, 329.(b) Lee, C.; Yang, W.; Parr, R. G. *Phys. Rev. B* **1988**, *37*, 785.

[12] (a) Becke, A. D. *J. Chem. Phys.* **1993**, *98*, 1372.(b) Becke, A. D. *J. Chem. Phys.* **1993**, *98*, 5648.

[13] Scheiner, A. C.; Baker, J.; Andzelm, J. W. *J. Comput. Chem.* **1997**, *18*, 775.

[14] Kristyan, S.; Pulay, P. *Chem. Phys. Lett.* **1994**, *229*, 175.

[15] Perez-Jorda, J. M.; Becke, A. D. *Chem. Phys. Lett.* **1995**, *233*, 134.

[16] Zhang, Y.; Pan, W.; Yang, W. *J. Chem. Phys.* **1997**, *107*, 7921.

[17] Sponer, J.; Hobza, P. *Chem. Phys. Lett.* **1997**, *267*, 263.

[18] Tsuzuki, S.; Lüthi, H. P. J. *Chem. Phys.* **2001**, *114*, 3949.

[19] Wu, Q.; Yang, W. *J. Chem. Phys.* **2002**, *116*, 515.

[20] (a) Champagne, B.; Perpete, A.; van Gisbergen, S. J. A.; Baerends, E. J.; Snijders, J. G.; Soubra-Ghaoui, C.; Robins, K. A.; Kirtman, B. *J. Chem. Phys.* **1998**, *109*, 10489.(b) Champagne, B.; Perpete, A.; Jacquemin, D.; van Gisbergen, S. J. A.; Baerends, E. J.; Soubra-Ghaoui, C.; Robins, K. A.; Kirtman, B. *J. Phys. Chem. A* **2000**, *104*, 4755.

[21] (a) Lee, K.; Seng, H.; Park, J. T. *Acc. Chem. Res.* **2003**, *36*, 78. (b) Nakamura, E.; Isobe, H. *Acc. Chem. Res.* **2003**, *36*, 807. (c) Balch, A.L.; Olmstead, M. N. *Chem. Rev.* **1998**, *98*, 2123.

[22] (a) Mulliken, R. S. *J. Chem. Phys.* **1955**, *23*, 1833.(b) Mulliken, R. S. *J. Chem. Phys.* **1955**, *23*, 1841.

[23] Reed, A. E.; Weinhold, F. *J. Chem. Phys.* **1985**, *83*, 1736.

[24] Löwdin, P. O. *J. Chem. Phys.* **1950**, *18*, 365.

[25] Wiberg, K. A. *Tetrahedron* **1966**, *24*, 1083.

[26] (a) Okada, T.; Fueno, T. *Bull. Chem. Soc. Jpn.* **1975**, *48*, 2025. (b) Okada, T.; Fueno, T. *Bull. Chem. Soc. Jpn.* **1976**, *49*, 1524.

[27] (a) Mayer, I. *Chem. Phys. Lett.* **1983**, *97*, 270.(b) Mayer, I. *Int. J. Quantum Chem.* **1983**, *23*, 341.

[28] Jug, K. *J. Comput. Chem.* **1984**, *5*, 555.

[29] Sannigrahi, A. B.; Kar, T. *Chem. Phys. Lett.* **1990**, *173*, 569.

[30] Kitaura, K.; Morokuma, K. *Int. J. Quantum Chem.* **1976**, *10*, 325.

[31] Ichikawa, H.; Yoshida, A. *Int. J. Quantum Chem.* **1999**, *71*, 35.

[32] Mayer, I. *Chem. Phys. Lett.* **2003**, *382*, 265.

[33] Nakai, H.; Kikuchi, Y. *Chem. Phys. Lett.* **2005**, *4*, 317.

[34] Sato, H.; Sakaki, S. *J. Phys. Chem. B* **2006**, *110*, 12714.

[35] Vyboishchikov, S. F.; Salvador, P.; Duran M. *J. Chem. Phys.* **2005**, *110*, 244110.

[36] Shaik, S.; Shurki, A. *Angew. Chem. Int. Ed.* **1999**, *38*, 586.

Part I

Binding Energy and Bonding Nature of Transition Metal Complexes of Large π Conjugated Molecules

Chapter 1

Binding Energy of Transition-Metal Complexes with Large π-Conjugate Systems. Density Functional Theory vs Post-Hartree-Fock Methods

1.1 Introduction

Density functional theory (DFT) is believed to be very useful, in particular for large systems, nowadays. However, several weak points have been pointed out. One of them is insufficient description of van der Waals interaction [1–5]. For instance, the conventional DFT method fails to evaluate the dispersion interaction, which plays important roles in van der Waals complexes, crystal packing of organic molecules, and three dimensional structures of biological systems [6–8]. Another weak point is the incorrect evaluation of polarizabilities and hyperpolarizabilities of large π-conjugate molecules. This weak point has been discussed in terms of the exchange-correlation functionals, which shows the hybrid functionals present better results than the pure functionals [9].

Recently, we theoretically investigated Pt(0) complexes of corannulene ($C_{20}H_{10}$), sumanene ($C_{21}H_{12}$), and C_{60} [10], because these transition-metal complexes have drawn considerable attention in wide areas of chemistry [11]. In the study, we observed that the DFT method underestimated the binding energy between $Pt(PH_3)_2$ and the π-conjugate system in comparison with the MP2 to MP4(SDQ) methods. This is another serious problem in the DFT method because many transition-metal complexes have been theoretically investigated with the DFT method.

Because $Pt(PH_3)_2(C_{20}H_{10})$, $Pt(PH_3)_2(C_{21}H_{12})$, and $Pt(PH_3)_2(C_{60})$ are Pt(0) complexes in

which the Pt center takes a d^{10} electron configuration, the π-back-donation interaction mainly participates in the coordinate bond [12, 13]. In Pt(II) and Pt(IV) complexes, on the other hand, not only the π-back-donation but also the σ-donation participates in the coordinate bond because Pt(II) and Pt(IV) atoms possess one and two unoccupied d orbitals, respectively. Actually, it was theoretically shown that the π-back-donation interaction mainly participates in the coordinate bond of a Pt(0) complex, $Pt(PH_3)_2(C_2H_4)$, and both the σ-donation and the π-back-donation interactions participate in the coordinate bond of a Pt(II) complex, $[PtCl_3(C_2H_4)]^-$ [12–14]. Thus, it is of considerable importance to clarify whether the DFT method underestimates the binding energy of the transitionmetal complex when only the π-back-donation participates in the coordinate bond or when both the π-back-donation and the σ-donation participate in the coordinate bond.

In the present study, we systematically investigated d^{10}, d^8, and d^6 transition-metal complexes of π-conjugate systems using various computational methods such as DFT, MP2 to MP4-(SDTQ), and CCSD(T). Our purposes here are to evaluate correctly their binding energies, to examine the reliability of the DFT method, and to clarify the reasons why the DFT method underestimates the binding energies of such d10, d8, and d6 metal complexes as $Pt(PH_3)_2(C_2H_{4-n}(CH{=}CH_2)_n)$, $Pd(PH_3)_2(C_2H_{4-n}(CH{=}CH_2)_n)$, $[PtCl_3(C_2H_{4-n}(CH{=}CH_2)_n)]^-$, $[PdCl_3(C_2H_{4-n}(CH{=}CH_2)_n)]^-$, and $[PtCl_5(C_2H_{4-n}(CH{=}CH_2)_n)]^-$ (n= 0-4). These complexes were selected here as typical examples of d^{10}, d^8, and d^6 transition-metal complexes.

1.2 Computational details

The geometry of $Pt(PH_3)_2(C_2H_4)$ was optimized by the MP2 and DFT methods, where B3LYP [15, 16] and B3PW91 [15, 17] functionals were used in the DFT calculation. Because the MP2- and DFT(B3PW91)-optimized geometries agree better with the experimental geometry than the DFT(B3LYP)-optimized one, as will be described below, the geometries of the other complexes were optimized by the DFT(B3PW91) method. In the geometry optimization, split-valence-type basis sets, (541/541/111/1) and (541/541/211/1), were used for the valence electrons of Pt and Pd, [18, 19] respectively, and the effective core potentials (ECPs) of Hay

and Wadt [18] were employed to replace their core electrons, where one f polarization function was added to each basis set [20]. For the other atoms, the 6-31G(d) basis sets were used [21]. This basis set system is named BS1.

The binding energies of these complexes were evaluated with the MP2 to MP4, CCSD(T) [22], and DFT methods using better basis set systems, BS2 and BS3. In the DFT calculation, various functionals such as SVWN [23, 24], BLYP [15, 16], BP86 [24, 26], B3LYP [15, 16], B3PW91 [15, 17], BHandHLYP [16, 23, 24], MPW1PW91 [17, 28], and PBE1PBE [29] were employed to investigate what functional presents good results. In BS2, the 6-311G(d) basis sets [30] were used for H, C, P, and Cl. For Pd and Pt, the core electrons were replaced with Stuttgarπ-Dresden-Bonn ECPs, and their valence electrons were represented by the (311111/-22111/411/11) basis set [31, 32]. We did not add the g polarization function here, because the MP4(SDQ)-calculated binding energy of $Pt(PH_3)_2(C_2H_4)$ changes little by addition of the g function [33]. In BS3, the core electrons of Pt were replaced with the ECPs of Hay and Wadt [18], and the (33111/31111/ 1111/111/11) basis set was used for its valence electrons [34]. For the C, P, and H atoms, the (63111/3111/11/1), (6311111/421111/111/11), and (3111/11) basis sets were employed [35], respectively. These basis sets were used in the G3MP2 calculation previously [34].

The Gaussian 03 program package was used for all calculations [36]. Population analysis was carried out with the method of Weinhold *et al.* [37] Orbital pictures were drawn with the MOLEKEL program package [38].

1.3 Results and discussions

1.3.1 Binding Energies of $Pt(PH_3)_2(C_2H_{4-n}(CH{=}CH_2)_n)$ (n = 0-4).

Because the DFT method underestimated the binding energies of the Pt(0) complexes of the large π-conjugate systems in our previous work [10], we evaluated the binding energy of $Pt(PH_3)_2(C_2H_{4-n}(CH{=}CH_2)_n)$ in which vinyl groups were introduced into the C=C double bond one after another, as shown in Figure 1.1. Our purpose here is to investigate whether the underestimation of the binding energy depends on the size of the π-conjugate system. Their

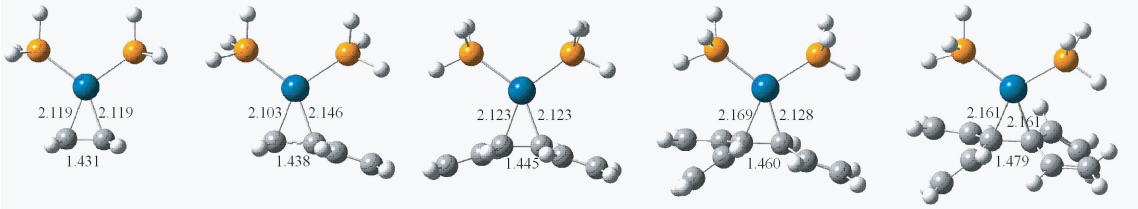

Figure 1.1: B3PW91-optimized structure of $Pt(PH_3)_2(C_2H_{4-n}(CH{=}CH_2)_n)$ (bond lengths in angstroms).

Table 1.1: Selected Bond Lengths (Å) of $Pt(PH_3)_2(C_2H_{4-n}(CH{=}CH_2)_n)$ (n = 0, 2) optimized by the MP2 and DFT Methods

	$Pt(PH_3)_2(C_2H_4)$			$Pt(PH_3)_2(C_6H_8)$	
	Pt-P	Pt-C	C=C	Pt-C	C=C
B3LYP	2.306	2.140	1.431	2.163	1.442
B3PW91	2.280	2.119	1.431	2.123	1.445
MP2	2.245	2.120	1.431	2.121	1.439
expt[a]	2.268	2.112	1.434		

a) Reference [39].

geometries were optimized with the DFT(B3PW91) method, because the DFT(B3PW91)-optimized geometry of $Pt(PH_3)_2(C_2H_4)$ agrees well with the experimental geometry of $Pt(PPh_3)_2$-(C_2H_4) [39] and the MP2-optimized geometry of $Pt(PH_3)_2(C_2H_4)$, as compared in Table 1.1; note that the DFT(B3LYP) method presents considerably longer Pt-C and Pt-P bonds than their experimental values. Interestingly, the Pt-C bond and the CdC bond coordinating with Pt become longer as the number of vinyl groups increases.

As shown in Table 1.2, the binding energy considerably fluctuates around the MP2 and MP3 levels but much less around the MP4(SDQ) and MP4(SDTQ) levels in all the complexes examined. The MP4(SDTQ) method tends to present a larger binding energy than the CCSD(T) method, and the inclusion of triple-excitation increases the binding energies in both the MP4 and CCSD calculations; see Table 1.2 for the MP4(SDQ)-, MP4(SDTQ)-, CCSD-, and CCSD(T)-calculated binding energies. As a result, the MP4(SDQ)-calculated binding energy is almost the same as the CCSD(T)-calculated value in these complexes. Thus, here we applied the MP4(SDQ) method to large systems which could not be calculated with the

CCSD(T) method due to the large size.

Though the MP4(SDQ)-calculated binding energies change little as the size of the π-conjugate system increases, as shown in Table 1.2, the DFT-calculated binding energy considerably decreases; [40] for instance, the B3LYP-calculated binding energy is 14.4, 6.7, and -1.1 kcal/mol for $Pt(PH_3)_2(C_2H_4)$, $Pt(PH_3)_2(C_2H_2(CH{=}CH_2)_2)$, and $Pt(PH_3)_2(C_2(CH{=}CH_2)_4)$, respectively. It is noted that the DFT-calculated binding energy decreases in all the functionals used here. For convenience, we defined $\Delta BE(B3LYP)$ and $\Delta BE(B3PW91)$ as the difference between the MP4(SDQ)- and DFT(B3LYP)-calculated binding energies (Eq. 1.1) and that between the MP4(SDQ)- and DFT(B3PW91)-calculated binding energies (Eq. 1.2),

$$\Delta BE(B3LYP) = \text{MP4(SDQ) binding energy} - \text{B3LYP binding energy} \quad (1.1)$$

$$\Delta BE(B3PW91) = \text{MP4(SDQ) binding energy} - \text{B3PW91 binding energy} \quad (1.2)$$

respectively. The $\Delta BE(B3LYP)$ and $\Delta BE(B3PW91)$ values increase as the size of the π-conjugate system increases; for instance, the $\Delta BE(B3LYP)$ and $\Delta BE(B3PW91)$ values become very large in $Pt(PH_3)_2(C_2(CH{=}CH_2)_4)$, that is, 22.2 and 13.3 kcal/mol, respectively.

It is noted that the binding energies calculated with the MP2-optimized geometries are almost the same as those calculated with the B3PW91-optimized geometry, suggesting that the MP4-(SDQ)//DFT(B3PW91) calculation presents a reliable binding energy; see the values in parentheses of Table 1.2 for the binding energy calculated with the MP2-optimized geometry.

We investigated $Pd(PH_3)_2(C_2H_{4-n}(CH{=}CH_2)_n)$ too. In these complexes, the MP4(SDQ)-calculated binding energy changes little as the size of the π-conjugate system increases, but the DFT-calculated binding energy considerably decreases, similar to that of $Pt(PH_3)_2(C_2H_{4-n}$-$(CH{=}CH_2)_n)$; see Figures 1.2 and 1.3 for the geometries and the binding energies of the Pd(0) complexes, respectively.

1.3.2 Basis Set Superposition Error (BSSE) Correction.

It is necessary to examine how much BSSE influences the binding energy. Because $Pt(PH_3)_2$-$(C_2H_{4-n}(CH{=}CH_2)_n)$ (n = 2-4) could not be calculated with the CCSD(T)/BS3 and MP4(SDQ)/-BS3 methods, due to the large size, we made a comparison between the MP4(SDQ)- and

Table 1.2: Binding Energies (kcal/mol) of $Pt(PH_3)_2(C_2H_{4-n}(CH{=}CH_2)_n)$ (n = 0-4)

Binding Energies Evaluated by the Post-Hartree-Fock Method							
n	MP2	MP3	MP4(DQ)	MP4(SDQ)	MP4(SDTQ)	CCSD	CCSD(T)
0	33.7 (32.7)[a]	16.7 (14.7)	22.3 (22.0)	22.2 (21.7)	28.0	19.1	22.2
1	34.0	15.8	22.3	22.5	29.7	19.6	22.6
2	34.0	13.9	21.5	22.1	30.1	18.5	21.9
3	35.2	12.5	21.6	22.6			
4	34.1	9.0	19.7	21.1			
Binding Energies Evaluated by the DFT Method with Various Functionals							
n	B3LYP	B3PW91	BLYP	SVWN	$\Delta BE(B3LYP)$	$\Delta BE(B3PW91)$	
0	14.4 (13.9)[a]	21.5 (21.2)	12.1 (11.2)	40.8 (41.0)	7.9	0.8	
1	11.3	18.4	8.3	38.2	11.3	3.9	
2	6.7	13.8	3.2	34.1	15.4	7.7	
3	4.0	11.3	0.4	32.7	18.7	10.4	
4	-1.1	6.5	-4.8	30.0	22.2	13.3	
n	BP86	BHHLYP	MPW1PW91	PBE1PBE			
0	21.8	14.5	23.5	25.3			
2	13.4	7.6	16.2	18.2			
4	6.3	-0.4	9.2	11.6			

a) In parentheses are given the binding energies calculated with the MP2-optimized geometry.

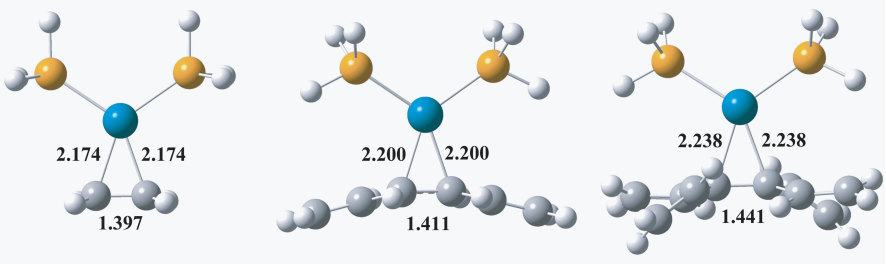

Figure 1.2: B3PW91-optimized structure of $Pd(PH_3)_2(C_2H_{4-n}(CH{=}CH_2)_n)$ (bond lengths in angstroms).

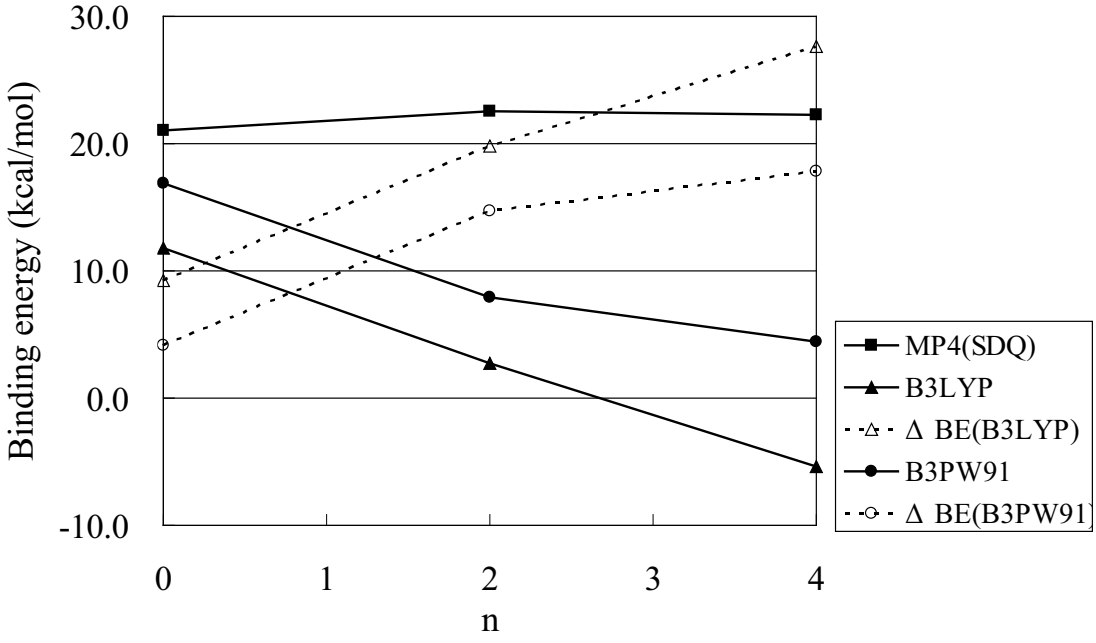

Figure 1.3: Binding energies of $Pd(PH_3)_2(C_2H_{4-n}(CH{=}CH_2)_n)$.

Table 1.3: BSSE-Corrected and BSSE-Non-Corrected Binding Energies (kcal/mol) of $Pt(PH_3)_2(C_2H_{4-n}(CH{=}CH_2)_n)$ (n = 0 or 1) calculated by the MP4(SDQ) and DFT(B3LYP) Methods with the BS2 and BS3 Basis Sets

	MP4(SDQ)		B3LYP	
	BSSE-non-corrected	BSSE-corrected	BSSE-non-corrected	BSSE-corrected
		$Pt(PH_3)_2(C_2H_4)$		
BS2	22.2	11.3	14.4	12.5
BS3	22.4	17.3	11.4	11.1
		$Pt(PH_3)_2(C_4H_8)$		
BS2	22.5	10.3	11.3	9.2
BS3	22.3	16.3	8.3	7.4

B3LYP-calculated binding energies of $Pt(PH_3)_2(C_2H_{4-n}(CH{=}CH_2)_n)$ (n = 0 or 1), as shown in Table 1.3, where the counterpoise method was employed to evaluate BSSE [41]. In the MP4(SDQ)/BS2 calculation, the binding energies with BSSE correction are significantly smaller than the binding energies without BSSE correction. In the DFT-(B3LYP)/BS2 calculations, on the other hand, the binding energies with BSSE correction are little different from those without BSSE correction. As a result, the BSSE-corrected ΔBE value becomes very small; for instance, the BSSE-corrected ΔBE value is -1.2 kcal/mol for $Pt(PH_3)_2(C_2H_4)$. Seemingly, these results mean that the large binding energy by the MP4-(SDQ) method arises from the large BSSE and that the DFT method presents a reliable binding energy due to the small BSSE. However, we must remember that the counterpoise method overestimates the BSSE correction.

It is expected that if the BSSE is large, the binding energy without BSSE correction should decrease and the binding energy with BSSE correction should increase as the basis sets used become better. However, the MP4(SDQ)-calculated binding energy without BSSE correction changes little when BS3 is used instead of BS2, while the binding energy with BSSE correction considerably increases, as shown in Table 1.3; for instance, it increases to 17.3 from 11.3 kcal/mol in $Pt(PH_3)_2(C_2H_4)$ and to 16.3 from 10.3 kcal/mol in $Pt(PH_3)_2(C_2H_3(CH{=}CH_2))$. These results are against the above-mentioned expectation. This discrepancy between the expectation and the computational results suggests that the BSSE is overcorrected by the counterpoise method and the binding energy calculated with the MP4(SDQ)/BS2 and MP4(SDQ)/BS3

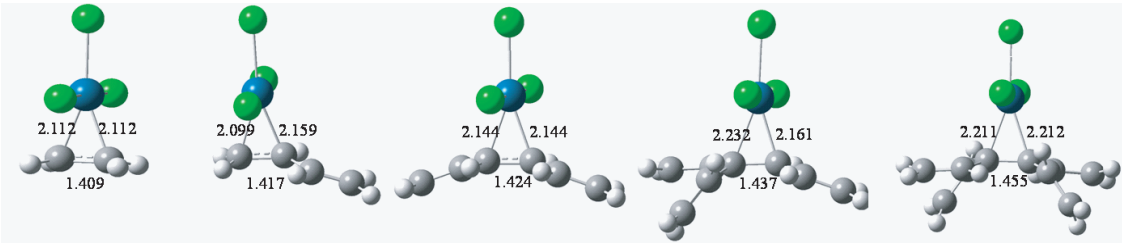

Figure 1.4: B3PW91-optimized structure of $[PtCl_3(C_2H_{4-n}(CH{=}CH_2)_n)]^-$ (bond lengths in angstroms).

methods are reliable. Similar results were reported recently; the BSSE evaluated with the counterpoise method is too large and should be decreased to 50 % [10]. Because much better basis sets were used here than in the previous work [10], the BSSE is much smaller here than in the previous work. From these results, it is likely that the BSSE is not significantly large.

1.3.3 Binding Energies of d^8 and d^6 Transition-Metal Complexes.

We investigated here d^8 metal complexes, $[PtCl_3(C_2H_{4-n}(CH{=}CH_2)_n)]^-$ (n = 0-4). Because of the presence of one unoccupied d orbital, both the σ-donation and the π-backdonation interactions participate in the coordinate bond of these complexes, as will be discussed below. Thus, their coordinate bonds are different from those of the d^{10} metal complexes $Pt(PH_3)_2C_2H_{4-n}$-$(CH{=}CH_2)_n$ in which the π-back-donation largely participates in the coordinate bond. From this investigation, we clarify whether the DFT method presents a reliable binding energy when both the σ-donation and the π-backdonation interactions participate in the coordinate bond.

Optimized structures of these complexes are shown in Figure 1.4. The Pt-C bond distance becomes longer as the size of the π-conjugate system increases. This bond lengthening is greater than in $Pt(PH_3)_2(C_2H_{4-n}(CH{=}CH_2)_n)$. Also, it is noted that the C=C double bond is shorter in these complexes than in $Pt(PH_3)_2(C_2H_{4-n}(CH{=}CH_2)_n)$. This is consistent with the fact that the π-back-donation is weaker in these complexes than in $Pt(PH_3)_2(C_2H_3(CH{=}CH_2))$, as will be discussed below in detail. The MP4(SDQ)-calculated binding energy decreases as the number of vinyl group increases by more than 2, as shown in Figure 1.5. On the other hand, the DFT-calculated binding energy decreases much more. Thus, it is concluded

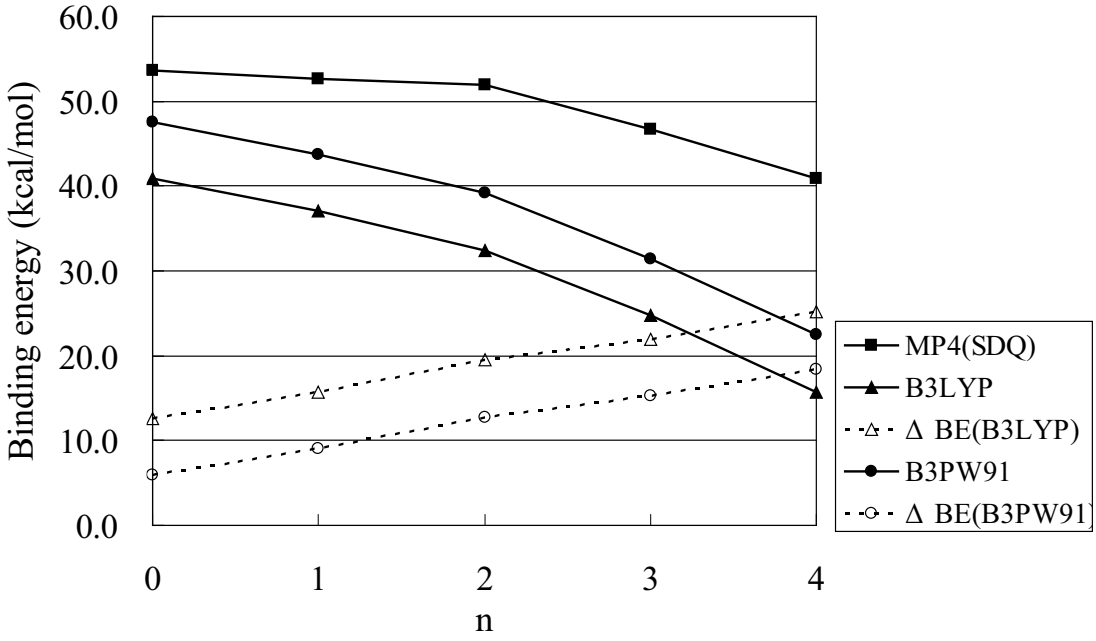

Figure 1.5: Binding energies of $[PtCl_3(C_2H_{4-n}(CH{=}CH_2)_n)]^-$.

that the DFT method underestimates the binding energies of these d^8 metal complexes when the π-conjugate system is large; for instance, the $\Delta BE(B3LYP)$ value is 25.2 kcal/mol for $[PtCl_3(C_2H_{4-n}(CH{=}CH_2)_n)]^-$, which is almost the same as that for $Pt(PH_3)_2(C_2(CH{=}CH_2)_4)$. Similar results are observed in the Pd analogues $[PdCl_3(C_2H_{4-n}(CH{=}CH_2)_n)]^-$; see Figures 1.6 and 1.7 for their optimized geometries and binding energies, respectively.

In $[PtCl_5(C_2H_{4-n}(CH{=}CH_2)_n)]^-$ (n = 0-4), the Pt center takes the +4 oxidation state with the d^6 electron configuration. This suggests that the σ-donation interaction becomes more important in these complexes than in the Pt(II) complexes, as will be discussed below. The Pt-C bond distance is considerably longer in these complexes than in $Pt(PH_3)_2(C_2H_{4-n}(CH{=}CH_2)_n)$ and $[PtCl_3(C_2H_{4-n}(CH{=}CH_2)_n)]^-$; for instance, it is 2.829 Åin $[PtCl_5(C_2H_{4-n}(CH{=}CH_2)_n)]^-$, as shown in Figure 1.8, indicating that the coordinate bond is weak. These results would arise from the weak π-back-donation and the large steric repulsion between the four Cl ligands and the π-conjugate system, as will be discussed below. In $[PtCl_5(C_2H_{4-n}(CH{=}CH_2)_n)]^-$, both the DFT- and MP4(SDQ)-calculated binding energies decrease as the size of the π-conjugate

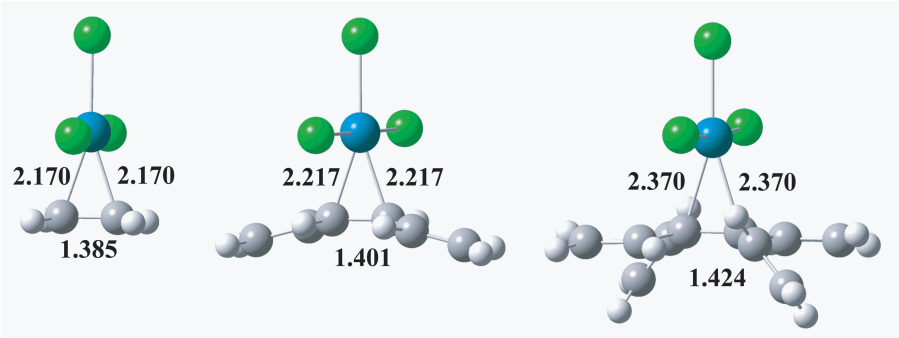

Figure 1.6: B3PW91-optimized structure of $[PdCl_3(C_2H_{4-n}(CH{=}CH_2)_n)]^-$ (bond lengths in angstroms).

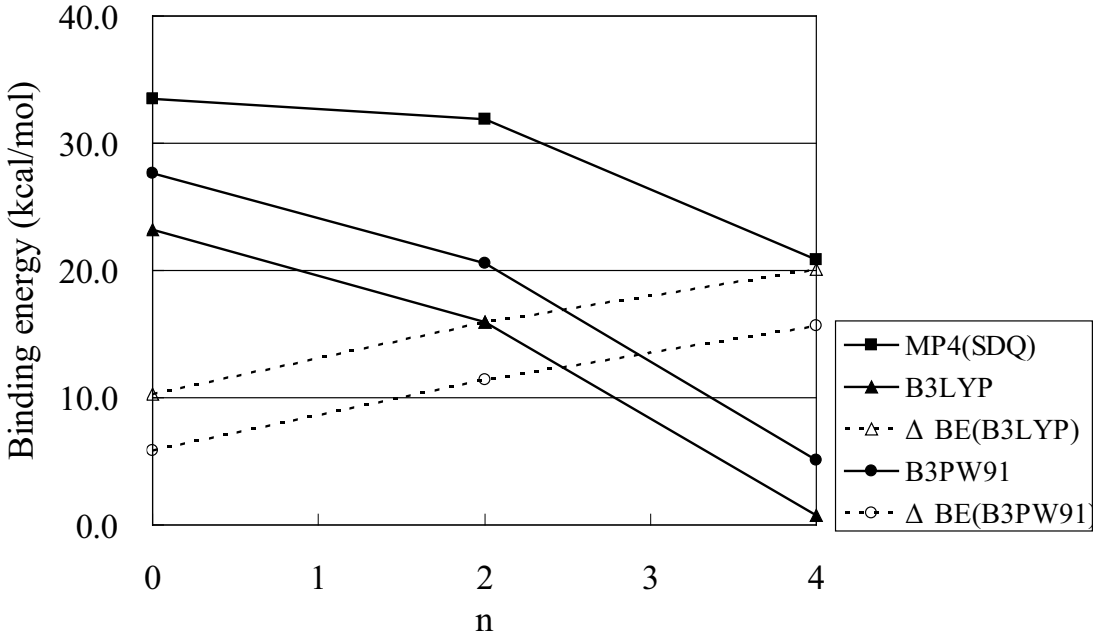

Figure 1.7: Binding energies of $[PdCl_3(C_2H_{4-n}(CH{=}CH_2)_n)]^-$.

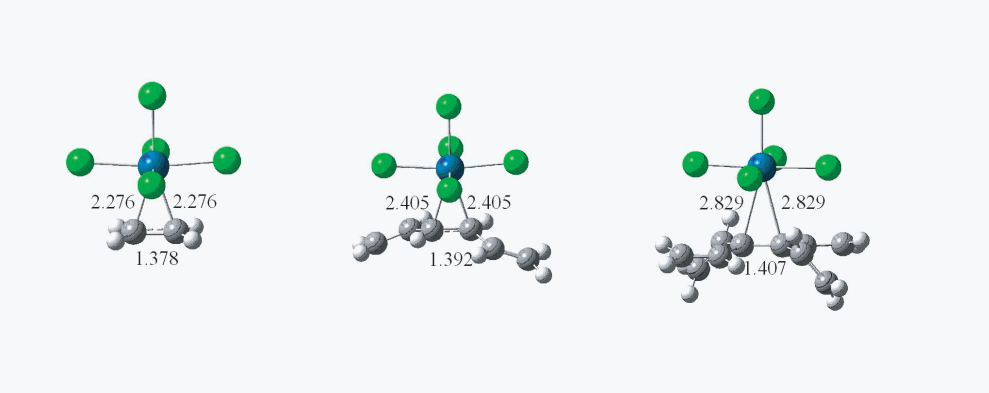

Figure 1.8: B3PW91-optimized structure of $[PtCl_5(C_2H_{4-n}(CH{=}CH_2)_n)]^-$ (bond lengths in angstroms).

system increases. However, it is noted that the DFT-calculated binding energy decreases more than the MP4(SDQ)-calculated value; actually, the $\Delta BE(B3LYP)$ and $\Delta BE(B3PW91)$ values of $[PtCl_5(C_2H_{4-n}(CH{=}CH_2)_n)]^-$ are very large, 26.6 and 23.6 kcal/mol, respectively, as shown in Figure 1.9. Thus, it is concluded that the DFTmethod underestimates the binding energies of these d^6 metal complexes, too, when the π-conjugate system is large.

1.3.4 Coordinate Bonding Nature and Electron Distribution.

Table 1.4 shows the natural atomic orbital (NAO) charge evaluated by the MP4(SDQ) and DFT(B3LYP) methods. The π-conjugate system is negatively charged, and its negative charge increases as the size of the π-conjugate system increases. These results clearly show that the π-back-donation interaction plays a more important role in $Pt(PH_3)_2(C_2H_{4-n}(CH{=}CH_2)_n)$ than the σ-donation interaction and becomes stronger with an increase of the size of the π-conjugate system. The DFTcalculated negative charge is slightly larger than the MP4(SDQ)-calculated value, indicating that the DFT method evaluates slightly stronger π-back-donation than the MP4(SDQ) method. It is noted that the difference in negative charge between the DFT and MP4(SDQ) calculations increases with an increase of the size of the π-conjugate system.

In the d^8 metal complex $[PtCl_3(C_2H_{4-n}(CH{=}CH_2)_n)]^-$, the π-conjugate systems are almost neutral, indicating that both the π-back-donation and the σ-donation interactions comparably participate in the coordinate bond of these complexes. In the d^6 metal complex

Table 1.4: NAO Charges of $C_2H_{4-n}(CH{=}CH_2)_n$ in $Pt(PH_3)_2(C_2H_{4-n}(CH{=}CH_2)_n)$, $[PtCl_3(C_2H_{4-n}(CH{=}CH_2)_n)]^-$, and $[PtCl_5(C_2H_{4-n}(CH{=}CH_2)_n)]^-$

	$Pt(PH_3)_2(C_2H_{4-n}(CH{=}CH_2)_n)$		$[PtCl_3(C_2H_{4-n}(CH{=}CH_2)_n)]^-$		$[PtCl_5(C_2H_{4-n}(CH{=}CH_2)_n)]^-$	
n	MP4(SDQ)	B3LYP	MP4(SDQ)	B3LYP	MP4(SDQ)	B3LYP
1	-0.356	-0.359	0.003	-0.002	0.184	0.209
2	-0.384	-0.393	-0.025	-0.013		
3	-0.419	-0.424	-0.041	-0.034	0.180	0.226
4	-0.436	-0.456	-0.065	-0.056		
5	-0.459	-0.470	-0.090	-0.074	0.171	0.199

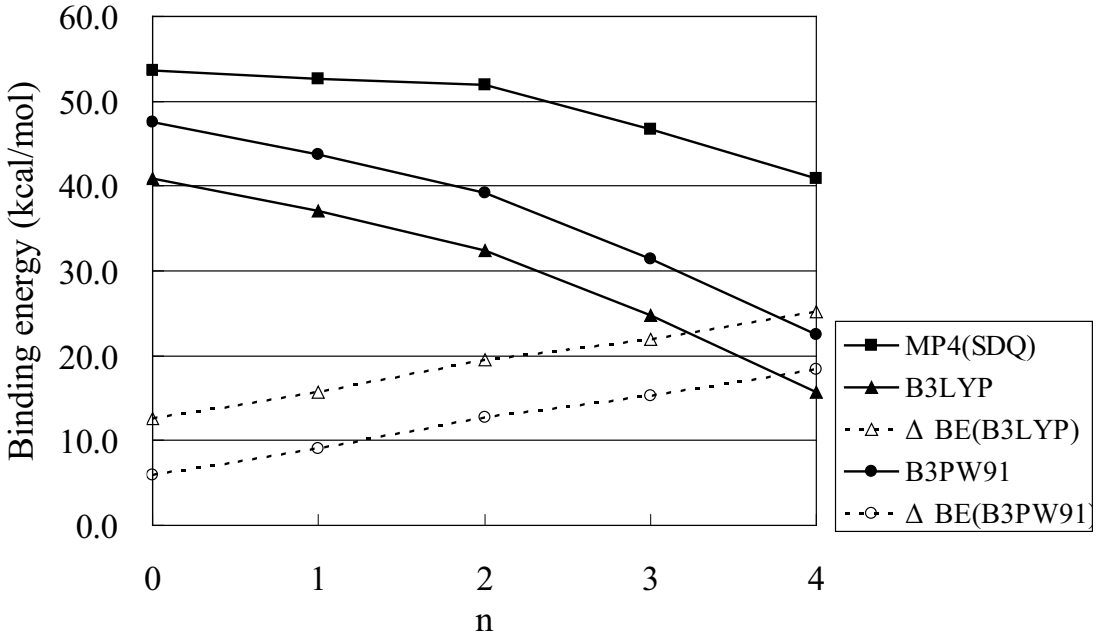

Figure 1.9: Binding energies of $[PtCl_5(C_2H_{4-n}(CH{=}CH_2)_n)]^-$.

$[PtCl_5(C_2H_{4-n}(CH{=}CH_2)_n)]^-$ the π-conjugate system is positively charged, indicating that the σ-donation participates more in the coordinate bond than the π-backdonation, as expected. In the d^8 and d^6 metal complexes, the DFT method tends to present a slightly less negative or a slightly more positive NAO charge of the π-conjugate system, respectively. This suggests that the σ-donation is calculated to be slightly stronger by the DFT method than by the MP4(SDQ) method.

To present more detailed information about the coordinate bonding nature, the molecular orbitals (MOs) of $Pt(PH_3)_2(C_2H_{4-n}(CH{=}CH_2)_n)$, $[PtCl_3(C_2H_{4-n}(CH{=}CH_2)_n)]^-$, and $[PtCl_5(C_2H_{4-n}(CH{=}CH_2)_n)]^-$ are represented by linear combination of the MOs of the fragments, as follows: [42]

$$\Psi_i(\text{A-B}) = \sum_k c_{i,k}\phi_k(\text{A}) + \sum_j d_{i,j}\varphi_k(\text{B}) \tag{1.3}$$

where $\phi_k(\text{A})$ is the kth MO of such a metal fragment A as $Pt(PH_3)_2$, $[PtCl_3]^-$, and $[PtCl_5]^-$, $\varphi_k(\text{B})$ is the jth MO of such a π-conjugate system B as $C_2H_{4-n}(CH{=}CH_2)_n$, and $c_{i,k}$ and $d_{i,j}$ are their expansion coefficients, respectively. The Mullikenlike population of each fragment

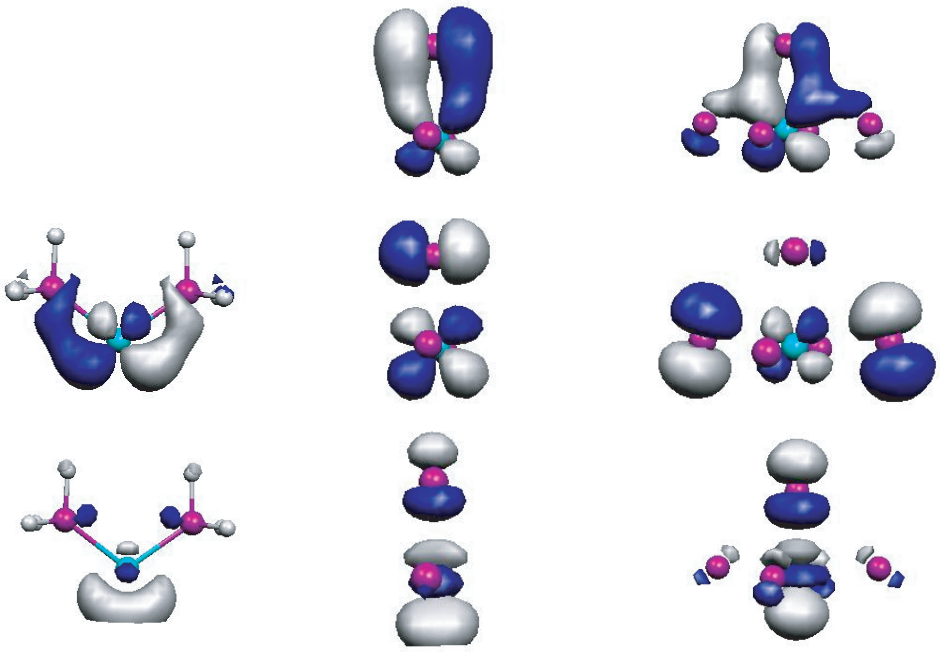

(a) $Pt(PH_3)_2$ (b) $[Pt(Cl_3)]^-$ (c) $[Pt(Cl_5)]^-$

Figure 1.10: d_π- and d_σ-type orbitals of (a) $Pt(PH_3)_2$, (b) $[PtCl_3]^-$, and (c) $[PtCl_5]^-$.

MO is represented by Eqs. 1.4 and 1.5.

$$\rho_k(\mathrm{A}) = \sum_{i}^{occ}[c_{i,k}^2 + \sum_{j} c_{i,k}d_{i,j}S_{k,j}] \tag{1.4}$$

$$\rho_j(\mathrm{B}) = \sum_{j}^{occ}[d_{i,j}^2 + \sum_{k} c_{i,k}d_{i,j}S_{k,j}] \tag{1.5}$$

where $S_{k,j}$ is the overlap integral between the kth MO of fragment A and the jth MO of fragment B. It is noted that the sum of these populations of the fragment is the same as the sum of the Mulliken atomic populations of fragment A. Table 1.5 summarizes the DFT(B3LYP)-evaluated Mulliken-like populations of the d_π occupied and σ-type unoccupied MOs of Pt-$(PH_3)_2$, $[PtCl_3]^-$ and $[PtCl_5]^-$ and those of the π and π^* MOs of C_2H_4 in $Pt(PH_3)_2(C_2H_4)$, $[PtCl_3$-$(C_2H_4)]^-$ and $[PtCl_5(C_2H_4)]^-$; see Figure 1.10 for these MOs. In the d^{10} metal complex $Pt(PH_3)_2$-(C_2H_4), the population (1.461e) of the d_π MO is significantly small, while it is 1.675e in the d^8 metal complex $[[PtCl_3(C_2H_4)]^-$ and 2.00e in the d^6 metal complex $[PtCl_5(C_2H_4)]^-$. These results clearly show that the π-back-donation interaction is considerably strong in the

Table 1.5: Mulliken-like Populations of Fragment MOs in $Pt(PH_3)_2(C_2H_4)$, $[PtCl_3(C_2H_4)]$-, and $[PtCl_5(C_2H_4)]$-

	$Pt(PH_3)_2(C_2H_4)$	$[PtCl_3(C_2H_4)]^-$	$[PtCl_5(C_2H_4)]^-$
	Pt Moiety		
d_π-type orbital[a]		1.962	1.938
d_π-type orbital[b]	1.461	1.675	1.977
d_σ-type unoccupied orbital[c]	0.310	0.474	0.560
	C_2H_4 Moiety		
π orbital	1.652	1.558	1.510
π^* orbital	0.556	0.390	0.174

a) This molecular orbital mainly consists of a d_π orbital which does not interact with the π^* orbital of the π-conjugate system.
b) This molecular orbital mainly consists of a d_π orbital which interacts with the π^* orbital of the π-conjugate system.
c) This molecular orbital mainly consists of a Pt 6s-like orbital in $Pt(PH_3)_2(C_2H_4)$ and a d_σ orbital in $[PtCl_3(C_2H_4)]^-$ and $[PtCl_5(C_2H_4)]^-$, where both interact with the π-orbital of the π-conjugate system.

d^{10} metal complex but becomes weaker in the d^8 metal complex than in the d^{10} metal complex and is not formed at all in the d^6 metal complex. On the other hand, the population of the σ-type unoccupied MO increases in the order $d^{10} < d^8 < d^6$. This result indicates that the σ-donation interaction becomes stronger in the order $d^{10} < d^8 < d^6$. Consistent with these results, the populations of the d and π^* MOs decrease in the order $d^{10} > d^8 > d^6$. All these results indicate that the π-back-donation is stronger than the σ-donation in the d^{10} metal complex, both are comparable in the d^8 metal complex, and only the σ-donation participates in the coordinate bond of the d^6 metal complex. Of course, we must consider the possibility that these population changes arise from polarization interaction. In these systems, however, the population changes in the d_π occupied and σ-type unoccupied MOs are similar to the population changes in the π^* and d MOs of the π-conjugate system, respectively. These results indicate that the population changes are induced by the CT interactions such as the σ-donation and the π-back-donation. From these results, it is concluded that the coordinate bonding nature is much different among these d^{10}, d^8, and d^6 metal complexes and that the DFT method underestimates the binding energies independently of the bonding nature when the π-conjugate system is large.

1.3.5 Why Does the DFT Method Underestimate Binding Energies When the π-Conjugate System Is Large?

It is important to clarify the reason why the DFT method underestimates the binding energy when the π-conjugate system is large. We must remember that the DFT method tends to overestimate the charge delocalization and cannot calculate well the dispersion interaction [1–4]. Here, we examine whether these tendencies lead to the underestimation of the binding energy.

Charge Delocalization.

As well-known, the DFT method overestimates electron delocalization. If the DFT method overestimated the CT interaction between the metal center and the π-conjugate system, it overestimated the binding energy and vice versa. In the Pt(0) complexes, the population analysis shows that the DFT method presents slightly stronger π-back-donation from the Pt center to

the π-conjugate system than the MP4-(SDQ) method, though the difference is not large. In the Pt(II) and Pt(IV) complexes, the DFT method moderately overestimates the σ-donation from the π-conjugate system to the Pt center, compared to the MP4(SDQ) method. These results suggest that the DFT method tends to overestimate the CT interaction in these complexes, as expected. This tendency would lead to the overestimation of the binding energy by the DFT method, which is not consistent with the underestimation of the binding energy by the DFT method.

Thus, we must consider another factor responsible for the underestimation of the binding energy. If the DFT method overestimated the delocalization of negative charge on the π-conjugate system which was induced by the π-back-donation, the DFT method underestimated the electrostatic interaction between the positive charge on Pt and the negative charge on the π-conjugate system, as shown in Scheme 1. Certainly, the coordinating C atoms are calculated to be more negatively charged and the C atoms of the vinyl groups are calculated to be less negatively charged by the MP4(SDQ) method than by the DFT method, though the differences are small; see Figure 1.11. Using these negative charges, we approximately evaluated the Coulomb interaction between the π-conjugate system and the positively charged Pt atom. When a +1 positive charge is placed on the Pt atom, the Coulomb interaction is -89.9 kcal/mol for the MP4(SDQ)-calculated electron distribution and -90.3 kcal/mol for the DFT(B3LYP)-calculated electron distribution. The difference is much smaller than that between the MP4(SDQ)- and DFT-(B3LYP)-calculated binding energies.

We also evaluated the interaction energy between a radical anion, [$C_2H_{4-n}(CH{=}CH_2)_n$]- (n = 0, 2, or 4), and a positive charge using the DFT and MP4(SDQ) methods, where the geometry of $C_2H_{4-n}(CH{=}CH_2)_n$ was taken to be the same as that in $Pt(PH_3)_2(C_2H_{4-n}(CH{=}CH_2)_n)$ and a positive charge was placed at the position of the Pt center. If the DFT method overestimated the delocalization of negative charge, the negative charge on the C1 atom decreased, where the C1 atom coordinates with the Pt center (Figure 1.12), which led to underestimation of the electrostatic interaction by the DFT method. As shown in Table 1.6, the energy difference between the DFT-(B3LYP) and MP4(SDQ) methods is less than 2 kcal/mol and that between the

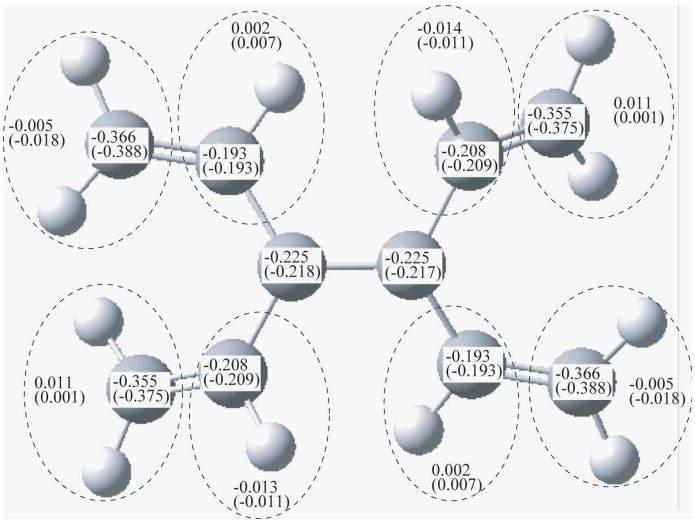

(a) Radical anion $[\bullet C_2(CH{=}CH_2)_4]^-$

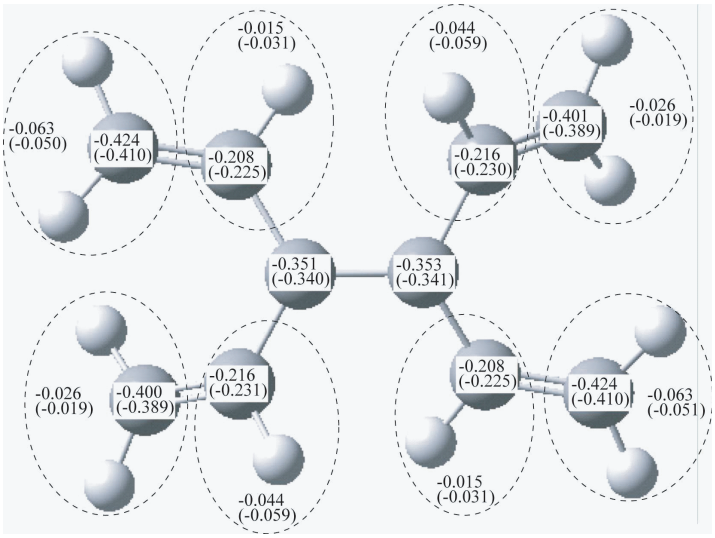

(b) $C_2(CH{=}CH_2)_4$ in $Pt(PH_3)_2(C_2(CH{=}CH_2)_4)$

Figure 1.11: The charge distribution of (a) radical anion $[\cdot\ C_2H_{4-n}(CH{=}CH_2)_n]^-$ and (b) $C_{10}H_{12}$ of $Pt(PH_3)_2(C_{10}H_{12})$ evaluated with MP4(SDQ) and B3LYP (values in parenthesis) method.

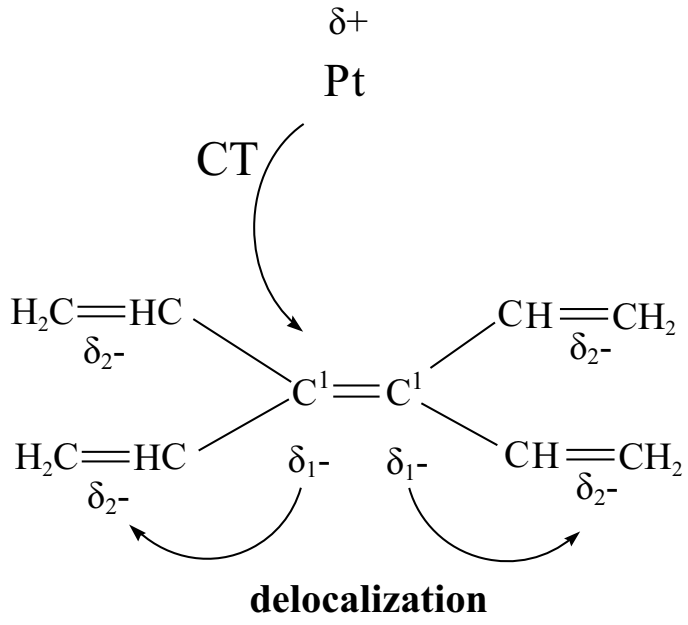

The delocalization decreases δ_1- and increases δ_2-.

⇓

Electrostatic interaction between Pt and C^1 decreases.

Figure 1.12: Delocalization Effect

Table 1.6: Interaction Energies (kcal/mol) between the Radical Anion $[\cdot C_2H_{4-n}(CH{=}CH_2)_n]^-$ and a Positive Charge

	n = 0	n = 2	n = 4
MP4(SDQ)	196.4	168.6	157.3
B3LYP	195.9	166.6	155.4
B3PW91	197.3	168.3	157.5

DFT(B3PW91) and MP4(SDQ) methods is less than 1 kcal/mol. These differences are much smaller than the difference between the DFT- and MP4(SDQ)-calculated binding energies; remember that the $\Delta BE(B3LYP)$ value is 22.2 kcal/mol and the $\Delta BE(B3PW91)$ value is 13.3 kcal/mol for $C_2(CH{=}CH_2)_4$. Moreover, the difference between the DFT and MP4(SDQ)-calculated electrostatic interaction energies changes little as the size of the π-conjugate system increases. From these results, it is concluded that the delocalization of the negative charge in the π-conjugate system is not responsible for the underestimation of the binding energy by the DFT method.

Dispersion Interaction

If the dispersion interaction contributed to the binding energy [1–5], the DFT method underestimated the binding energy. Here, we investigate whether the dispersion interaction contributes to the binding energy. However, we cannot estimate the energy stabilization by the dispersion interaction between $Pt(PH_3)_2$ and the vinyl group, because the vinyl group contributes not only to the dispersion interaction but also to the CT interaction with the Pt center. We investigated here $Pt(PH_3)_2(C_2H_{4-n}(CH_3)_n)$ in which methyl groups are introduced to the C=C double bond, because the methyl group forms a dispersion interaction but not a CT interaction with the Pt moiety. The optimized geometries and binding energies of these complexes are shown in Figures 1.13 and 1.14, respectively. In these complexes, the ΔBE value increases, in other words, the DFT-calculated binding energy decreases, as the number of methyl groups increases, whereas the MP4(SDQ)-calculated value decreases little. This behavior is similar to that of $Pt(PH_3)_2(C_2H_{4-n}(CH{=}CH_2)_n)$.

If this underestimation arises from the poor description of the dispersion interaction, a similar underestimation should occur in the interaction between $Pt(PH_3)_2$ and the methyl substituents. We evaluated the interaction energy between $Pt(PH_3)_2$ and two methane molecules, as shown in Figure 1.15, where we employed methane instead of the methyl substituent because the methyl radical would form a covalent interaction with $Pt(PH_3)_2$. The positions of the methanes were taken to be the same as those of the methyl groups in $Pt(PH_3)_2$(trans-

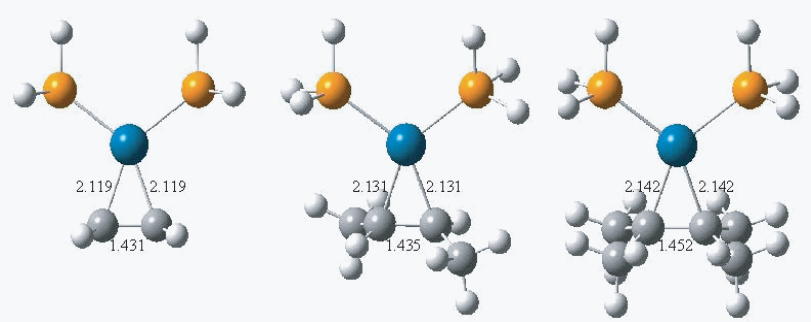

Figure 1.13: B3PW91-optimized structure of $Pt(PH_3)_2(C_2H_{4-n}(CH_3)_n)$ (bond lengths in angstroms).

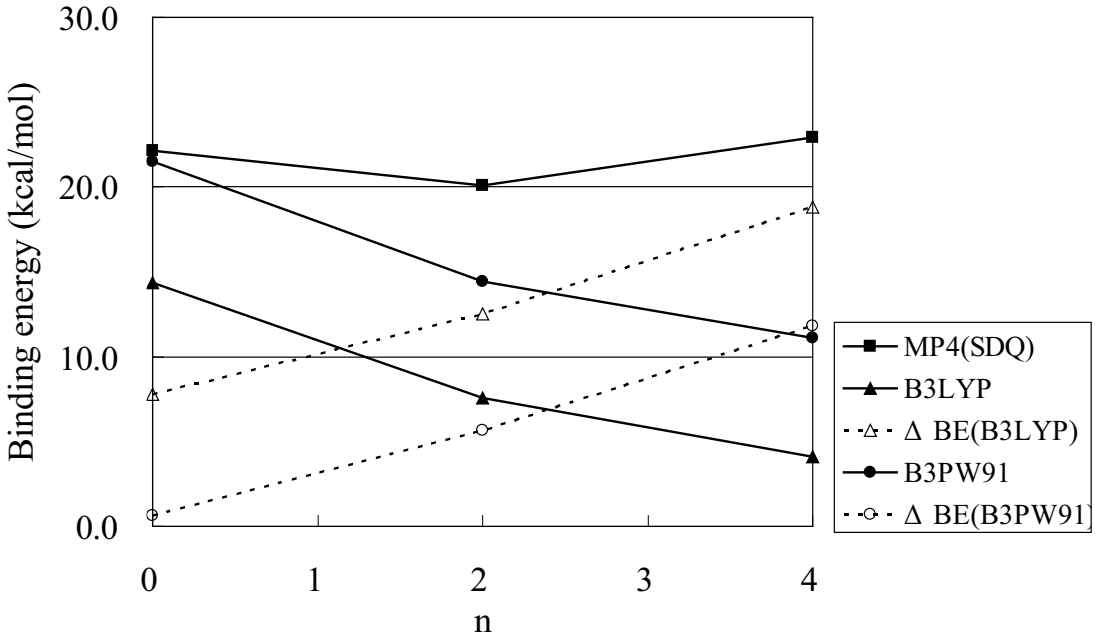

Figure 1.14: Binding energies of $Pt(PH_3)_2(C_2H_{4-n}(CH_3)_n)$.

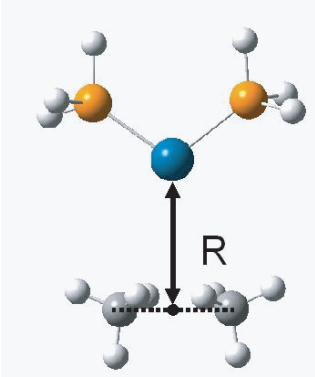

Figure 1.15: System which consists of $Pt(PH_3)_2$ and two methane molecules

MeHC=CHMe). The MP4(SDQ) and CCSD(T) methods present a considerably large energy stabilization around R = 2.8 Å, as shown in Figure 1.16. However, the B3LYP and B3PW91 methods present an energy destabilization around there. The difference between the DF-Tand MP4(SDQ)-calculated binding energies of $Pt(PH_3)_2$(trans-MeHC=CHMe) is about 12.5 kcal/mol, but we must remember that the binding energy of $Pt(PH_3)_2(C_2H_4)$ is different by 7.8 kcal/mol between these two methods. Thus, two methyl groups induce an energy difference of 4.7 kcal/mol, which is similar to the difference (5.8 kcal/mol) in the interaction energy of $Pt(PH_3)_2(CH_4)_2$ between the DFT and MP4(SDQ) calculations, where the distance between Pt and the centers of the two C atoms was taken to be the same as that of $Pt(PH_3)_2$(trans-MeHC=CHMe). Because the stabilization energy between $Pt(PH_3)_2$ and CH_4 is considered to arise from the dispersion interaction, these results lead to the conclusion that the insufficient description of the dispersion interaction by the DFT method is one of the reasons for the underestimation of the binding energy [43].

Other Factors

The B3PW91 functional presents energy stabilization of the methane-methane interaction like the CCSD(T) method [4]. Because methane-methane interaction mainly arises from the dispersion interaction, the B3PW91 functional is not very bad at evaluating the dispersion interaction. Nevertheless, the DFT(B3PW91)-calculated binding energy decreases as the size of the π-conjugate system increases, unlike the MP4(SDQ)-calculated value.

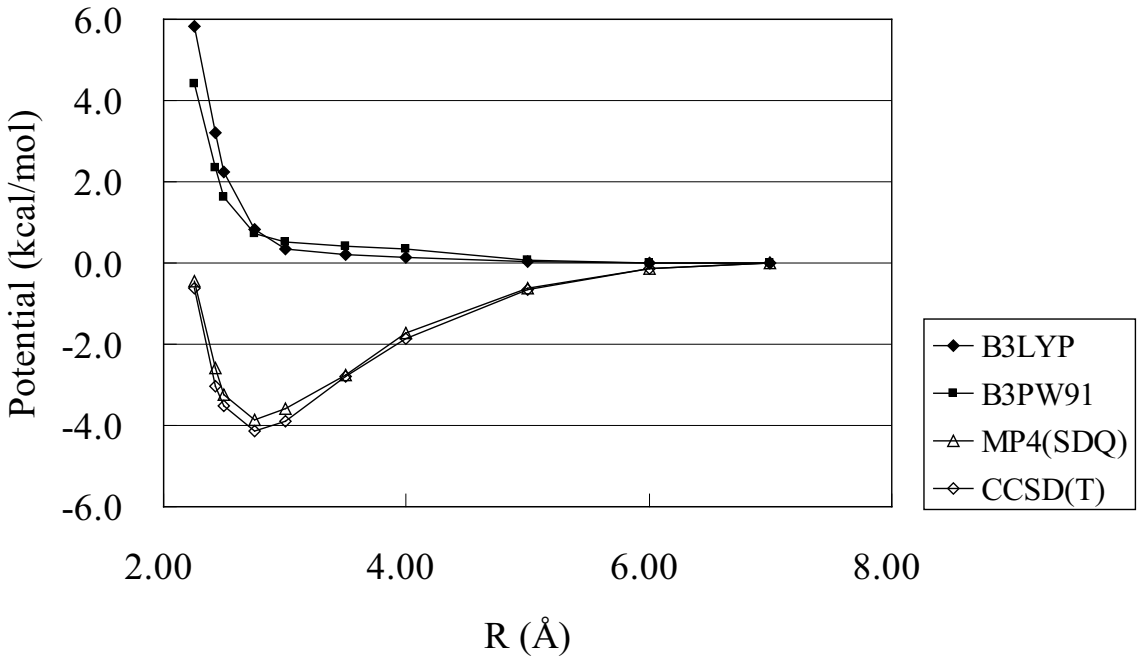

Figure 1.16: Potential energy curves in $Pt(PH_3)_2(CH_4)_2$. R represents the distance between Pt and the centers of the two C atoms.

Table 1.7: Binding Energies (kcal/mol) of Pt(C_2H_{4-n}(CH=CH_2)$_n$)

Binding Energies Evaluated by the Post-Hartree-Fock Method						
n	MP2	MP3	MP4(DQ)	MP4(SDQ)	CCSD	CCSD(T)
0	86.6	61.0	67.3	70.7	67.5	72.4
2	85.8	56.6	64.8	69.0		
4	88.5	54.8	66.0	71.1		
Binding Energies Evaluated by the DFT Method with Various Functionals						
n	B3LYP	B3PW91	$\Delta BE(B3LYP)$	$\Delta BE(B3PW91)$		
0	62.8	69.6	8.0	1.2		
2	55.9	63.2	13.1	5.9		
4	52.1	60.0	19.0	11.1		

Table 1.8: Binding Energies (kcal/mol) of Pt(PH_3)$_2$(C_2H_{4-n}(CH=CH_2)$_n$) (n = 0-4) calculated with the Hartree-Fock Method

	n = 0	n = 1	n = 2	n = 3	n = 4
BE	3.2	0.4	-2.5	-5.5	-10.8

We investigated here the complexes of a bare Pt(0) atom with the π-conjugate systems, Pt(C_2H_{4-n}(CH_3)$_n$). In these complexes, the DFT-calculated binding energy considerably decreases to an extent similar to that of Pt(PH_3)$_2$(C_2H_{4-n}(CH_3)$_n$) as the size of the π-conjugate system increases (see Table 1.7), while the MP4(SDQ)-calculated binding energy decreases little. Because the dispersion interaction between the ligandsandsubstituents is not involved in Pt(C_2H_{4-n}(CH_3)$_n$), these results suggest that not only the dispersion interaction but also another factor is responsible for the underestimation.

We also evaluated the binding energy of Pt(PH_3)$_2$(C_2H_{4-n}(CH_3)$_n$) at the Hartree-Fock level. Interestingly, the binding energy decreases as the size of the π-conjugate system increases, as shown in Table 1.8. This behavior is the same as that of the DFT method.

From all these results, it should be concluded that if the electron correlation effects are not sufficiently taken into consideration in the calculation, the binding energy decreases as the size of the π-conjugate system increases. It is likely that the use of a single-determinant wave function is one of the reasons that the DFT method underestimates the binding energy of the transition-metal complexes with a π-conjugate system when the size of the π-conjugate system

is large [44].

1.4 Conclusion

In this study, we systematically evaluated the binding energies of d^{10}, d^8, and d^6 transition-metal complexes of π-conjugate systems using the MP2 to MP4, CCSD(T), and DFT methods with triple-u-quality basis sets. The binding energy of $Pt(PH_3)_2(C_2H_{4-n}(CH{=}CH_2)_n)$ considerably fluctuates around the MP2 and MP3 levels but much less upon going to MP4(SDQ) from MP3. The binding energy moderately increases upon going from MP4(SDQ) to MP4(SDTQ) and from CCSD to CCSD(T). The MP4(SDTQ) method tends to present a moderately larger binding energy than the CCSD(T) method. Thus, the MP4(SDQ) method presents a binding energy similar to that of the CCSD(T) method, which indicates that the MP4(SDQ) method provides a reliable binding energy from a practical point of view.

It should be noted that the MP4(SDQ)- and CCSD(T)-calculated binding energies of $Pt(PH_3)_2(C_2H_{4-n}(CH{=}CH_2)_n)$ change little as the size of the π-conjugate system increases, while the DFT-calculated binding energy considerably decreases. The difference between the DFT- and MP4(SDQ)-calculated binding energies reaches about 25 kcal/mol for n = 4. The DFTcalculated binding energies of such d8 and d6 metal complexes as $[PtCl_3(C_2H_{4-n}(CH{=}CH_2)_n)]^-$, its Pd analogue, and $[PtCl_5(C_2H_{4-n}(CH{=}CH_2)_n)]^-$ decrease similarly.

Population analysis based on the fragment MOs and usual natural atomic population leads to the conclusion that the bonding nature is quite different in these complexes; the π-back-donation mainly participates in the coordinate bond of the Pt(0) complex, the σ-donation and π-back-donation comparably participate in the coordinate bond of the Pt(II) complex, and the σ-donation largely participates but the π-back-donation participates little in the coordinate bond of the Pt(IV) complex. Thus, it is concluded that the DFT method underestimates the binding energy independently of the coordinate bonding nature when the π-conjugate system is large.

The reason for the underestimation was investigated with model systems $Pt(PH_3)_2(C_2H_{4-n}(CH_3)_n)$ and $Pt(PH_3)_2 + 2CH_4$. We found that the DFT method underestimated the interaction

between $Pt(PH_3)_2$ and two methane molecules to an extent similar to that of the binding energy of $Pt(PH_3)_2$(trans-MeCH=CHMe). This result suggests that the dispersion interaction is one of the reasons for the underestimation of the binding energy by the DFT method [43]. However, it is noted that the DFTcalculated binding energy between the bare Pt(0) atom and the π-conjugate system decreases with an increase of the size of the π-conjugate system but the MP4(SDQ)-calculated value changes little, indicating that not only the dispersion interaction between the substituents and the metal moiety but also another factor is responsible for the underestimation [44]. The Hartree-Fock-calculated binding energy of $Pt(PH_3)_2(C_2H_{4-n}$-$(CH{=}CH_2)_n)$ also decreases as the size of the π-conjugate system increases. From these results, we present several conclusions, as follows.

- The DFT method underestimates the binding energies of these d10, d8, and d6 metal complexes with a large π-conjugate system.
- The DFT method tends to moderately overestimate the CT interaction, which is not responsible for the underestimation of the binding energy.
- One of the reasons for the underestimation is the poor description of the dispersion interaction between the substituents of the C=C double bond and the metal moiety [43].
- The insufficient incorporation of the electron correlation effects is one of the reasons that the DFT method underestimates the binding energy of these complexes when the π-conjugate system is large [44].

The present examination was made for the late-transitionmetal complexes. It would be interesting to investigate the binding energies of the middle- and early-transition-metal complexes, because the electronic structure would be very different among the early-, middle-, and late-transition-metal complexes.

Bibliography

[1] Kristyan, S.; Pulay, P. *Chem. Phys. Lett.* **1994**, *229*, 175.

[2] Perez-Jorda, J. M.; Becke, A. D. *Chem. Phys. Lett.* **1995**, *233*, 134.

[3] Zhang, Y.; Pan, W.; Yang, W. *J. Chem. Phys.* **1997**, *107*, 7921.

[4] Tsuzuki, S.; Lüthi, H. P. J. *Chem. Phys.* **2001**, *114*, 3949.

[5] Wu, Q.; Yang, W. *J. Chem. Phys.* **2002**, *116*, 515.

[6] Meyer, E. A.; Castellano, R. K.; Diederich, F. *Angew. Chem. Int. Ed.* **2003**, *42*, 1210.

[7] Sponer J.; Hobza, P. *Chem. Phys. Lett.* **1997**, *267*, 263.

[8] Aravinda, S.; Shamala, N.; Das, C.; Sriranjini, A.; Karle, I. L.; Balaram, P. *J. Am. Chem. Soc.* **2003**, *125*, 5308.

[9] (a) Champagne, B.; Perpete, A.; van Gisbergen, S. J. A.; Baerends, E. J.; Snijders, J. G.; Soubra-Ghaoui, C.; Robins, K. A.; Kirtman, B. *J. Chem. Phys.* **1998**, *109*, 10489. (b) Champagne, B.; Perpete, A.; Jacquemin, D.; van Gisbergen, S. J. A.; Baerends, E. J.; Soubra-Ghaoui, C.; Robins, K. A.; Kirtman, B. *J. Phys. Chem. A* **2000**, *104*, 4755.

[10] Kameno, Y.; Ikeda, A.; Nakao, Y.; Sato, H.; Sakaki, S. *J. Phys. Chem. A* **2005**, *109*, 8055.

[11] (a) Lee, K.; Song, H.; Park, J. T. *Acc. Chem. Res.* **2003**, *36*, 78. (b) Nakamura, E.; Isobe, H. *Acc. Chem. Res.* **2003**, *36*, 807. (c) Balch, A. L.; Olmstead, M. M. *Chem. Rev.* **1998**, *98*, 2123..

[12] Albright, T. A.; Hoffmann, R.; Thibeault, J. C.; Thorn, D. L. *J. Am. Chem. Soc.* **1979**, *101*, 3801.

[13] Sakaki, S.; Ieki, M. *Inorg. Chem.* **1991**, *30*, 4218.

[14] Hay, P. J. *J. Am. Chem. Soc.* **1981**, *103*, 1390.

[15] (a) Becke, A. D. *J. Chem. Phys.* **1986**, *84*, 4524. (b) Becke, A. D. *Phys. Rev. A* **1988**, *38*, 3098. (c) Becke, A. D. *J. Chem. Phys.* **1993**, *98*, 5648.

[16] Lee, C.; Yang, W.; Parr, R. G. *Phys. Rev. B* **1988**, *37*, 785.

[17] (a) Perdew, J. P.; Chevary, J. A.; Vosko, S. H.; Jackson, K. A.; Pederson, M. R.; Singh, D. J.; Fiolhais, C. *Phys. Rev. B* **1992**, *46*, 6671. (b) Perdew, J. P.; Chevary, J. A.; Vosko, S. H.; Jackson, K. A.; Pederson, M. R.; Singh, D. J.; Fiolhais, C. *Phys. Rev. B* **1993**, *48*, 4978. (c) Perdew, J. P.; Burke, K.; Wang, Y. *Phys. Rev. B* **1996**, *54*, 16533.

[18] Hay, P. J.; Wadt, W. R. *J. Chem. Phys.* **1985**, *82*, 299.

[19] Couty, M.; Hall, M. B. *J. Comput. Chem.* **1996**, *17*, 1359.

[20] Ehlers, A. W.; Böhme, M.; Dapprich, S.; Gobbi, A.; Höllwarth, A.; Jonas, V.; Köhler, K. F.; Stegmann, R.; Veldkamp, A.; Frenking, G. *Chem. Phys. Lett.* **1993**, *208*, 111.

[21] (a) Hebre, W. J.; Ditchfield, R.; Pople, J. A. *J. Chem. Phys.* **1972**, *56*, 2257. (b) Hariharan, P. C.; Pople, J. A. *Mol. Phys.* **1974**, *27*, 209. (c) Hariharan, P. C.; Pople, J. A. *Theoret. Chim. Acta* **1973**, *28*, 213. (d) Francl, M. M.; Pietro, W. J.; Hebre, W. J.; Binkley, J. S.; Gordon, M. S.; DeFrees, D. J.; Pople, J. A. *J. Chem. Phys.* **1982**, *77*, 3654.

[22] (a) Cizek, J. AdV. *Chem. Phys.* **1969**, *14*, 35. (b) Purvis, G. D.; Bartlett, R. J. *J. Chem. Phys.* **1982**, *76*, 1910. (c) Scuseria, G. E.; Janssen, C. L.; Schaefer, H. F., III. *J. Chem. Phys.* **1988**, *89*, 7382. (d) Scuseria, G. E.; Schaefer, H. F., III. *J. Chem. Phys.* **1990**, *90*, 3700. (e) Pople, J. A.; Heaπ-Gordon, M.; Raghavachari, K. *J. Chem. Phys.* **1987**, *87*, 5968.

[23] Slater, J. C. *Phys. ReV.* **1951**, *81*, 385.

[24] Vosko, S. J.; Wilk, L.; Nusair, M. *Can J. Phys.* **1980**, *58*, 1200.

[25] Becke, A. D. *Phys. ReV.* **1988**, *438*, 3098.

[26] Perdew, J. P. *Phys. Rev. B* **1986**, *33*, 8822.

[27] Beche, A. D. *J. Chem. Phys.* **1988**, *88*, 1053.

[28] Adamo, C.; Barone, V. *J. Chem. Phys.* **1998**, *108*, 664.

[29] (a) Perdew, J. P.; Burke, J.; Ernzerkof, M. *Phys. Rev. Lett.* **1996**, *77*, 3865. (b) Perdew, J. P.; Burke, J.; Ernzerkof, M. *Phys. Rev. Lett.* **1997**, *78*, 1396.

[30] (a) Krishnan, R.; Binkley, J. S.; Seeger, R.; Pople, J. A. *J. Chem. Phys.* **1980**, *72*, 650. (b) McLean, A. D.; Chandler, G. S. *J. Chem. Phys.* **1980**, *72*, 5639.

[31] Dolg, M.; Stoll, H.; Preuss, H.; Pitzer, R. M. *J. Phys. Chem.* **1993**, *97*, 5852.

[32] Martin, J. M. L.; Sundermann, A. *J. Chem. Phys.* **2001**, *114*, 3408.

[33] The MP4(SDQ)-calculated binding energy of $Pt(PH_3)_2(C_2H_4)$ is 21.7 and 22.2 kcal/mol with and without the g polarization function, where either (311111/22111/411/11/1) or (311111/22111/411/11) was employed for Pt. [34]

[34] Yates, B. F. *J. Mol. Struct. (THEOCHEM)* **2000**, *506*, 223.

[35] Curtiss, L. A.; Redfern, P. C.; Raghavachari, K.; Rassolov, V.; Pople, J. A. *J. Chem. Phys.* **1999**, *110*, 4703.

[36] Pople, J. A.; *et al.* Gaussian 03, revision C.02; Gaussian, Inc.: Wallingford, CT, 2004.

[37] (a) Reed. A. E.; Weinhold, F. *J. Chem. Phys.* **1983**, *78*, 4066. (b) Reed, A. E.; Curtiss, L. A.; Weinhold, F. *Chem. Rev.* **1988**, *88*, 899.and references therein.

[38] (a) Flukiger, P.; Lu ¨ thi, H. P.; Portmann, S.; Weber, J. Swiss Center for Scientific Computing, Manno, Switzerland, 2000-2002. (b) Portman, S.; Luthi, H. P. MOLEKEL: An Interactive Molecular Graphics Tool. *Chimia* **2000**, *54*, 766.

[39] Cheng, P. -T.; Cook, C. D.; Nyburg, S. C.; Wan, K. Y. *Inorg. Chem.* **1971**, *10*, 2210.

[40] (a) The binding energy of $Pt(PPh_3)_2(C_2H_4)$ was experimentally reported, while those of the other complexes with large π-conjugate systems have not been experimentally reported. Therefore, the calculated binding energy cannot be compared with the experimental value except for $Pt(PH_3)_2(C_2H_4)$. The CCSD(T)-calculated binding energy of $Pt(PH_3)_2(C_2H_4)$ is smaller than one experimental value but larger than the other Binding Energy of Transition-Metal Complexes *J. Phys. Chem. A* **2007**, *111*, 7131.experimental value. The calculated value in this work is almost the same as the theoretical value which was previously calculated with the CCSD(T) method using a good basis set. These results suggest that the CCSπ-(T)/BS2 and MP4(SDQ)/BS2 methods present a reliable binding energy. (b) Kirkham, W. G.; Lister, M. W.; Lister, R. B. *Thermochim. Acta* **1975**, *11*, 89. (c) Mortimer, C. T. *Inorg. Chem.* **1984**, *6*, 233.(d) Martinho Simoes, J. A.; Beauchamp, J. L. *Chem. Rev.* **1990**, *90*, 629.

[41] Boys, S. F.; Bernardi, F. *Mol. Phys.* **1970**, *19*, 553.

[42] Similar methods were reported in several papers: Kato, S.; Yamabe, S.; Fukui, K. *J. Chem. Phys.* **1974**, *60*, 572..and Dapprich, S.; Frenking, G. *J. Phys. Chem.* **1995**, *99*, 9352.

[43] Usually the dispersion interaction is small. Thus, the poor description of the dispersion interaction by the DFT method is one of the reasons that the DFT method underestimates the binding energy when the size of the π-conjugate system is large. Another reason is responsible for the underestimation.

[44] Because the polarization is very important in the coordinate bond, it is likely that the incorrect evaluation of the polarizability and hyperpolarizability by the DFT method is

another reason for the underestimation of the binding energy by the DFT method. It is likely that the electron correlation effects should be well incorporated with a multiconfiguration wave function to calculate the polarizability and hyperpolarizability.

Chapter 2

Binding Energies and Bonding Nature of $MX(CO)(PH_3)_2(C_{60})$ (M = Rh or Ir; X = H or Cl): Theoretical Study

2.1 Introduction

Transition-metal complexes of fullerene are of considerable interest, because they are expected to be new materials with interesting properties [1]. Since the first syntheses of $OsO_4(NC_5H_4CMe_3)(C_{60})$ and $Pt(PPh_3)_2(C_{60})$ [2, 3], various transition-metal η^2-fullerene [1, 4–7] and η^5-fullerene complexes [8] have been reported so far. Also, several theoretical studies have been carried out; for instance, $Pt(PH_3)_2(C_{60})$ was investigated with Fenske-Hall [9], Hartree-Fock [10–12], and extended Hückel MO methods [13] previously and with the DFT method [14] recently. Also, the possibility of the existence of η^6-C_{60} complex was theoretically investigated with the semi-empirical and Hartree-Fock MO methods [15, 16]. However, all those theoretical works of the η^2-C_{60} complex were limited to $M(PH_3)_2(C_{60})$ type complexes (M = Ni, Pd, or Pt) and the other type of the η^2-C_{60} complex has not been theoretically investigated yet, to our knowledge. For instance, no theoretical work has been reported on Vaska type complexes of C_{60} such as $IrCl(CO)(P(PH_3)_2)(C_{60})$ [17] and $RhH(CO)(P(PH_3)_2)(C_{60})$ [18], despite of the importance of Vaska type complexes in coordination and organometallic chemistries.

In this work, we theoretically investigated $MH(CO)(PH_3)_2(C_{60})$ and $MCl(CO)(PH_3)_2(C_{60})$ (M = Rh or Ir) with DFT and MP2 to MP4(SDQ) methods. Our purposes here are to evaluate binding energies of this kind of transitionmetal η^2-C_{60} complexes and to make comparisons of the binding energy of these complexes with those of ethylene complexes and

$Pt(PH_3)_2(C_{60})$. From these investigations, we wish to theoretically clarify the characteristic features of $MH(CO)(PPH_3)2(C_{60})$ and $MCl(CO)(PPH_3)_2$-(C_{60}).

2.2 Computational details

Geometries were optimized by the DFT method with the B3LYP functional [19, 20]. In the geometry optimization, LANL2DZ basis sets [21] were used for Ir and Rh and usual 6-31G basis sets [22, 23] were employed for P, Cl, C, and H atoms. This basis set system is called BS-1 hereafter. The binding energy was evaluated with the MP2 and ONIOM(MP4(SDQ);UFF) [24, 25] methods, because the DFT method significantly underestimated the binding energy of $Pt(PH_3)_2(C_{60})$, as reported recently by us [26]. In the ONIOM calculation, we separated high and low level regions. In evaluation of the binding energy, we employed better basis set systems, BS-2 and BS-3; in BS-2, (541/541/211/1) and (541/541/111/1) basis sets were used for Rh and Ir [21, 27, 28], respectively, with the same effective core potentials as those of LANL2DZ. For the other atoms, usual 6-31G basis sets were employed [22, 23] except for P for which LANL2DZ basis set augmented with one d polarization function was used [29, 30]. In BS-3, usual 6-31G(d) basis sets were used for all atoms except for transition-metal elements for which the same basis sets and the same ECPs as those of BS-2 were used.

Gaussian 98 program package was used for all calculations [31]. Orbital plots were drawn with MOLEKEL program package [32].

2.3 Results and discussions

2.3.1 Optimized Geometries of $IrH(CO)(PH_3)_2(C_{60})$ (1), $IrCl(CO)(PH_3)_2$-(C_{60}) (2), and $RhH(CO)(PH_3)_2(C_{60})$ (3)

Experimental works reported that the transition metal interacted with C_{60} at the C-C bond between two six-member rings in these complexes [17, 18]. In $Pt(PR_3)_2(C_{60})$, experimental [3] and theoretical works [10, 26] showed that the Pt center interacted with C_{60} at the same C-C bond. Thus, we optimized geometries of these complexes in this coordination structure.

All these complexes take pseudo-trigonal bipyramidal structure around the metal center, in

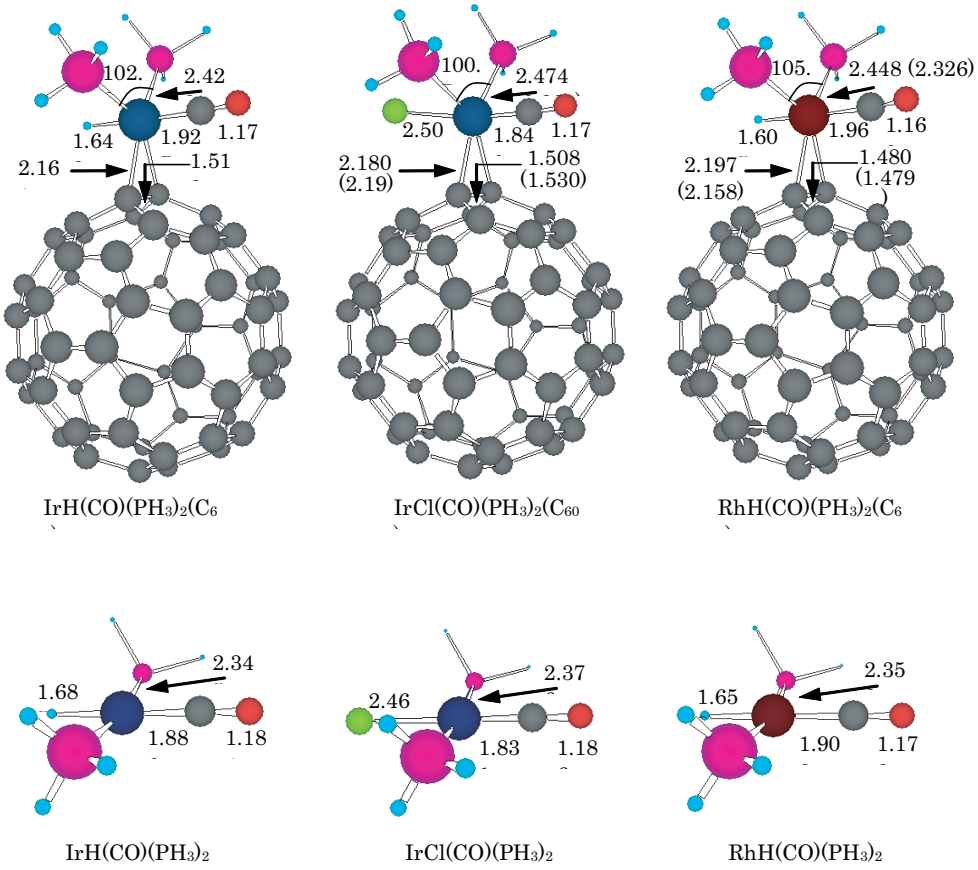

Figure 2.1: Optimized structures of $IrH(CO)(PH_3)_2(C_{60})$, $IrCl(CO)(PH_3)_2(C_{60})$, $RhH(CO)(PH_3)_2(C_{60})$, $IrH(CO)(PH_3)_2$, $IrCl(CO)(PH_3)_2$ and $RhH(CO)(PH_3)_2$. Bond length in Åand bond angle in degree. In parentheses are experimental values.

which the X (X = H or Cl) and CO ligands are at the axial positions, while two PH_3 ligands and the C-C bond of C_{60} are on the equatorial plane. This is because anion and strongly donating ligands tend to take a position on the C_{3v} axis but either electron-withdrawing ligand and less donating one tend to take a position on the equatorial plane [33]. In **2**, the optimized Ir-C1 and C1-C2 distances agree well with the experimental values [17], as shown in Figure 2.1. In **3**, the Rh-C1 and C1-C2 distances also agree well with the experimental values [18]. The C1-C2 bond distance becomes longer in the order **3** $<$ **2** $<$ **1**. Consistent with this longer C1-C2 distances of **1** and **2** than that of **3**, the Ir-C1 and Ir-C2 distances of **1** and **2** are shorter than those of **3** [34]. Although the C1-C2 distance is similar in **1** and **2**, the Ir-C1 and Ir-C2 distances of **1** are shorter than those of **2**. These results suggest that C_{60} more strongly

coordinates with the Ir center in **1** than in **3**, and in **1** than in **2**, as will be discussed below in more detail. Although moderate deviations of the optimized geometries from the experimental ones [17, 18] are observed in the M-P distance [35], it is likely that reliable discussion of the coordinate bond of C_{60} can be presented on the basis of the optimized geometries here because the geometry of the M-C_{60} moiety is reproduced well by the optimization.

Geometry changes induced by the coordination with C_{60} are worthy of note. In all these complexes, the Ir-P distance becomes longer than that of $IrX(CO)(PH_3)_2$, as shown in Figure 2.1. In 2, the Ir-Cl distance becomes somewhat longer than that of $IrCl(CO)(PH_3)_2$, while the Ir-CO distance little changes by the coordination with C_{60}. The similar geometry changes are observed in the ethylene analogue. In **1** and **3**, on the other hand, the M-H distance becomes moderately shorter than those of $MH(CO)(PH_3)_2$, while the M-P and M-CO distances become longer by the coordination with C_{60}. The lengthening of the M-P distance by the C_{60} coordination is easily understood in terms of the interaction between the lone pair orbital of PH_3 and the d orbital of the metal center in the trigonal bipyramidal d^8 metal complex, as follows: in the trigonal bipyramidal d^8 metal complex, only one d_{z^2} orbital along the C_{3v} axis is empty and the others are doubly occupied, as shown in Figure 2.2. The lone pair orbital of phosphine overlaps with the empty dr orbital in square planar structure, as shown in Figure 2.2, but it must overlap well with the doubly-occupied dxy and $d_{x^2-y^2}$ orbitals in the trigonal bipyramidal structure, to induce four-electron repulsion with these occupied d orbitals, as shown in Figure 2.2. As a result, the M-P distance becomes longer in the trigonal bipyramidal d^8 metal complex. The lengthening of the M-CO distance by the C_{60} coordination in **1** and **3** is also interpreted in terms that the strong π-back donation from the M center to C_{60} weakens the π-back donation from the M center to CO; see the discussion below for the strong π-back donation to C_{60}. In **2**, however, the Ir-CO distance little changes upon the coordination with C_{60} unlike those of **1** and **3**. This unexpected result is related to the Ir-Cl bond lengthening in **2**, as follows: The lengthening of the M-Cl bond of **2** is in contrast to the shortening of the M-H bonds of **1** and **3**. In the trigonal bipyramidal d^8 metal complex, one d_σ orbital interacts with two axial ligands, as shown in Figure 2.2, while it interacts with four ligands in the square planar structure (Figure

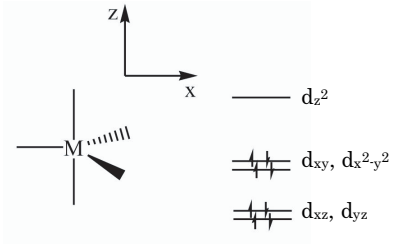

(A) d orbital occupation of d^8 trigonal bypyramidal complex.

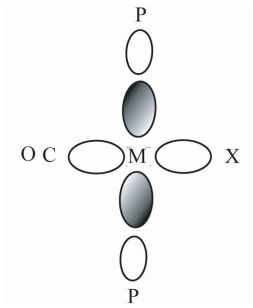

(B) Bonding interaction of phosphine lone pair orbitals with empty d_σ

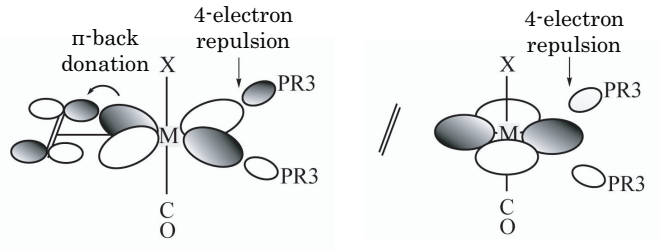

(C) Antibonding overlap of phosphine lone pair orbitals with doubly occupied d_{xy} and $d_{x^2-y^2}$ orbitals in d^8 trigonal bypyramidal complex.

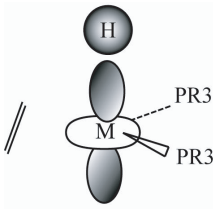

(D) Bonding interaction between H 1S and M d_{z^2} orbitals.

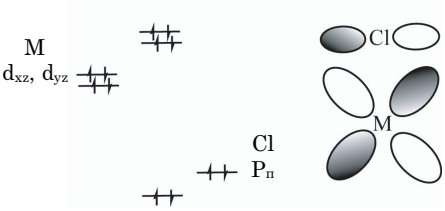

(E) The d_π–P_π anti-bonding interaction between M and Cl in trigonal bipyramidal d^8 complex.

Figure 2.2: (a) d orbital occupation of d^8 trigonal bipyramidal complex. (b) Bonding interaction of phosphine lone pair orbitals with empty d_σ orbital. (c) Anti-bonding overlap of phosphine lone pair orbitals with doubly-occupied dxy and $d_{x^2-y^2}$ orbitals in d^8 trigonal bipyramidal complex. (d) Bonding interaction between H 1s and M d_{z^2} orbitals. (e) The d_π-p_π anti-bonding interaction between M and Cl in trigonal bipyramidal d^8 complex.

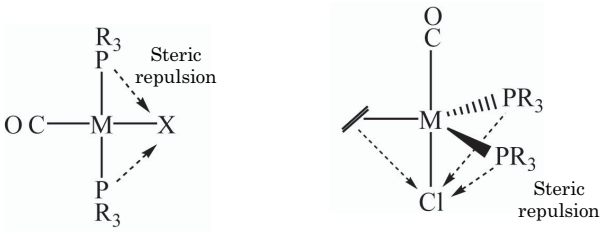

Figure 2.3: Illustration of steric repulsion.

2.2). As a result, the M-H distance becomes shorter in the trigonal bipyramidal d^8 complex than in the square planar complex. Contrary to the above discussion, the Ir-Cl distance becomes longer in the trigonal bipyramidal C_{60} complex than in the square planar complex. The similar lengthening of the Ir-Cl bond is observed in $IrCl(CO)(PH_3)_2(C_2H_4)$ in which the Ir-Cl distance lengthens by 0.06 Å. The Cl ligand is different from the H ligand in the larger size and the presence of doubly-occupied pp orbitals. Considering that the doubly-occupied pp orbitals of Cl overlap with the doubly-occupied d_{xz} and d_{yz} orbitals in an anti-bonding way (see Figure 2.2) but not with the d_{xy} orbital which mainly participates in the π-back donation from the M center to C_{60}, the π-back donation does not influence very much the M-Cl bond distance. This means that the other factor should be responsible for the lengthening of the M-Cl bond. One of such candidates is the steric repulsion of the large Cl ligand with the other ligands; Cl suffers from steric repulsion with two phosphine ligands in the square planar complex but from steric repulsion with C_{60} (or C_2H_4) in addition to two phosphine ligands in the trigonal bipyramidal complex, as shown in Figure 2.3. In the case of the less bulky H ligand, on the other hand, it is likely that the bonding interaction with the dr orbital plays more important role to shorten the Ir-H bond rather than the steric repulsion lengthens the Ir-H bond in the trigonal bipyramidal structure. Such Ir-Cl bond lengthening of **2** leads to the strengthening of the Ir-CO bond, which compensates the Ir-CO bond weakening by the π-back donation to C_{60}. As a result, the Ir-CO bond distance little changes by coordination with C_{60} in **2**.

Table 2.1: Binding energy (BE in kcal/mol) of $IrH(CO)(PH_3)_2(C_{60})$ (**1**), $IrCl(CO)(PH_3)_2(C_{60})$ (**2**), $RhH(CO)(PH_3)_2(C_{60})$ (**3**), and their ethylene analogues

	1	**2**	**3**	$Pt(PH_3)_2(C_{60})$
	C_{60} complexes			
B3LYP/BS-2	16.1	2.5	8.3	14.2
B3LYP/BS-3	16.9	3.1	8.8	14.9
MP2/BS-2	63.1	49.3	57.2	50.0
MP2/BS-3	68.0	53.4	60.2	55.0
ONIOM(MP2/BS-2:UFF)	61.3	47.4	55.8	48.5
ONIOM(MP4(SDQ)/BS-2:UFF)	54.9	39.9	45.5	42.8
ONIOM(MP2/BS-3:UFF)	65.9	51.1	58.6	53.2
ONIOM(MP4(SDQ)/BS-3:UFF)	[59.4][a]	[43.5][a]	[48.2][a]	[47.5][a]
	1'[b]	**2'**[b]	**3'**[b]	$Pt(PH_3)_2(C_2H_4)$
	C_2H_4 complexes			
B3LYP/BS-2	16.5	8.8	7.9	13.0
B3LYP/BS-3	18.4	10.6	9.1	15.0
MP2/BS-2	37.5	27.5	28.6	33.2
MP2/BS-3	44.7	34.3	33.2	33.5
MP3	26.1	17.6	12.8	19.7
MP4(DQ)	34.3	24.6	23.3	23.2
MP4(SDQ)	33.8	24.9	24.2	24.2
CCSD(T)	32.4	24.1	-	24.3

a) The binding energy at the ONIOM(MP4(SDQ)/BS-3:UFF) level was estimated from the ONIOM(MP4(SDQ)/BS-2:UFF)-calculated binding energy by adding the basis set effects on the binding energy (Δ E) which was evaluated at the MP2 level, as follows: ΔE = BE[ONIOM(MP2/BS-3:UFF)] - BE[OINOM(MP2/BS-2:UFF)].
b) Abbreviations, **1'**, **2'**, and **3'** represent ethylene analogues of **1**, **2**, and **3**, respectively.

2.3.2 Binding energies of $IrH(CO)(PH_3)_2(C_{60})$ (1), $IrCl(CO)(PH_3)_2(C_{60})$ (2), and $RhH(CO)(PH_3)_2(C_{60})$ (3)

As shown in Table Figure 2.1, the DFT-calculated binding energies (BE) are much smaller than the MP2-calculated ones in all these complexes, as reported previously [26]. Although the basis sets used here are not extremely good, the BE values are not different very much between the MP2/BS-2 and MP2/BS-3 calculations. In our previous theoretical work, the basis set effects on the BE value were carefully examined in $Pt(PH_3)_2(C_2H_4)$, which indicated that the BE value little changed upon going to BS-3 from BS-2 [26]. Also, we found that the MP4(SDQ)/BS-3 and CCSD(T)/BS-3 methods presented almost the same BE value

in $Pt(PH_3)_2(C_2H_4)$ [26]. As shown in Table 1, the BE values of $IrH(CO)(PH_3)_2(C_2H_4)$ **1'**, $IrCl(CO)(PH_3)_2$-(C_2H_4) **2'**, and $RhH(CO)(PH_3)_2(C_2H_4)$ **3'** moderately fluctuate at MP2/BS-3 and MP3/BS-3 levels but converge upon going to MP4(SDQ)/BS-3 from MP3/BS-3 and almost the same binding energy was calculated with the MP4(SDQ)/BS-3 and CCSD(T)/BS-3 methods, as reported previously in $Pt(PH_3)_2(C_2H_4)$ [26]. From these results, it is reasonably concluded that the MP4(SDQ)/BS-3 method presents reliable BE values in these Ir(I) and Rh(I) complexes.

However, we could not perform MP4(SDQ)/BS-3 calculations of $MX(CO)(PH_3)_2(C_{60})$ because of the very large size. Although the ONIOM method is useful to evaluate the binding energy of large system, the ONIOM(MP4-(SDQ)/BS-3:UFF) method could not be applied to these complexes due to their large sizes, too. Thus, we evaluated the binding energies of these complexes with the ONIOM(MP4(SDQ)/BS-2:UFF) method and then made correction of basis set effects by considering the difference in the BE value between ONIOM(MP2/BS-2:UFF) and ONIOM(MP2/BS-3:UFF) calculations. The reliability of this procedure was clearly shown in our previous work [26]. This calculated BE values are given in brackets of Table 2.1. Apparently, the BE values of these Ir and Rh complexes of C_{60} are much larger than those of the ethylene analogues. This is because the π^* orbital of C_{60} is at much lower energy than that of ethylene, as reported [26]. Also, it is noted that the BE value decreases in the order **1** $>$ **3** $>$ **2**; in other words, the hydride complex and the Ir complex yields larger BE value than the chloride complex and the Rh complex, respectively. The factors to determine the BE values will be discussed below.

2.3.3 Electron population changes by coordination with C_{60}

The electron population of the metal moiety considerably decreases and that of the C_{60} moiety considerably increases (see Table 2.2). In particular, the metal d orbital population considerably decreases. On the other hand, the atomic population of metal center considerably increases. These population changes clearly show that the π-back donation predominantly participates in the coordinate bond of C_{60}, as reported previously in $M(PH_3)_2(C_{60})$ and also

Table 2.2: Population changes[a] by coordination of C_{60} with the Ir center

	1	**2**	**3**
C_{60}	0.162	0.092	0.214
Ir	0.258	0.269	0.234
d	-0.149	-0.113	-0.198
CO	-0.146	-0.158	-0.115
H or Cl	-0.110	-0.070	-0.101
PH_3	-0.091	-0.067	-0.116

a) Relative to $MX(CO)(PH_3)_2$ with distorted geometry taken in the total complex.

that the σ-donation from CO and PH_3 to the s and p orbitals of the metal center is enhanced by the coordination of C_{60}. The importance of the π-back donation is clearly shown by the orbital picture, as shown in Figure 2.4, in which the π^* orbital of C_{60} overlaps well with the dp orbital of the metal center in these complexes.

The charge transfer from the metal moiety to C_{60} decreases in the order **3** $>$ **1** $>$ **2**, which is parallel to the decreasing order of the metal d orbital population. However, it is somewhat different from the decreasing order of the BE value and the d_π orbital energy, unexpectedly; see Tables 1 and 3 for the BE value and dp orbital energy, respectively. These results request us to investigate the relation between the binding energy and the coordinate bonding nature, in more detail.

2.3.4 Relation between binding energy (BE) and d orbital energy

The binding energy (BE) decreases in the order **1** $>$ **3** $>$ **2**, as mentioned above, which agrees with the decreasing order of the dp orbital energy $\epsilon(d_\pi)$ of $MX(CO)(PH_3)_2$ taking the same structure as that in the total complex, as shown in Table 2.3. This result seemingly indicates that the π-back donation from the metal center to C_{60} plays an important role and the d_{pi} orbital energy is a key factor to determine the binding energy. However, the discrepancy between the trend of the BE value and that of the electron population of C_{60} is observed, as discussed above.

Here, the intrinsic binding energy (E_{INT}) is defined as stabilization energy by the interaction between C_{60} and $MX(CO)(PH_3)_2$ taking the distorted geometry in the total complex, and the

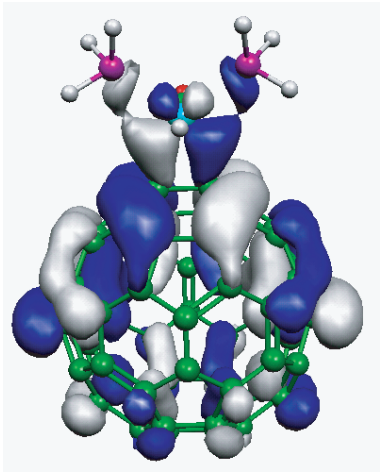

$IrH(CO)(PH_3)_2(C_{60})$

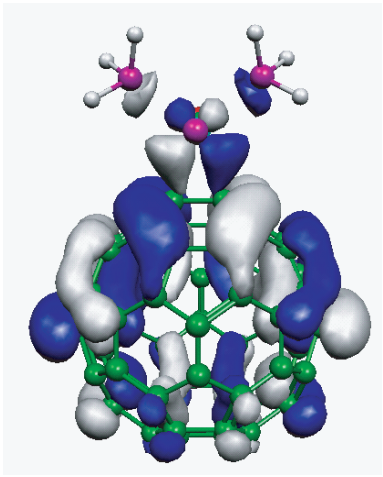

$IrCl(CO)(PH_3)_2(C_{60})$

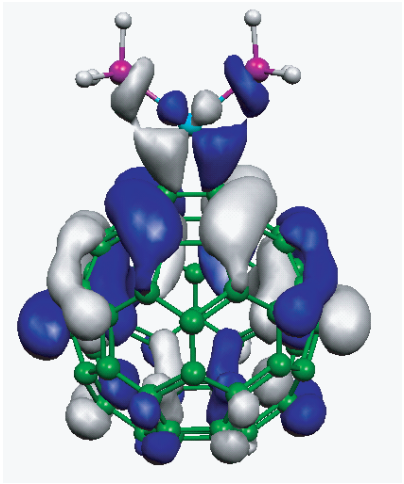

$Pt(PH_3)_2(C_{60})$

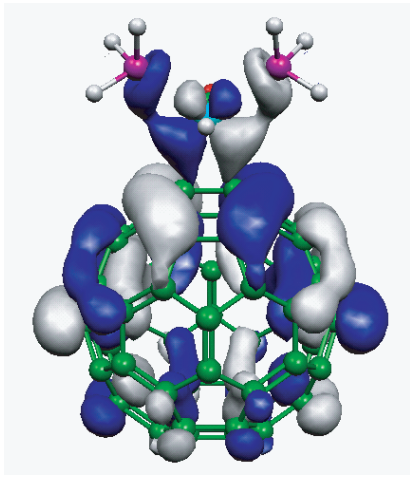

$RhH(CO)(PH_3)_2(C_{60})$

Figure 2.4: Orbital pictures of π-back donation. Note: Kohn-Sham orbital (DFT/BS-III).

Table 2.3: Intrinsic interaction energy (E_{INT})[a] of MX(CO)(PH_3)$_2$(C_{60}), and distortion energy (E_{DIST})[b] and dp orbital energy[c] of MX(CO)(PH_3)$_2$

	IrH(CO)(PH_3)$_2$	IrCl(CO)(PH_3)$_2$	RhH(CO)(PH_3)$_2$	Pt(PH_3)$_2$
E^a_{INT}	97.0	90.0	75.8	83.4
E^b_{DIST}	37.6	46.5	27.6	35.9
ϵ(d_π)	-7.04	-7.76	-7.66	-6.72
	(-4.51)	(-4.98)	(-4.71)	(-4.37)
ϵ(d_σ)	1.15	0.79	1.34	1.46
	(-2.32)	(-2.87)	(-1.98)	(-1.73)
Square of LCMO coefficient in the occupied space of MX(CO)(PH_3)$_2$(C_{60})[d]				
π HOMO - 6	0.888	0.877	0.924	0.909
	(0.952)	(0.945)	(0.984)	(0.961)
HOMO - 9	0.903	0.884	0.933	0.926
	(0.915)	(0.911)	(0.949)	(0.941)
π^* LUMO	0.152	0.129	0.107	0.135
	(0.130)	(0.104)	(0.077)	(0.120)
LUMO + 3	0.061	0.056	0.045	0.058
	(0.068)	(0.058)	(0.044)	(0.064)
LUMO + 6	0.030	0.031	0.023	0.031
	(0.042)	(0.039)	(0.029)	(0.043)

a) Stabilization energy (in kcal/mol) of MX(CO)(PH_3)$_2$(C_{60}) relative to the sum of C_{60} and the distorted MX(CO)(PH_3)$_2$ taken in the total complex, where the MP4(SDQ) method was employed.
b) Destabilization energy (in kcal/mol) of MX(CO)(PH_3)$_2$ is the energy difference between the equilibrium structure and the distorted one taken in the total complex, where the MP4(SDQ) method was employed.
c) Hartree-Fock orbital energy (in eV) of MX(CO)(PH_3)$_2$ with the distorted structure taken in the total complex. In parentheses are Kohn-Sham orbital energies.
d) Kohn-Sham orbitals were analyzed. In parentheses are results from Hartree-Fock orbitals.

distortion energy (E_{DIST}) is defined as destabilization energy of MX(CO)(PH_3)$_2$ upon going from the equilibrium geometry to the distorted one taken in the total complex. The BE value is the sum of E_{INT} and E_{DIST}, BE = E_{INT} + E_{DIST}. The E_{INT} value directly relates to the dp orbital energy of the distorted MX(CO)(PH_3)$_2$, if the π-back donation predominantly contributes to the coordinate bond. However, the E_{INT} value decreases in the order **1** $>$ **2** $>$ **3**, whereas the dp orbital lowers in energy in the order **1** $>$ **3** $>$ **2**. This disagreement indicates that not only dp orbital energy but also the other factor is responsible for the interaction. One of the candidates is the orbital overlap S(d_π -π^*) between the d orbital of the metal center and the π^* orbital of C_{60} [36]. Actually, the S(d_π -π^*) value of **3** is much smaller than those of **1** and **2**; S(d_π -π_1^*) is 0.146, 0.131, and 0.111 for **1**, **2**, and **3**, respectively, where π_1^* is LUMO of C_{60}. This is because the 5d orbital more expands than the 4d orbital in general [37]. The larger S(d_π-π^*) value of **2** leads to the stronger coordinate bond of **2** than that of **3**. As a result, the E_{INT} value of **2** is much larger than that of **3**. In spite of this large E_{INT} value of **2**, the BE value of **2** is smaller than that of **3**. This is because E_{DIST} value of **2** is much larger than that of **3**. Although the details are ambiguous, it is likely that the large E_{DIST} value in **2** is attributed to the considerable lengthening of the Ir-Cl bond upon going to the distorted geometry in **2** from the equilibrium one; remember that the M-H bond moderately shortens in **1** and **3** but the Ir-Cl bond considerably lengthens in **2** compared to that of IrCl(CO)(PH_3)$_2$.

Summarizing the above discussion, the E_{INT} value of **2** is considerably larger than that of **3** because of the large overlap S(d_π-π^*), despite of the low dp orbital energy. However, the large E_{DIST} value decreases very much the BE value. The BE and E_{INT} values of 1 are the largest in these complexes because of the highest dp orbital energy, the largest S(d_π-π_1^*) value, and the smallest E_{DIST} value which arises from the small size of H.

It is necessary to clarify the reason that the population increase of C_{60} is the largest in **3** but the E_{INT} value is the smallest in **3**, whereas the dp orbital of RhH(CO)(PH_3)$_2$ is at much lower energy than that of IrH(CO)(PH_3)$_2$. This means that not the back donation but the other factor leads to the largest negative charge of C_{60} in **3**. One important characteristic features of MX(CO)(PH_3)$_2$ is the presence of the unoccupied dr orbital unlike M(PH_3)$_2$. This d_σ orbital

contributes to the σ donation from C_{60} to the M center in $MX(CO)(PR_3)_2(C_{60})$. We evaluated how much π and π^* orbitals of C_{60} participate in the occupied space of $MX(CO)(PH_3)_2(C_{60})$ by representing the molecular orbitals of $MX(CO)(PH_3)_2(C_{60})$ as linear combinations of molecular orbitals of fragments, $MX(CO)(PH_3)_2$ and C_{60} [38]. As shown in Table 3, the sum of the squares of coefficients of the π^* orbital decreases in the order **1** $>$ **2** $>$ **3**, and the sum of the squares of coefficients of the p orbital increases in the order **2** $<$ **1** $<$ **3**. These results suggest that the pback donation is the strongest in **1** but the σ-donation of **2** is moderately stronger than that of 1 [39]. This is because the dp and dr orbitals of $IrH(CO)(PH_3)_2$ are at higher energies than those of the Cl analogue, as shown in Table 3. The larger E_{INT} value of **1** than that of **2** indicates that the π-back donation is more important than the σ-donation. Interestingly, both the σ-donation and the π-back donation are the weakest in **3**. This means that the large electron population of C_{60} in **3** results from the weakest σ-donation from C_{60} to the M center, which leads to the smallest E_{INT} value of **3**. The weakest π-back donation arises from the facts that S(d_π-π^*) value of **3** is smaller than those of **1** and **2** and the d_π orbital is at lower energy in **3** than in **1**. The weakest σ-donation is interpreted in terms of the d_σ orbital at high energy and the small overlap between the d_σ orbital and the π orbital of C_{60}; note that the S(d_σ-π) value is parallel to the S(d_π-π^*) value; S(d_σ-π^1) is 0.114, 0.112, and 0.090 for **1**, **2**, and **3**, respectively, where π^1 is HOMO of C_{60}.

Also, this analysis clearly shows the interesting difference between $M(PH_3)_2(C_{60})$ and $MX(CO)(PH_3)_2(C_{60})$, as follows: Interestingly, the E_{INT} value of $Pt(PH_3)_2(C_{60})$ is smaller than that of $IrX(CO)(PH_3)_2(C_{60})$ despite of the dp orbital of $Pt(PH_3)_2$ at higher energy than that of $IrX(CO)(PH_3)_2$. Apparently, the sum of the squares of the π orbitals in $Pt(PH_3)_2(C_{60})$ are much larger than those in **1** and **2**, indicating the very weak σ-donation from C_{60} to $Pt(PH_3)_2$. This is because $Pt(PH_3)_2$ does not have empty dr orbital unlike $IrX(CO)(PH_3)_2$. The presence of doublyoccupied dσ orbital also disfavors the coordination of C_{60} with the Pt center due to four-electron repulsion between d_σ orbital of Pt and π orbital of C_{60}. In other words, the smaller E_{INT} value of $Pt(PH_3)_2(C_{60})$ than that of IrX $(CO)(PH_3)_2(C_{60})$ is attributed to the absence of empty d_σ orbital.

2.4 Conclusion

The MP2 toMP4(SDQ) and DFT methods were applied to IrH(CO)(PH_3)$_2$(C_{60}) (**1**), IrCl(CO)-(PH_3)$_2$(C_{60}) (**2**), and RhH(CO)(PH_3)$_2$(C_{60}) (**3**), to estimate their binding energies and clarify the bonding nature. The DFT method presents much smaller binding energies than the MP2 method, as reported previously [26]; for instance, the binding energy of **1** was evaluated to be 16.9 kcal/mol with the DFT/BS-3 method but 68.0 kcal/mol by the MP2/BS-3 method [26].

The binding energies of **1**, **2**, and **3** were evaluated to be 59.4, 43.5, and 48.2 kcal/mol, respectively, with the ONIOM(MP4(SDQ)/BS-3:UFF) method, where the basis set effects upon going to BS-3 from BS-2 were evaluated at the MP2 level. This decreasing order is different from that of the E_{INT} value **1** $>$ **2** $>$ **3**. The E_{INT} value is easily interpreted in terms of π-back donation and σ-donation; in **3**, both π-back donation and σ-donation are the weakest, which leads to the smallest E_{INT} value. The weakest π-back donation of **3** arises from the less expansion of the d orbital and the d_π orbital at the low energy. The weakest σ-donation is due to the d_σ orbital at the high energy and the less expansion of the d orbital. The E_{INT} value of **2** is much larger than that of **3**, which arises from the larger expansion of the d orbital. However, the larger E_{DIST} value leads to the smaller BE value of **2** than that of **3**. The largest BE and E_{INT} values of **1** are interpreted in terms of the d_π orbital at the highest energy and the largest overlap S(d_π-π^*) value. The smaller BE and E_{INT} values of Pt(PH_3)$_2$(C_{60}) than that of **1** is interpreted in terms of the presence of the doubly-occupied dr orbital in the Pt(0) center.

Bibliography

[1] (a) Lee, K.; Seng, H.; Park, J. T. *Acc. Chem. Res.* **2003**, *36*, 78. (b) Nakamura, E.; Isobe, H. *Acc. Chem. Res.* **2003**, *36*, 807. (c) Balch, A.L.; Olmstead, M. N. *Chem. Rev.* **1998**, *98*, 2123.

[2] Hawkins, J. M.; Meyer, A.; Lewis, T. A.; Loren, S.; Hollander, F. J. *Science* **1991**, *252*, 312.

[3] (a) P.J. Fagan, J.C. Calabrese, B. Malone, *Science* **1911**, *252*, 1160. (b) P.J. Fagan, J.C. Calabrese, B. Malone, *J. Am. Chem. Soc.* **1991**, *113*, 9408.

[4] V.V. Bashilov, P.V. Petrovskii, V.I. Sokolov, S.V. Lindeman, I.A. Guzey, Y.T. Struckkov, *Ø* **1993**, *12*, 991.

[5] H. Nagashima, H. Yamaguchi, Y. Kato, Y. Saito, M. Haga, K. Itoh, *Chem. Lett.* **1993**, *212153*

[6] (a) L.C. Song, .J.T. Liu, Q.M. Hu, L.H. Weng, *Organometallics* **2000**, *19*, 1643. (b) L.C. Song, J.T. Liu, Q.M. Hu, G.F. Wang, P. Zanello, M. Fontani, *Organometallics* **2000**, *19*, 5342.and references therein for the reports before about 2000.

[7] (a) A.J. Badcock, J. Li, K. Lee, J.R. Sharpley, *Organometallics* **2002**, *21*, 3940. (b) K. Lee, H. Song, B. Kim, J.T. Park, S. Park, M.-G. Choi, *J. Am. Chem. Soc.* **2002**, *100*, 2872.and references therein 2000-2002.

[8] (a) M. Sawamura, H. Iikura, E. Nakamura, *J. Am. Chem. Soc.* **1996**, *118*, 12850. (b) M. Sawamura, H. Iikura, A. Hirai, E. Nakamura, *J. Am. Chem. Soc.* **1998**, *120*, 8285. (c) M.

Sawamura, M. Toganoh, Y. Kuninobu, S. Kato, E. Nakamura, *Chem. Lett.* **2000**, *20*, 270. (d) M. Sawamura, H. Iikura, T. Ohama, U. Hackier, E. Nakamura, *J. Organomet. Chem.* **2000**, *599*, 32. (e) M. Sawamura, M. Toganoh, K. Suzuki, A. Hirai, H. Iikura, E. Nakamura, *Org. Lett.* **2000**, *2*, 1919. (f) M. Sawamura, Y. Kuninobu, M. Toganoh, Y. Matsuo, M. Yamanaka, E. Nakamura, *J. Am. Chem. Soc.* **2000**, *122*, 12407. (g) E. Nakamura, M. Sawamura, *Pure Appl. Chem.* **2001**, *73*, 355. (h) M. Sawamura, M. Toganoh, H. Iikura, Y. Matsuo, A. Hirai, E. Nakamura, *J. Mater. Chem.* **2002**, *12*, 2109. (i) M. Sawamura, Y. Kuninobu, M. Toganoh, M.Y. Matsuo, M. Yamanaka, E. Nakamura, *J. Am. Chem. Soc.* **2002**, *124*, 9354. (j) M. Tognoh, Y. Matsuo, E. Nakamura, *J. Am. Chem. Soc.* **2003**, *125*, 13974. (k) Y. Matsuo, E. Nakamura, *Organometallics* **2003**, *22*, 2554. (m) M. Tognoh, Y. Matsuo, E. Nakamura, *J. Organomet. Chem.* **2003**, *683*, 295. (o) Y. Kuninobu, Y. Matsuo, M. Tognoh, M. Sawamura, E. Nakamura, *Organometallics* **2004**, *23*, 3259.

[9] (a) D.L. Lichtenberger, L.L. Wright, N.E. Gruhn, M.E. Rempe, *Synth. Met.* **1993**, *59*, 353. (b) D.L. Lichtenberger, L.L. Wright, N.E. Gruhn, M.E. Rempe, *J. Organomet. Chem.* **1994**, *478*, 213.

[10] N. Koga, K. Morokuma, *Chem. Phys. Lett.* **1993**, *202*, 330.

[11] H. Fujimoto, Y. Nakao, K. Fukui, *J. Mol. Struct. (THEOCHEM)* **1993**, *300*, 425.

[12] C. Bo, M. Costas, J.M. Poblet, *J. Phys. Chem.* **1995**, *99*, 5914.

[13] J.A. Lopez, C. Mealli, *J. Organomet. Chem.* **1994**, *478*, 161.

[14] F. Nunzi, A. Sgamellotti, N. Re, C. Floriani, *Organometallics* **2000**, *19*, 1628.

[15] (a) J.R. Rogers, D.S. Marynick, *Chem. Phys. Lett.* **1993**, *205*, 197. (b) S.K. Goh, D.S. Marynick, *Int. J. Quantum Chem.* **2001**, *22*, 1881.

[16] E.D. Jemmis, M. Manoharan, P. Sharma, *Organometallics* **2000**, *19*, 1879.

[17] (a) A.L. Balch, V.J. Catalano, J.W. Lee, *Inorg. Chem.1991* **30**, *3980 (b) A.L. Balch*, .J.W. Lee, B.C. Noll, M.M. Olmstead, *J. Am. Chem. Soc.* **1992**, *114*, 10984. (c) A.L. Balch, J.W. Lee, B.C. Noll, M.M. Olmstead, *Inorg. Chem.* **1994**, *33*, 5238.

[18] A.L. Balch, J.W. Lee, B.C. Noll, M.M. Olmstead, *Inorg. Chem.* **1993**, *32*, 3577.

[19] (a) A.D. Becke, *Phys. Rev. A* **1988**, *38*, 3098. (b) A.D. Becke, *J. Chem. Phys.* **1983**, *98*, 5648.

[20] C. Lee, W. Yang, R.G. Parr, *Phys. Rev. B* **1988**, *37*, 785.

[21] P.J. Hay, W.R. Wadt, *J. Chem. Phys.* **1985**, *82*, 299.

[22] (a) R. Ditchfiled, W.J. Hehre, J.A. Pople, *J. Chem. Phys.* **1971**, *54*, 724. (b) P.C. Hariharan, J.A. Pople, *Mol. Phys.* **1974**, *27*, 209.

[23] M.M. Francl, W.J. Pietro, W.J. Hehre, J.S. Binkley, M.S. Gordon, D.J. DeFrees, J.A. Pople, *J. Chem. Phys.* **1982**, *77*, 3654.

[24] (a) T. Vreven, K. Morokuma, *J. Comput. Chem.* **2000**, *21*, 1419.and references therein. (b) F. Maseras, K. Morokuma, *J. Comput. Chem.* **1995**, *16*, 1170.

[25] A.K. Rappe, C.J. Casewit, K.S. Colwell, W.A. Goddard III, W.M. Skiff, *J. Am. Chem. Soc.* **1992**, *114*, 10024.

[26] Y. Kameno, A. Ikeda, Y. nakao, H. Sato, S. Sakaki, *J. Phys. Chem. A* **2005**, *109*, 8055.

[27] M. Couty, M.B. Hall, *J. Comput. Chem.* **1996**, *17*, 1359.

[28] A.W. Ehlers, M. Böhme, S. Dapprich, A. Gobbi, A. Höllwarth, V. Jonas, K.F. Köhler, R. Stegmann, A. Veldkamp, G. Frenking, *Chem. Phys. Lett.* **1993**, *208*, 111.

[29] W.R. Wadt, P.J. Hay, *J. Chem. Phys.* **1985**, *82*, 284.

[30] A. Höllwarth, M. Böhme, S. Dapprich, A.W. Ehlers, A. Gobbi, V. Jonas, K.F. Köhler, R. Stegmann, A. Veldkamp, G. Frenking, *Chem. Phys. Lett.* **1993**, *208*, 237.

[31] J.A. Pople et al., GAUSSIAN 98 and 03, Gaussian Inc., Pittsburgh, PA, 1998.

[32] G. Schaftenaar, J.H. Noordik, *J. Comput. Aided Mol. Des.* **2000**, *14*, 123.

[33] A.R. Ropssi, R. Hoffmann, *Inorg. Chem.* **1975**, *14*, 365.

[34] The Rh-C1 and Rh-C2 distances of **3** are slightly longer than the Ir-C1 and Ir-C2 distances of **2** in our calculation, which is consistent with the longer C1-C2 distance of **2** than that of **3**. However, the experimental workswith X-ray analysis reported that the Rh-C1 and Rh-C2 distances of $RhH(CO)(PMe_3)_2(C_{60})$ are longer than the Ir-C1 and Ir-C2 distances of $IrCl(CO)(PMe_3)_2(C_{60})$. This result seems against our expectation that the stronger M-C interaction leads to the shorter C-C distance.

[35] The M-P distance is overestimated here, because the d polarization function is omitted in the basis set for P to save the computation time.

[36] There are several important π^* orbitals which participate in the backdonation. For all those π^* orbitals, $S(d_\pi - \pi^*)$ values decrease in the order **1** $>$ **2** $>$ **3**. In evaluation of this overlap integral, the minimal basis set was employed for the metal atom.

[37] S. Fraga, K.M.S. Saxena, J. Karwowski, Handbook of Atomic Data, Elsevier, Amsterdam, 1976.

[38] H. Fujimoto, S. Kato, S. Yamabe, K. Fukui, *J. Chem. Phys.* **1974**, *60*, 572.

[39] Strictly speaking, not only charge transfer but also polarization changes the contributions of π and π^* orbitals in the occupied space. However, it is likely that π and π^* orbital populations change mainly due to the donation and back-donation interactions.

Part II

Developlement and Application of New Resonance Theory

Chapter 3

A New Analysis of Molecular Orbital Wave Functions Based on Resonance Theory

We have traditionally considered that molecules are built up of atoms that link each other through chemical bonding. The nature of the chemical bond has been discussed in terms of resonance between covalent and ionic-type interactions in many cases. The concepts of covalency, ionicity, and resonance still play important roles in chemistry, because these enable us to classify the various molecules according to the nature of the chemical bond. In this sense, it is highly desirable to present a method by which results of electronic structure calculations of molecules are interpreted with these chemical concepts.

Most of modern ab initio calculations are based on the molecular orbital (MO) method. However, it is hard to obtain the weights of covalency and ionicity from the wave function calculated by the MO method, because MOs are delocalized over the whole molecule, and the wave function is quite different from the valence bond wave function that directly describes covalent-ionic resonance. Various methods have been developed to make up for deficiencies in the MO method. Good examples are population analysis [1–3] and bond order indexes [4–6]. One goal of extension of these developments is to calculate the weights of each resonance structure from the wave function. Many evaluation methods of weights of resonance structures from the wave function have been developed over a long period.

The most important of this research [7] was reported by Hiberty *et al.* They constructed complete sets of valence bond wave functions from atomic orbital basis sets, and then, a Hartree-Fock (HF) wave function was expanded with these valence bond wave functions. This is one of

the important pioneering works, though not practical enough. Recently, natural resonance theory [8] (NRT), which was based on natural bond orbital (NBO) analysis, has been developed by Glendening and Weinhold. Additionally, Karafiloglou reported another method to calculate weights of resonance structures from NBO analysis [9].

In this paper, we would like to present a new method to calculate the weights of resonance structures from HF wave function. The range of application of the present method is limited to the molecular orbital wave functions in which each MO can be localized to either one- or two-center orbitals. At the present stage, it is difficult to apply the method to molecules involving more than three-center LMOs, such as conjugated molecules. However, for molecules for which the electronic structures are well localizable, the method is a simple and useful tool to link MOs with the concept of resonance.

First order density matrix $(\mathbf{PS})_{\mu\nu}$ of LCAO wave function $|\Psi\rangle$ is given by Eq. 3.1,

$$\begin{aligned}(\mathbf{PS})_{\mu\nu} &= \langle\Psi|\chi_\nu^+\psi_\mu^-|\Psi\rangle \\ &= 2\sum_i^{occ}\sum_n C_{i,\mu}C_{i,n}S_{n\nu}, \end{aligned} \tag{3.1}$$

where χ_ν^+ is creation operator related to atomic orbital (AO) basis χ_ν and ψ_μ^- is annihilation operator related to the biorthogonal AO basis ψ_μ. $\mathbf{C}_{i,\mu}$ is LCAO coefficient of MO i and $\mathbf{S}_{n\nu}$ is element of the overlap matrix.

$|\Psi\rangle$ is invariant to localization (unitary transformation) among doubly occupied orbitals. When we use localized MOs (LMOs) $\phi_i^{local} = \sum_{\mu=i}^{m} L_{i,\mu}\chi_\mu$, we can define local density matrices for the orbital i, as follows,

$$(\mathbf{PS})_{\mu\nu}^{local,i} = 2\sum_n L_{i,\mu}L_{i,n}S_{n\nu}. \tag{3.2}$$

It is noted that these local density matrices hold the idempotency and number of electrons is conserved in each LMO.

$$(\mathbf{PS})_{\mu\mu}^{local,i} = \frac{1}{2}\sum_\nu (\mathbf{PS})_{\mu\nu}^{local,i}(\mathbf{PS})_{\nu\mu}^{local,i} \tag{3.3}$$

$$2 = \sum_\mu (\mathbf{PS})_{\mu\mu}^{local,i}. \tag{3.4}$$

According to Eqs. 3.3 and 3.4, we can obtain a simple equation,

$$\begin{aligned} 1 &= \frac{1}{4}\sum_{\mu}\sum_{\nu}(\mathbf{PS})^{local,i}_{\mu\nu}(\mathbf{PS})^{local,i}_{\nu\mu} \\ &= \sum_{M}\sum_{N} w^{i}_{MN}. \end{aligned} \tag{3.5}$$

where $w^{i}_{MN} = \frac{1}{4}\sum_{\mu\in M}\sum_{\nu\in N}(\mathbf{PS})^{local,i}_{\mu\nu}(\mathbf{PS})^{local,i}_{\nu\mu}$. It is important that $(\mathbf{PS})^{local,i}_{\mu\nu} \times (\mathbf{PS})^{local,i}_{\nu\mu}$ is the expectation value of operator, $\chi^{\sigma_1+}_{\nu}\chi^{\sigma_2+}_{\mu}\psi^{\sigma_2-}_{\nu}\psi^{\sigma_1-}_{\mu}$, where σ_1 and σ_2 are spin variables ($\sigma_1 \neq \sigma_2$).

$$\frac{1}{4}(\mathbf{PS})^{local,i}_{\mu\nu}(\mathbf{PS})^{local,i}_{\nu\mu} = \langle\phi^{local}_{i}|\chi^{\sigma_1+}_{\nu}\chi^{\sigma_2+}_{\mu}\psi^{\sigma_2-}_{\nu}\psi^{\sigma_1-}_{\mu}|\phi^{local}_{i}\rangle \tag{3.6}$$

In the case of $\mu \neq \nu$, sum of $\frac{1}{4}(\mathbf{PS})^{local,i}_{\mu\nu}(\mathbf{PS})^{local,i}_{\nu\mu}$ and $\frac{1}{4}(\mathbf{PS})^{local,i}_{\nu\mu}(\mathbf{PS})^{local,i}_{\mu\nu}$ represents the weight of the state in which two electrons are singlet-coupled between AO μ and ν. In the case of $\mu = \nu$, $\frac{1}{4}(\mathbf{PS})^{local,i}_{\mu\mu}(\mathbf{PS})^{local,i}_{\mu\mu}$ is that of the state in which two electrons occupy the same AO μ. According to this interpretation, we can see that $2w^{i}_{MN} = w^{i}_{MN} + w^{i}_{NM}$ is the weight of the state in which two electrons in ϕ^{local}_{i} are shared between M and N atoms, and w^{i}_{MM} is that of the state in which two electrons in ϕ^{local}_{i} are belonging to atom M.

When ϕ^{local}_{i} is a two-center LMO between A and B atoms, two electrons are localized in the bond between A and B, and we can rewrite Eq. 3.5 as

$$\begin{aligned} 1 &= w^{i}_{AA} + 2w^{i}_{AB} + w^{i}_{BB} + \left\{ \begin{array}{l} all\ other\ N^{local,i}_{MN}, in\ which \\ (M,N)\ is\ not\ (A or B)\ at\ the\ same\ time. \end{array} \right\} \\ &= w^{i}_{AA} + 2w^{i}_{AB} + w^{i}_{BB} + \bar{w}^{i}. \end{aligned} \tag{3.7}$$

The term $\bar{w}^{i}$, sum of all terms in $\{\}$, is virtually very small as shown below. The weights of ionic and covalent bonds between A and B can be calculated by using Eq. 3.7. w^{i}_{AA} is the weight of the ionic structure ($A^{-}B^{+}$), w^{i}_{BB} is that of the ionic structure ($A^{+}B^{-}$), and $2w^{i}_{AB}$ is that of the covalent structure (A$-$B). If each MO can be localized into either one-center or two-center orbital and the property of bond described in LMOs can be regarded to be independent on each other, the weights of resonance structures of a whole molecule can be obtained by multiplication of the weights of the participating two-center bonding between two atoms.

$$1 = \prod_{i}^{LMOs}(w^{i}_{AA} + 2w^{i}_{AB} + w^{i}_{BB} + \bar{w}^{i}) \tag{3.8}$$

The choice of wi in each LMO i is actually related to choice of valence bond configuration. Because sum of the values in () is 1 in Eq. 3.8, the total sum of the weights calculated by the present procedure is always 1. It is confident that all the weights continuously and reasonably change with respect to nuclear coordinate even if the symmetry is broken.

This method was applied to H_2O, BH_3, and H_3O^+. Two two-center LMOs for H_2O and three for BH_3 and H_3O^+ are selected. All calculations were performed with the program code GAMESS modified by us.

At first, we apply the method to the H_2O (H1-O-H2) molecule using 6-31G(d,p) basis sets [10]. We obtained two two-center valence LMOs, ϕ_4^{local} and ϕ_5^{local}, and then calculated the weights of covalent and ionic bonds for OH1 and OH2. In the present case, Eq. 3.8 is written as

$$\begin{aligned} 1 = &(w_{OO}^4 + 2w_{OH1}^4 + w_{H1H1}^4 + \bar{w}^4) \\ &\times(w_{OO}^5 + 2w_{OH2}^5 + w_{H2H2}^5 + \bar{w}^5) \end{aligned} \tag{3.9}$$

For example, the weight of the structure $H1^+O^-{-}H2$ was obtained as $w_{OO}^4 \times 2w_{OH2}^5$ are shown in Table 3.1. "Other" represents the sum of all terms containing $\bar{w}$. The most important structure is $H^+O^-{-}H$ for which the weight is 0.399. The weights of the ionic structures which consist of O^-H^+ are larger than that of O^+H^-. This result agrees well with our chemical intuition. It is noted that the "Other " term is very small.

The results of BH_3 and H_3O^+ are shown in Table 3.2. The results by our method with STO-3G basis sets are in excellent agreement with those by Hiberty *et al.* Characteristic differences are observed between BH_3 and H_3O^+. In BH_3, the most important resonance structure consists of two covalent bonds ($B{-}H$) and one ionic (B^+H^-) bond. On the other hand, in H_3O^+, the most important resonance structure consists of one covalent bond ($O{-}H$) and two ionic bonds (O^-H^+). These results are consistent with the fact that the electronegativity of oxygen is larger than that of boron. In both, the results from various basis sets are little different. Thus, the weights computed by the present method minimally depend on the selection of basis sets.

In this paper, the method was used in conjunction with Mulliken type of $\mathbf{PS}$ matrices. However, the analysis by this method can be successfully combined with density matrices based on

Table 3.1: The weights of resonance structure in H_2O Computed with 6-31G(d,p)

	Weight
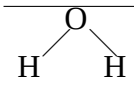	0.212
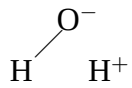	0.399
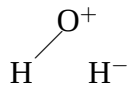	0.112
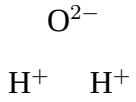	0.188
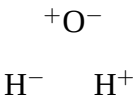	0.106
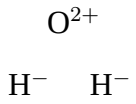	0.015
Other	-0.032
Total	1.000

Löwdin orbitals in the case of simple molecule. Both Löwdin and Mulliken types of density matrices produced qualitatively similar results. The comparison between two kinds of density matrices and the inspection of the basis set dependency will be presented in the forthcoming paper.

Table 3.2: Weights of Resonance Structures of BH_3 and H_3O^+ Calculated with Various Basis Sets. In each structure, upper and lower values represent X = B and X = O, respectively. BS1, BS2, BS3, and BS4 are, respectively, STO-3G, 6-31G, 6-31G(d,p), and 6-311G(d,p).

		Hiberty	BS1	BS2	BS3	BS4
1	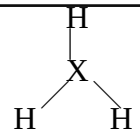	0.127	0.128	0.133	0.132	0.137
		0.086	0.077	0.038	0.057	0.067
2	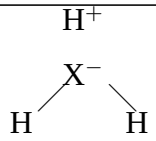	0.216	0.219	0.241	0.237	0.231
		0.045	0.048	0.015	0.029	0.039
3	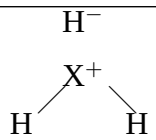	0.165	0.167	0.164	0.166	0.183
		0.291	0.279	0.214	0.248	0.259
4	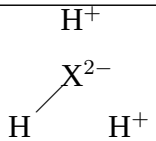	0.120	0.126	0.146	0.142	0.130
		0.006	0.010	0.002	0.005	0.008
5	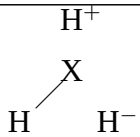	0.072	0.073	0.068	0.069	0.082
		0.333	0.334	0.402	0.363	0.334
6	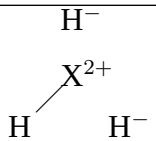	0.186	0.191	0.199	0.198	0.206
		0.114	0.116	0.057	0.085	0.101
7	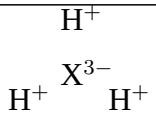	0.023	0.024	0.030	0.028	0.024
		0.000	0.001	0.000	0.000	0.000
8	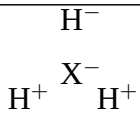	0.010	0.011	0.009	0.010	0.012
		0.127	0.134	0.252	0.177	0.143
9	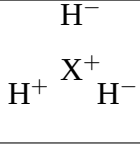	0.042	0.042	0.041	0.041	0.046
		0.072	0.070	0.053	0.062	0.065

Table 3.2:

		Hiberty	BS1	BS2	BS3	BS4
10	H^- X^{3+} H^- H^-	0.054	0.055	0.060	0.059	0.058
		0.012	0.012	0.004	0.007	0.010
	Other	-0.015	-0.035	-0.091	-0.084	-0.109
		-0.086	-0.081	-0.037	-0.032	-0.025
	Total	1.000	1.000	1.000	1.000	1.000
		1.000	1.000	1.000	1.000	1.000

Bibliography

[1] (a) Mulliken, R. S. *J. Chem. Phys.* **1955**, *23*, 1833.(b) Mulliken, R. S. *J. Chem. Phys.* **1955**, *23*, 1841.

[2] Löwdin, P. O. *J. Chem. Phys.* **1950**, *18*, 365.

[3] Reed, A. E.; Weinhold, F. *J. Chem. Phys.* **1985**, *83*, 1736.

[4] Wiberg, K. A. *Tetrahedron* **1966**, *24*, 1083.

[5] (a) Mayer, I. *Chem. Phys. Lett.* **1983**, *97*, 270. (b) Mayer, I. *Int. J. Quantum Chem.* **1983**, *23*, 341.

[6] Sannigrahi, A. B.; Kar, T. *Chem. Phys. Lett.* **1990**, *173*, 569.

[7] Hiberty, P.C.; Leforestier, C. *J. Am. Chem. Soc.* **1978**, *100*, 2012.

[8] Glendening, E. D.; Weinhold, F. *J. Comput. Chem.* **1998**, *19*, 593.

[9] Karafiloglou, P. *J. Comput. Chem.* **2001**, *22*, 306.

[10] Hariharan, P. C.; Pople, J. A. *Theoret. Chim. Acta* **1973**, *28*, 213.

Chapter 4

The Invariance of the Analysis Based on Resonance Theory. Dependence on Basis Set, Localization Scheme and Density Matrix.

4.1 Introduction

Undoubtedly, chemical bond is the central concept in chemistry. Valence bond (VB) method, which allows us to understand the chemical bond, is one of the most useful methods. The concepts of covalency, ionicity, and their resonance, which came from the VB method, play important roles in chemistry [1]. On the other hand, most of modern electronic structure theories are based on molecular orbital (MO) method. The wave functions obtained by MO calculation are quite different from those obtained by VB calculation. If VB-like characterization of MO wave function can be achieved, not only the total electron distribution and total energy but also the detailed bonding nature become available.

Several methods have been developed for such purpose. The pioneering work was reported by Hiberty *et al.* [2]. In their method, MO wave function is expanded into a complete set of VB type of wave functions which consist of determinants based on atomic orbitals (AOs). Weinhold *et al.* reported quite different method, called natural resonance theory (NRT) [3]. This is based on NBO analysis, in which superpositions of density matrices play key role. Karafiloglou reported another method, which is based on natural atomic orbitals [4]. CASVB by Robb *et al.* [5] and by Hirao and coworkers [6], which are based on CASSCF-type wave function, can offer similar information on a molecule.

Very recently, we reported a new method to evaluate the weights of resonance structures and

applied the method to solvated systems [7]. Our method is based on orbital localization and second quantization of singlet-coupling. The computational cost of the method is very low, and the results show excellent agreement with our chemical intuitions and results by Hiberty *et al.* [2]. When MOs can be well localized, the method is very useful to understand the results of MO calculations with the concept of resonance.

In our previous report [7], we introduced the method in conjunction with Mulliken-population related biorthogonal operator [8,9] and Boys-Foster [10] localization. In the present study, the formulation is generalized to Löwdin-population related operators [11]and the method is combined with various localizations. We take investigate the dependency of the results on the choice of operator types, localization schemes, and basis sets. Here, we take H_2, H_2O, NH_3 and H_2CO molecules for instance.

4.2 Method

The first order density matrix $(\mathbf{D})_{\mu\nu}$ of a wave function $|\Psi\rangle$ is given by Eq. 4.1,

$$(\mathbf{D})_{\mu\nu} = \langle\Psi|a_\nu^+ a_\mu^-|\Psi\rangle, \tag{4.1}$$

where a_ν^+ and a_μ^- are the creation and annihilation operators related to atomic orbitals (AOs) ν and μ, respectively [9].

$|\Psi\rangle$ is invariant to any unitary transformation among occupied orbitals. With localized MOs (LMOs) ϕ_i^{local}, we can define local density matrices (LDMs) for a LMO i ($i = 1, 2, \cdots$), as follows,

$$(\mathbf{D}^i)_{\mu\nu} = \langle\phi_i^{local}|a_\nu^+ a_\mu^-|\phi_i^{local}\rangle. \tag{4.2}$$

It is noted that these LDMs hold the idempotency and number of electrons is conserved in each LMO.

$$(\mathbf{D}^i)_{\mu\mu} = \frac{1}{2}\sum_\nu (\mathbf{D}^i)_{\mu\nu}(\mathbf{D}^i)_{\nu\mu} \tag{4.3}$$

$$2 = \sum_\mu (\mathbf{D}^i)_{\mu\mu}. \tag{4.4}$$

According to Eqs. 4.3 and 4.4, a simple equation is obtained,

$$\begin{aligned} 1 &= \frac{1}{4}\sum_{\mu}\sum_{\nu}(\mathbf{D}^i)_{\mu\nu}(\mathbf{D}^i)_{\nu\mu} \\ &= \sum_{M,N} W^i_{MN}, \end{aligned} \tag{4.5}$$

where M, N are atom labels and $W^i_{MN} = \frac{1}{4}\sum_{\mu\in M}\sum_{\nu\in N}(\mathbf{D}^i)_{\mu\nu}(\mathbf{D}^i)_{\nu\mu}$. Importantly, $(\mathbf{D}^i)_{\mu\nu}(\mathbf{D}^i)_{\nu\mu}$ is the expectation value of an operator, $a_\nu^{\sigma_1+}a_\mu^{\sigma_2+}a_\nu^{\sigma_2-}a_\mu^{\sigma_1-}$, where σ_1 and σ_2 are spin variables ($\sigma_1 \neq \sigma_2$).

$$\frac{1}{4}(\mathbf{D}^i)_{\mu\nu}(\mathbf{D}^i)_{\nu\mu} = \langle\phi_i^{local}|a_\nu^{\sigma_1+}a_\mu^{\sigma_2+}a_\nu^{\sigma_2-}a_\mu^{\sigma_1-}|\phi_i^{local}\rangle \tag{4.6}$$

In the case of $\mu \neq \nu$, the sum of $\frac{1}{4}(\mathbf{D}^i)_{\mu\nu}(\mathbf{D}^i)_{\nu\mu}$ and $\frac{1}{4}(\mathbf{D}^i)_{\nu\mu}(\mathbf{D}^i)_{\mu\nu}$ represents the weight of the state in which two electrons are singlet-coupled between AOs μ and ν. In the case of $\mu = \nu$, $\frac{1}{4}(\mathbf{D}^i)_{\mu\mu}(\mathbf{D}^i)_{\mu\mu}$ represents the weight of the state in which two electrons occupy the same AO μ. Thus, $2W^i_{MN} = W^i_{MN} + W^i_{NM}$ is considered as the weight of the state in which two electrons in ϕ_i^{local} are shared between M and N atoms, and W^i_{MM} is that of the state in which two electrons in ϕ_i^{local} are belonging to the atom M.

When ϕ_i^{local} is a two-center LMO between A and B atoms, two electrons are localized in the bond between A and B, and we can rewrite Eq. 4.5 to Eq. 4.7.

$$\begin{aligned} 1 &= W^i_{AA} + 2W^i_{AB} + W^i_{BB} + \left\{\begin{array}{l}\text{all other } W^i_{MN}\text{, in which} \\ (M,N) \text{ is not } (A \text{ or } B) \text{ at the same time.}\end{array}\right\} \\ &= W^i_{AA} + 2W^i_{AB} + W^i_{BB} + \bar{W}^i. \end{aligned} \tag{4.7}$$

$\bar{W}^i$, which is the sum of all the terms in braces, corresponds to many-body term and is virtually very small as will be shown below. The weights of ionic and covalent bonds between A and B can be calculated by Eq. 4.7. W^i_{AA} is the weight of the ionic structure (A^-B^+), W^i_{BB} is that of the ionic structure (A^+B^-), and $2W^i_{AB}$ is that of the covalent structure (A−B). If each MO can be localized into either one-center or two-center orbitals and the LMO character is independent on each other, the weights of resonance structures of a whole molecule can be presented by multiplications of the weights of the participating two-center bonding between two atoms.

$$1 = \prod_i^{LMOs}(W^i_{AA} + 2W^i_{AB} + W^i_{BB} + \bar{W}^i) \tag{4.8}$$

The sum of the weights including $\bar{W}^i$ is named many-body contribution because of its above mentioned origin. Since the sum of the terms in parenthesis is 1, normalization of all the weights is always garantied.

LDMs can be expressed with various AO basis. Both nonorthogonal AO and orthogonal AO based LDMs were examined in this study. In the former case, we used nonorthogonal AO creation operator χ_ν^+ and biorthogonal AO annihilation operator ϕ_μ^- [9]. In the latter case, the creation and annihilation operators, l_ν^+ and l_μ^-, related to Löwdin orbitals l_ν and l_μ were used. Using these operators, we can express both of LDMs of LMO i in overlap matrix $\mathbf{S}$ and local P-matrix $(\mathbf{P}^i)_{\mu\nu}$, as follows,

$$(\mathbf{D}^i)_{\mu\nu} = (\mathbf{P}^i\mathbf{S})_{\mu\nu} \quad (a_\nu^+ = \chi_\nu^+ \text{ and } a_\mu^- = \phi_\mu^-), \tag{4.9}$$

$$(\mathbf{D}^i)_{\mu\nu} = (\mathbf{S}^{\frac{1}{2}}\mathbf{P}^i\mathbf{S}^{\frac{1}{2}})_{\mu\nu} \quad (a_\nu^+ = l_\nu^+ \text{ and } a_\mu^- = l_\mu^-), \tag{4.10}$$

where $(\mathbf{P}^i)_{\mu\nu} = 2(\mathbf{C})_{\mu i}(\mathbf{C})_{\nu i}$ and $(\mathbf{C})_{\mu i}$ is the LCAO coefficient of LMO i. The former and the latter density matrices are Mulliken type and Löwdin type of LDMs, respectively [8] [11].

In this study, we compared the weights calculated by Boys-Foster (BF), Edmiston-Ruedenberg (ER) [12] and Pipek-Mezey (PM) [13] localizations. Hereafter, these weight were called BF-, ER- and PM-weights, respectively.

For all atoms, DZ, DZP, TZ, TZP and TZP+ basis sets were used [14]. Since Löwdin population analysis with 6d-orbitals is not rotationally invariant [15, 16], we used 5d-orbitals in all calculations.

All calculations were performed with program code GAMESS [17] modified by us.

4.3 Results and discussion

4.3.1 H_2: A trivial example.

At first, we calculated the weights of resonance structures of H_2, as a trivial example. In this case, we need not perform any orbital localization, because H_2 is a two-electron system. In all cases of basis sets and LDMs, the weight of covalent structure H−H was 50 % and that of ionic structure H^+H^- (and H^-H^+) was 50 %. Thus, our method reproduced the fact that

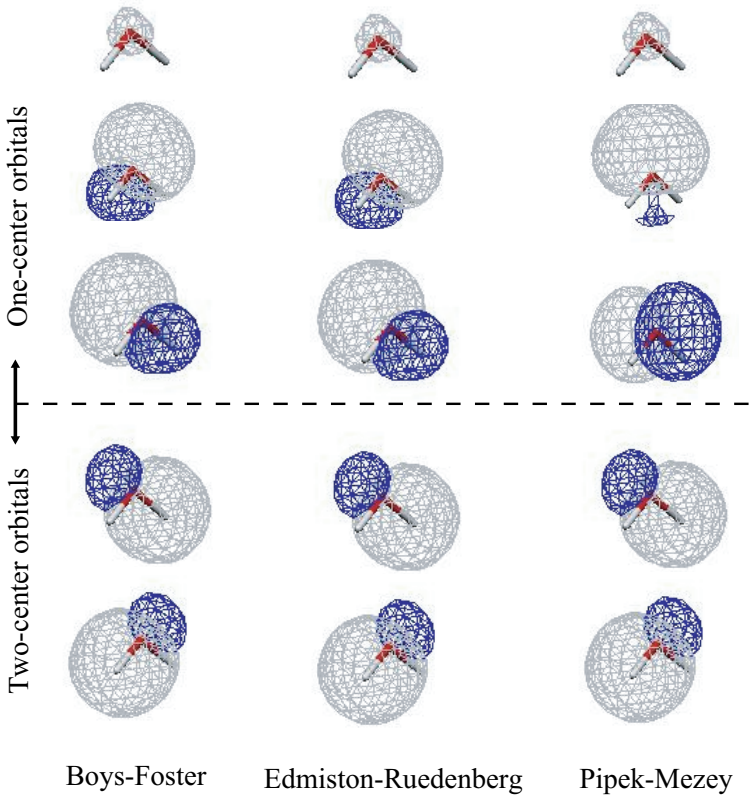

Figure 4.1: Three one-center and two two-center BF-, ER-, and PM-orbitals of H_2O. TZP basis sets were used.

HF wave function of H_2 is half-covalent and half-ionic. In the case of homonuclear diatomic molecule, the method is completely independent from the choice of basis set as well as atomic population analysis. It is noted that the population of H is 1 and the bond order is also 1, in all cases.

4.3.2 H_2O and NH_3

Next, we applied the method to H_2O molecule with various basis sets, localization schemes, and LDMs. BF, ER and PM orbitals of H_2O are shown in Fig. 4.1. Three one-center and two two-center orbitals were obtained by each localization method. In the case of one-center orbitals, PM localization method produces an in-plane lone pair orbital and an out-of-plane one, whereas BF and ER localizations produce two equivalent lone pair orbitals. On the other hand, in the case of two-center orbitals, BF, ER and PM localization methods present similar

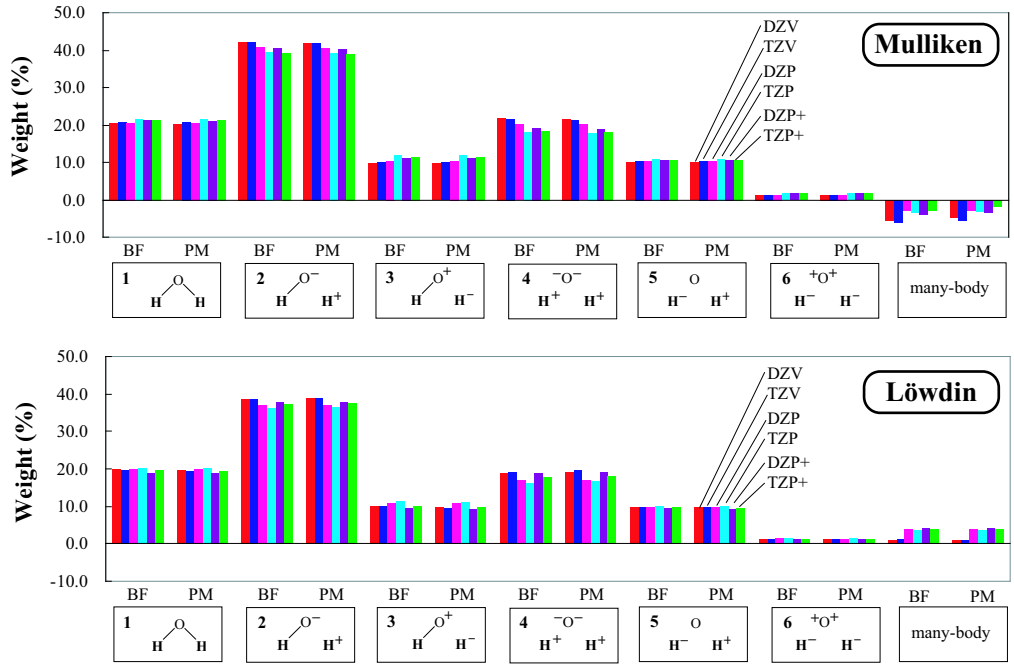

Figure 4.2: Weights (%) of resonance structures of H_2O evaluated with Mulliken and Löwdin LDMs.

localized orbitals.

In Fig. 4.2, the BF- and PM-weights calculated with various basis sets and LDMs are plotted. Because the differences between the BF- and ER-weights are less than 0.1 % in all the resonance structures, the ER-weights are omitted in the figure. In all cases, the most important resonance structure is **2**, in which one O-H bond is ionic and one is covalent. The totally covalent structure **1** is comparable with a totally ionic structure **4**.

The PM-weights are almost the same as BF-weights. This result is reasonable since BF, ER and PM two-center orbitals are similar. Thus, in the case of H_2O, the choice of localization schemes doesn't have a significant effect on the result. All basis sets provides almost similar results and the choice of basis sets also doesn't have a significant effect. The results calculated with Löwdin type of LDMs are essentially the same as those in the case of Mulliken type. The weights of **2** and **4** evaluated with Löwdin type of LDMs are slightly smaller than those with Mulliken type of LDMs. This difference is consistent with the result that the Löwdin populations on O atom is smaller than the Mulliken's one; Mulliken and Löwdin population

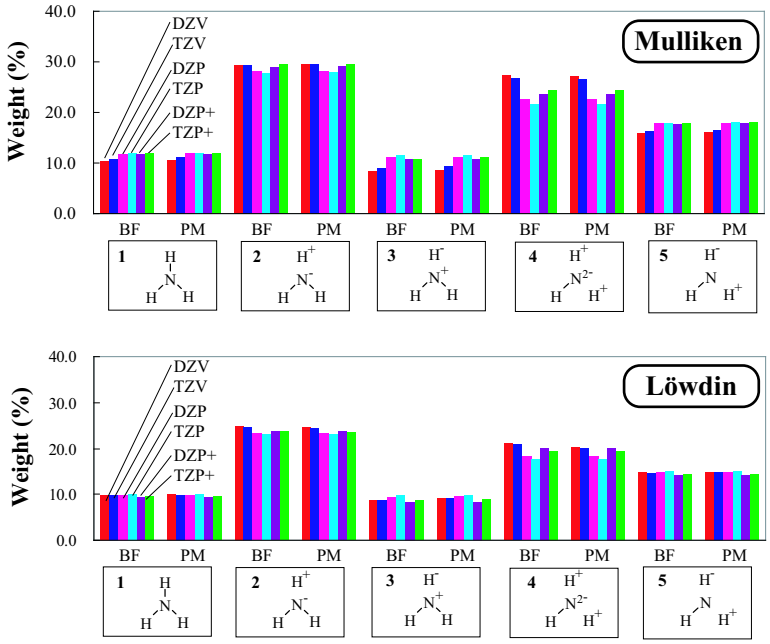

Figure 4.3: Weights (%) of important resonance structures of NH_3 evaluated with Mulliken and Löwdin LDMs.

calculated with TZP basis sets are 8.615 and 8.397, respectively. The 'many-body' term is negligible, like that of Mulliken type of LDMs, but positive, unlike that of Mulliken type of LDMs. This difference can be understood in terms of the fact that only Mulliken population analysis often gives negative population due to the non-orthogonality of AOs. However, it's to be noted that these differences are quite small and two LDMs provide essentially the same results, which means that the present procedure is virtually independent from the choice of LDMs.

NH_3 was also analyzed to examine the dependence on localization schemes, basis sets, and LDMs. The two-center orbitals obtained by BF, ER, and PM localizations are similar, as in the case of H_2O. The BF- and PM-weights were plotted in Fig. 4.3. In all cases, the most important resonance structure is **2**, which consists of two covalent (N−H) and one ionic (N^-H^+) bonds. Next is **4**, which consists of one covalent (N−H) and two ionic (N^-H^+) bonds.

The BF- and PM-weights are almost similar and all the basis sets present similar weights. In **2** and **4**, which have negative charged N atom, the weights calculated with Löwdin type

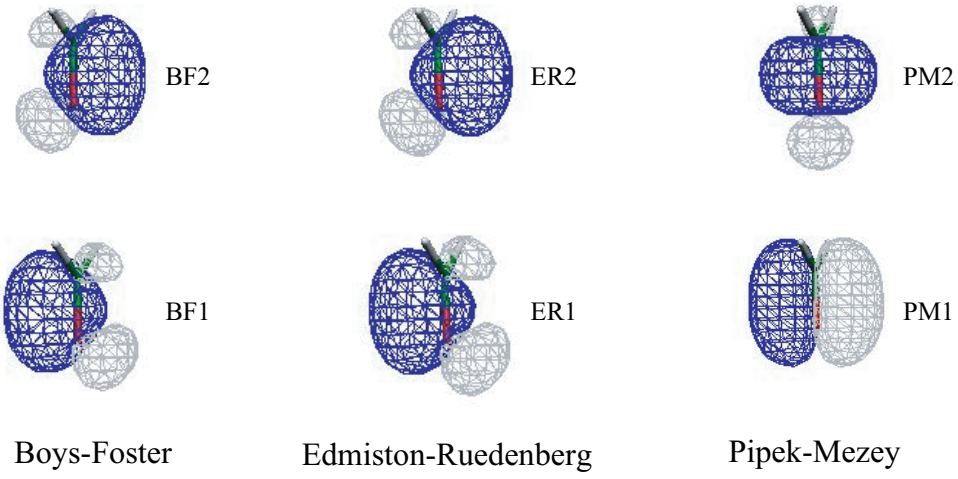

Figure 4.4: Two two-center BF-, ER-, and PM-orbitals of H_2CO, corresponding to C=O bond. TZP basis sets were used.

of LDMs are slightly smaller than those with Mulliken type of LDMs. All these results are similar to those of H_2O.

4.3.3 H_2CO

Finally, a double bond C=O in H_2CO is focused. In H_2O and NH_3, it's reasonable that BF-, ER-, and PM-weights are almost similar, because BF, ER and PM bonding orbitals are almost similar. However, in the case of double bond, BF and ER localization give two equivalent σ-π mixed orbitals (denorted by BF1, BF2, ER1, and ER2 in Fig. 4.4) and PM localization give one σ and one π orbital (denorted by PM1 and PM2 in Fig. 4.4). Therefore, it is not clear the analysis is independent from the choice of localization schemes.

In the present procedure, the weight of resonance structure is calculated by the products of the weights of covalent or ionic bonds. Table 4.1 shows the BF- and PM-weights, and thoes definitions. The PM-weights are almost the same as BF-weights, even in the case of H_2CO. For example, we focus the most important resonance structure **2**, which is composed from one ionic and one covalent bond. The BF- and PM-weights of **2** are 35.0 % and 35.6 %, respectively. As shown in Table 1, the weight of **2** was calculated as follows,

$$\text{The BF-weight of } C^+ - O^- \quad = \quad 2W_{CO}^{BF1} \times W_{OO}^{BF2} + W_{OO}^{BF1} \times 2W_{CO}^{BF2},$$

Table 4.1: The BF- and PM-weights (%) of resonance structure of H_2CO evaluated with Mulliken LDMs and TZP basis sets.

No.		BF	PM	
1	C=O	22.2	21.7	$= 2W^1_{CO} \times 2W^2_{CO}$
2	C^+-O^-	35.0	35.6	$= 2W^1_{CO} \times W^2_{OO} + W^1_{OO} \times 2W^2_{CO}$
3	C^--O^+	14.1	13.4	$= 2W^1_{CO} \times W^2_{CC} + W^1_{CC} \times 2W^2_{CO}$
4	$C^{2+}O^{2-}$	13.8	14.4	$= W^1_{OO} \times W^2_{OO}$
5	$C^{\pm}O^{\mp}$	11.1	11.2	$= W^1_{CC} \times W^2_{OO} + W^1_{OO} \times W^2_{CC}$
6	$C^{2-}O^{2+}$	2.2	2.1	$= W^1_{CC} \times W^2_{CC}$
	many-body	1.6	1.7	
	total	100.0	100.0	

Table 4.2: The weights (%) of covalent and ionic bond in H_2CO calculated by using BF1, BF2, PM1 and PM2 orbitals. Mulliken LDMs and TZP basis sets were used.

	W_{CC}	$2W_{CO}$	W_{OO}
BF1	14.9	47.1	37.2
BF2	14.9	47.1	37.2
PM1	16.5	47.9	34.7
PM2	12.4	45.4	41.4

$$\text{The PM-weight of } C^+ - O^- \quad = \quad 2W^{PM1}_{CO} \times W^{PM2}_{OO} + W^{PM1}_{OO} \times 2W^{PM2}_{CO}.$$

Table 4.2 shows the weights of covalent and ionic bond calculated with BF- and PM-orbitals. The weights obtained with BF-orbitals are intermediate between those with PM1 and PM2. For example, W^{BF1}_{OO} and W^{BF2}_{OO} are 37.2 %, and W^{PM1}_{OO} and W^{PM2}_{OO} are 34.7 and 41.4 %, respectively. This means the BF-orbital have intermediate character between the orbitals PM1 and PM2. As a result of summation of both contributions from W^{PM1}_{OO} and W^{PM2}_{OO}, the PM-weights become almost similar to BF-weights.

Fig. 4.5 shows the BF- and PM-weights calculated with various basis sets and LDMs. In all cases, the most important resonance structure is **2** and the next is **1**, which is doubly-bonded resonance structure. This clearly shows the double bond C=O is polarized. All basis sets provides almost similar results and the weights calculated with Löwdin type of LDMs are slightly smaller than those with Mulliken type of LDMs, as in the case of H_2O and NH_3. In all cases, BF-weights are similar to PM-weights, and hence, the results are independent from the

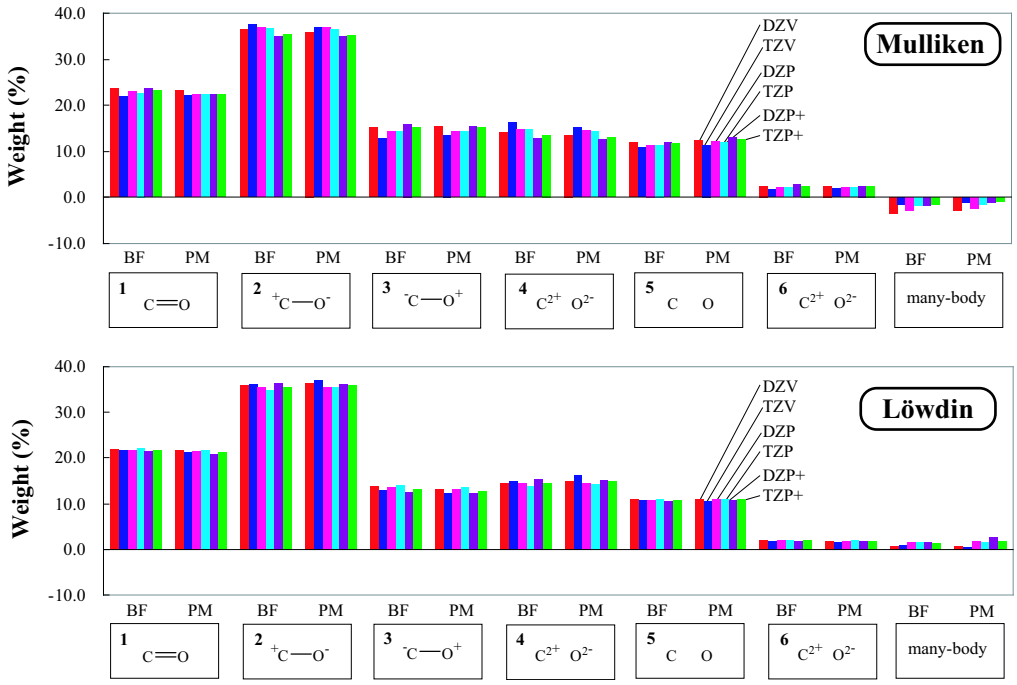

Figure 4.5: Weights (%) of resonance structures of H_2CO evaluated with Mulliken and Löwdin LDMs.

choice of localization schemes.

4.4 Conclusions

In this paper, we introduced the general formulation of the method to evaluate the weights of resonance structures. We investigated the resonance structure of H_2, H_2O, NH_3 and H_2CO using the two LDMs, Mulliken and Löwdin type, and three orbital localization schemes, BF, ER, and PM localizations, and various basis sets. The results are virtually independent from the choice of LDMs, namely operator types, and basis sets. The results are also independent from localization schemes in the cases of H_2O, NH_3 and even H_2CO, in which the character of PM bonding orbitals are quite different from those of BF and ER.

Acknowledgements

We acknowledge financial support by grant-in Aid for Scientific Research on Priority Areas ‘Water and biomolecule’ (430-18031019) and ‘Molecular Theory’ (461) from the Ministry of Education, Science, Sports, and Culture (MONBU SHO) in Japan.

Bibliography

[1] Shaik, S.; Shurki, A. *Angew. Chem. Int. Ed.* **1999**, *38*, 586.

[2] Hiberty, P. C.; Leforestier, C. *J. Am. Chem. Soc.* **1978**, *100*, 2012.

[3] Glendening, E. D.; Weinhold, F. *J. Comput. Chem.* **1998**, *19*, 593.

[4] Karafiloglou, P. *J. Comput. Chem.* **2001**, *22*, 306.

[5] McDouall, J. J. W.; Robb, M. A. *Chem. Phys. Lett.* **1986**, *132*, 319.

[6] Hirao, K.; Nakano, H.; Nakayama, K.; Dupuis, M. *J. Chem. Phys.* **1996**, *105*, 9227.

[7] (a) Ikeda, A.; Nakao, Y.; Sato, H.; Sakaki, S. *J. Phys. Chem. A* **2006**, *110*, 9028.(b) Ikeda, A.; Yokogawa, D.; Sato, H.; Sakaki, S. *Chem. Phys. Lett.* **2006**, *424*, 499.(c) Ikeda, A.; Yokogawa, D.; Sato, H.; Sakaki, S. Int. J. Quantum Chem. in press.

[8] (a) Mulliken, R. S. *J. Chem. Phys.* **1955**, *23*, 1833.(b) Mulliken, R. S. *J. Chem. Phys.* **1955**, *23*, 1841.

[9] (a) Mayer, I. *Chem. Phys. Lett.* **1983**, *97*, 270.(b) Mayer, I. *Int. J. Quantum Chem.* **1983**, *23*, 341..

[10] Boys, S. F., in Lowdin PO(eds.), *Quantum Theory of Atoms, Molecules, and the Solid State*,, Academic, New York, pp. 253, 1996.

[11] Löwdin, P. O. *J. Chem. Phys.* **1950**, *18*, 365.

[12] Edmiston, C.; Ruedenberg, K. *J. Chem. Phys.* **1965**, *43*, S97.

[13] Pipek, J.; Mezey, P. G. *J. Chem. Phys.* **1989**, *90*, 4916..

[14] (a) Dunning, T. H. *J. Chem. Phys.* **1971**, *55*, 716.. (b) Huzinaga, S. *J. Chem. Phys.* **1965**, *42*, 1293.

[15] Takahashi, O.; Sawahata, H.; Ogawa, Y.; Kikuchi, O. *J. Mol. Struct. (THEOCHEM)* **1997**, *393*, 141.

[16] Mayer, I. *Chem. Phys. Lett.* **2004**, *393*, 209.

[17] Schmidt, M. W.; Baldridge, K. K.; Boatz, J. A.; Elbert, S. T.; Gordon, M. S.; Jensen, J. H.; Koseki, S.; Matsunaga, N.; Nguyen, K. A.; Su, S. J.; Windus, T. L.; Dupuis, M.; Montgomery, J. A. *J. Comput. Chem.* **1993**, *14*, 1347.

Chapter 5

A New Resonance Theory Consistent with Mulliken Population Analysis

5.1 Introduction

Chemist's traditional approach to molecule is based on the resonance theory. In resonance theory, molecules are discussed in terms of resonance between several resonance structures, which built up of atoms with linking each other through ionic and covalent types of chemical bond. The resonance theory is still useful because that provides simple understanding of the reactivity and character of molecules. However, most of modern ab-initio calculations are based on the molecular orbital (MO) theory. Because MO theory is quite different from resonance theory, it is hard to extract the traditional picture of molecule from a MO wave function. To extract such pictures, we need the analysis of MO wave function based on the resonance theory. For such purpose, Hiberty *et al.* [1] reported the method to calculate the weights of resonance structures by using a MO wave function. In their method, MO wave function is expanded into a complete set of VB type of wave functions which consist of determinants based on hybrid orbitals. Weinhold *et al.* reported quite different method, called natural resonance theory (NRT) [2]. This is based on natural bond orbital (NBO) analysis. Karafiloglou reported another method [3], which is based on natural atomic orbitals [4]. CASVB by Robb *et al.* [5] and by Hirao and coworkers [6], which are based on CASSCF-type wave function, can offer similar information on a molecule.

On the other hand, other type of wave function analysis have been developed steadily. The most basic ones are Mulliken population analysis (MPA) and ab-initio bond order analysis

(BOA). A theoretical background of MPA [7] became very clear by Mayer's reformulation using mixed formalism of the second quantization for nonorthogonal orbitals [8]. BOA was developed as an extension of Wiberg's pioneering work [9] by Okada *et al.* [10] and Mayer [8], independently. Furthermore, several definitions, interpretations, and extensions of atomic population and bond order have been developed by various researchers [11–14].

We recently reported a method to evaluate the weights of resonance structures [15] from Hartree-Fock (HF) wave function, which is based on an orbital localization and a second quantized expression of BOA. The results show excellent agreement with our chemical intuitions and results by Hiberty *et al.* However, the previous method can not be applied to the system in which electrons are delocalized, like transition states and conjugated molecules.

In this work, we developed a novel method to calculate the weights of resonance structures, which is innovative extension of the previous method and natural extension of MPA and BOA. The present method is not only applicable to the system in which electrons are delocalized, but also consistent with MPA and BOA. In general, a resonance structure r have the corresponding and integer-valued atomic population (A_r) and bond order ($\mathrm{A\text{-}B}_r$) for atoms A and B. Let us consider H_2 as a trivial example. In the case of the resonance structure $\mathrm{H}_a - \mathrm{H}_b$, the population of H_a and H_b is 1, and the bond order is 1. In the case of $\mathrm{H}_a^- \mathrm{H}_b^+$, the populations of H_a and H_b are 2 and 0, respectively, and the bond order is 0. For consistency with MPA and BOA, it is desirable that the calculated weights W_i of resonance structures i satisfy the following equations.

$$\sum_r W_r \times \mathrm{A}_r = \text{Mulliken population of atom A} \tag{5.1}$$

$$2\sum_r W_r \times \mathrm{A\text{-}B}_r = \text{ab-initio bond order between A and B atoms} \tag{5.2}$$

The present method satisfies Eqs. 5.1 and 5.2, exactly.

The organization of this paper is follows. In Sec 2, we overviewied our previous method and formulated the new method. In Sec 3, we applied the new method to LiH and $\mathrm{H_2O}$ molecules, to investigate the consistency with MPA, BOA and our previous method. Next, we applied the present method to trans-butadiene and S_N2 reaction, to which cannot be applied the previous

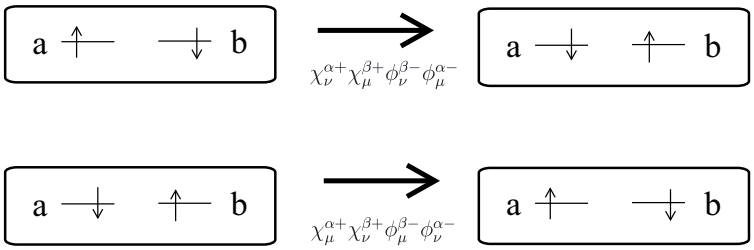

Figure 5.1: Action of $\chi_b^{\alpha+}\chi_a^{\beta+}\phi_b^{\beta-}\phi_a^{\alpha-}$ and $\chi_a^{\alpha+}\chi_b^{\beta+}\phi_a^{\beta-}\phi_b^{\alpha-}$.

method, because electrons in those systems are delocalized. The conclusion was summarized in Sec 4.

5.2 Theory

5.2.1 A reformulation of BOA

Ab-initio bond order between atomic orbitals a and b can be defined as follows,

$$b_{a-b}^1 = \frac{1}{2}\mathbf{PS}_{ab}\mathbf{PS}_{ba} \tag{5.3}$$

Here, $\mathbf{S}$ is overlap matrix and $\mathbf{P}$ is defined as $\mathbf{P}_{ab} = 2\sum_i^{occ}\mathbf{C}_{a,i}\mathbf{C}_{b,i}$, where $\mathbf{C}_{a,i}$ is LCAO coefficient of molecular orbital i. By using b^1, ab-initio bond order between atoms A and B is calculated as $2\sum_{a\in A,b\in B} b_{a-b}^1$.

Now, we can construct the second quantized operator of which HF expectation value is b_{a-b}^1.

$$b_{a-b}^1 = \langle\Psi_{HF}|\chi_b^{\alpha+}\chi_a^{\beta+}\phi_b^{\beta-}\phi_a^{\alpha-} + \chi_a^{\alpha+}\chi_b^{\beta+}\phi_a^{\beta-}\phi_b^{\alpha-}|\Psi_{HF}\rangle \tag{5.4}$$

Here, χ_b^+ is creation operator of nonorthogonal atomic orbital b and ϕ_a^- is annihilation operator of biorthogonal atomic orbital a. When and only when the ket is the states in which two atomic orbitals a and b are singly occupied by one α electron and one β electron, the operators $\chi_b^{\alpha+}\chi_a^{\beta+}\phi_b^{\beta-}\phi_a^{\alpha-}$ and $\chi_a^{\alpha+}\chi_b^{\beta+}\phi_a^{\beta-}\phi_b^{\alpha-}$ transform α and β electrons into β and α electrons, respectively (Figure 5.1). This shows ab-initio bond order is corresponding to the probability of the state in which two electrons are singlet-coupled between atomic orbitals.

5.2.2 The previous method

Let us consider a localized orbital ϕ_i between two atomic centers, A and B, which can be obtained by standard orbital localization of HF wave function. Next, we define the ab-initio bond order between atomic orbitals a and b, for two electron system related to the localized orbital ϕ_i.

$$b^{1(i)}_{a-b} = \langle \phi_i \bar{\phi}_i | \chi^{\alpha+}_b \chi^{\beta+}_a \phi^{\beta-}_b \phi^{\alpha-}_a + \chi^{\alpha+}_a \chi^{\beta+}_b \phi^{\beta-}_a \phi^{\alpha-}_b | \phi_i \bar{\phi}_i \rangle \tag{5.5}$$

By using $b^{1(i)}$, we can define the weights of ionic and covalent bonds between atoms A and B as

$$W^i(\mathrm{A}^-\mathrm{B}^+) = \frac{1}{2} \sum_{a \in A} \sum_{b \in A} b^{1(i)}_{a-b}, \tag{5.6}$$

$$W^i(\mathrm{A}-\mathrm{B}) = \sum_{a \in A} \sum_{b \in B} b^{1(i)}_{a-b}, \tag{5.7}$$

$$W^i(\mathrm{A}^+\mathrm{B}^-) = \frac{1}{2} \sum_{a \in B} \sum_{b \in B} b^{1(i)}_{a-b}. \tag{5.8}$$

We consider the weights of ionic and covalent bonds for each bond in whole molecule are independent from each, and the weights of resonance structures are calculated by the product of those.

5.2.3 The present method

Above-described procedure didn't provide significant error for the molecules, in which two electrons are localized in one chemical bond, However, in the case of the conjugated molecules and transition states, this must be violated.

For avoiding this problem, we develope the second-order ab-initio bond order $b^2_{a-b,c-d}$, which is related to the probability of the state in which four electrons make two singlet-coupled pairs, like $a-b$ and $c-d$. By extending the operators in Eq. 5.4, we get following six operators,

$$\hat{X}_1 = \chi^{\alpha+}_d \chi^{\beta+}_c \chi^{\alpha+}_b \chi^{\beta+}_a \phi^{\beta-}_d \phi^{\alpha-}_c \phi^{\beta-}_b \phi^{\alpha-}_a,$$

$$\hat{X}_2 = \chi^{\alpha+}_c \chi^{\beta+}_d \chi^{\alpha+}_b \chi^{\beta+}_a \phi^{\beta-}_c \phi^{\alpha-}_d \phi^{\beta-}_b \phi^{\alpha-}_a,$$

$$\hat{X}_3 = \chi^{\alpha+}_d \chi^{\beta+}_c \chi^{\alpha+}_a \chi^{\beta+}_b \phi^{\beta-}_d \phi^{\alpha-}_c \phi^{\beta-}_a \phi^{\alpha-}_b,$$

$$
\begin{aligned}
\hat{X}_4 &= \chi_c^{\alpha+}\chi_d^{\beta+}\chi_a^{\alpha+}\chi_b^{\beta+}\phi_c^{\beta-}\phi_d^{\alpha-}\phi_a^{\beta-}\phi_b^{\alpha-}, \\
\hat{X}_5 &= \chi_d^{\alpha+}\chi_b^{\beta+}\chi_c^{\alpha+}\chi_a^{\beta+}\phi_d^{\beta-}\phi_b^{\alpha-}\phi_c^{\beta-}\phi_a^{\alpha-}, \\
\hat{X}_6 &= \chi_c^{\alpha+}\chi_a^{\beta+}\chi_d^{\alpha+}\chi_b^{\beta+}\phi_c^{\beta-}\phi_a^{\alpha-}\phi_d^{\beta-}\phi_b^{\alpha-}.
\end{aligned}
$$

These operators transform α and β electrons into β and α electrons in four electron systems, as shown in Figure 5.2. In these operators, $\hat{X}_1$, $\hat{X}_2$, $\hat{X}_3$, and $\hat{X}_4$ are related to the state $a-b, c-d$. Now, we define second-order bond index $b^2_{a-b,c-d}$ as follows,

$$
\begin{aligned}
b^2_{a-b,c-d} &= \langle\Psi_{HF}|\hat{X}_1+\hat{X}_2+\hat{X}_3+\hat{X}_4-\hat{X}_5-\hat{X}_6|\Psi_{HF}\rangle, \qquad (5.9)\\
&= \frac{1}{4}\mathbf{PS}_{ab}\mathbf{PS}_{ba}\mathbf{PS}_{cd}\mathbf{PS}_{dc}-\frac{1}{8}\mathbf{PS}_{ac}\mathbf{PS}_{cd}\mathbf{PS}_{db}\mathbf{PS}_{ba} \\
&- \frac{1}{8}\mathbf{PS}_{ab}\mathbf{PS}_{bd}\mathbf{PS}_{dc}\mathbf{PS}_{ca}-\frac{1}{8}\mathbf{PS}_{ab}\mathbf{PS}_{bc}\mathbf{PS}_{cd}\mathbf{PS}_{da} \\
&- \frac{1}{8}\mathbf{PS}_{ad}\mathbf{PS}_{dc}\mathbf{PS}_{cb}\mathbf{PS}_{ba}+\frac{1}{8}\mathbf{PS}_{ac}\mathbf{PS}_{cb}\mathbf{PS}_{bd}\mathbf{PS}_{da} \\
&+ \frac{1}{8}\mathbf{PS}_{ad}\mathbf{PS}_{db}\mathbf{PS}_{bc}\mathbf{PS}_{ca}. \qquad (5.10)
\end{aligned}
$$

Based on this definition of $b^2_{a-b,c-d}$, the consistency with MPA and BOA is guaranteed. Namely, $b^2_{a-b,c-d}$ satisfies following relations,

$$
\begin{aligned}
\sum_b\sum_c\sum_d b^2_{(a-b,c-d)} &= (N_e-2)PS_{aa}, \qquad (5.11)\\
\sum_c\sum_d b^2_{(a-b,c-d)} &= (N_e-2)b^1_{a-b}, \qquad (5.12)
\end{aligned}
$$

where, N_e is the number of electrons. Eq. 5.12 mean that b^2 is a natural extension of b^1. It is noted that $b^2_{a-b,c-d}$ is also consistent with the requirement: Two covalent bonds must not use same atomic orbitals. In the case of VB theory, such wave functions like $|\,ab\,ac\,|$ can not be defined. In our method, $b^2_{a-b,c-d}$ becomes 0, when a or b is equivalent to c or d.

We define the weights of resonance structures by using $b^2_{a-b,c-d}$. Let us consider two localized orbitals ϕ_i and ϕ_j among atomic centers, A, B, C, and D. Next, we define second-order ab-initio bond order, for four electron system related to a localized orbital ϕ_i and ϕ_j.

$$
b^{2(i,j)}_{a-b,c-d} = \langle\phi_i\bar{\phi}_i\phi_j\bar{\phi}_j|\hat{X}_1+\hat{X}_2+\hat{X}_3+\hat{X}_4-\hat{X}_5-\hat{X}_6|\phi_i\bar{\phi}_i\phi_j\bar{\phi}_j\rangle \qquad (5.13)
$$

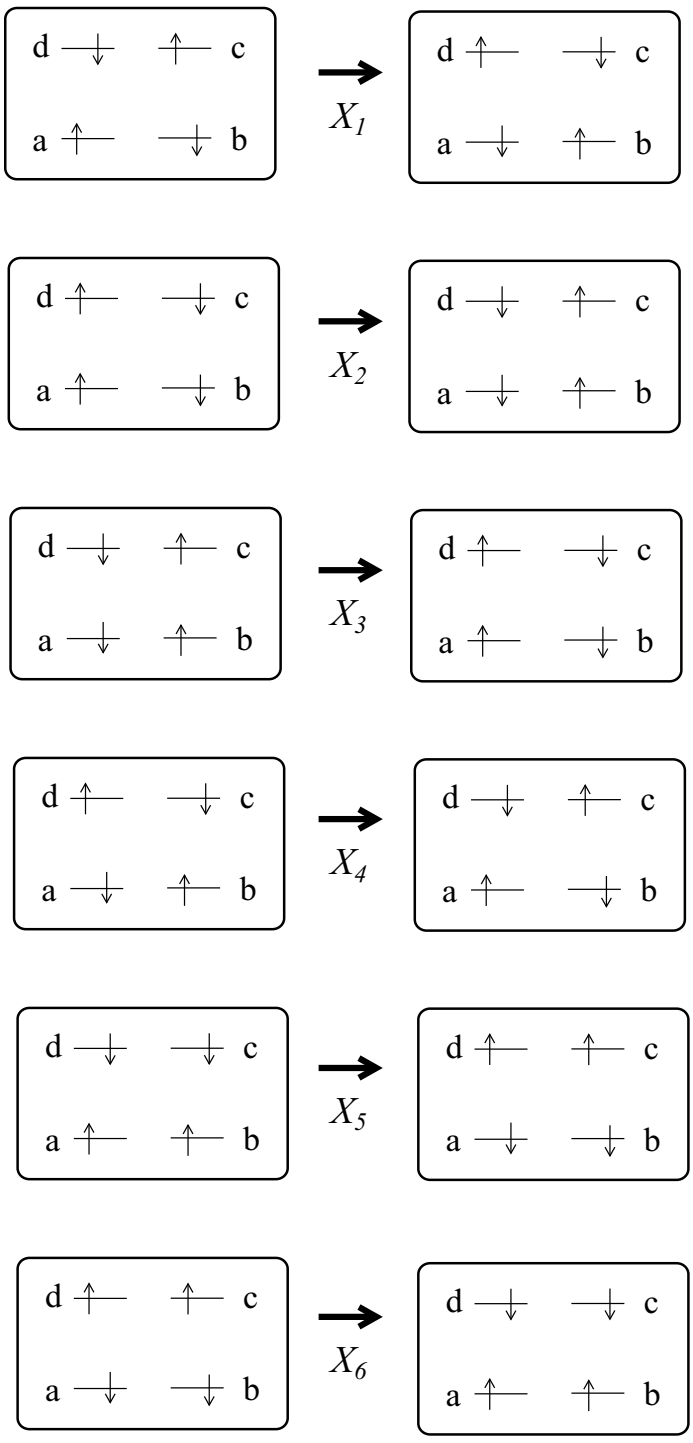

Figure 5.2: Action of $\hat{X}_1$, $\hat{X}_2$, $\hat{X}_3$, $\hat{X}_4$, $\hat{X}_5$ and $\hat{X}_6$.

By using $b^{2(i,j)}$, we can define the weights of resonance structure for four electron systems in the similar manner to the previous method. For example, the weight of totally covalent resonance structure $\mathrm{A}-\mathrm{B},\mathrm{C}-\mathrm{D}$ can be expressed as follows,

$$W^{i,j}(\mathrm{A}-\mathrm{B},\mathrm{C}-\mathrm{D}) = \sum_{a\in A}\sum_{b\in B}\sum_{c\in C}\sum_{d\in D} b^{2(i,j)}_{a-b,c-d}. \tag{5.14}$$

Because $b^2_{a-b,c-d}$ satisfy Eqs. 5.11 and 5.12, the calculated weights satisfy Eqs. 5.1 and 5.2. It is noted that Eqs. 5.11 and 5.12 also guarantees that the sum of all weights becomes exactly 1.

In this work, we calculated HF wave function and then applied the present method. According to need, the Pipek-Mezey orbital localization [16] was emploied. For all atoms, STO-3G, DZV, DZP and TZP basis sets were used [17]. All calculations were performed with program code GAMESS [18] modified by us.

5.3 Numerical results and discussion

5.3.1 LiH and H_2O: Consistency with MPA, BOA and the previous method.

To demonstrate the consistency with MPA and BOA, we apply the present method to LiH molecule, as a typical four electron system. The weights of resonance structures, populations of Li and H, and bond orders calculated by MPA, BOA, and the present method are shown in Table 5.1. The charges and bond orders calculated by the present method are exactly equal to MPA and BOA values in all the basis sets. The weights slightly depend on the choice of basis set, and this dependency is also consistent with MPA and BOA. In all basis set, the weight of $\mathrm{Li}^+\mathrm{H}^-$ is larger than $\mathrm{Li}^-\mathrm{H}^+$, and then it is cleared the bond between Li and H is polarized. In the case of TZP basis set, the weight of $\mathrm{Li}^+\mathrm{H}^-$ and $\mathrm{Li}^-\mathrm{H}^+$ are 45.3 % and 10.7 %.

Both the previous and present method can be applied to the system in which two electrons are localized in one chemical bond. As a typical example, we applied the methods to H_2O molecule. The orbital localization are employed to extract two two-center orbitals related to OH bonds. The calculated weights are shown in Table 5.2. In all basis sets, the weights by the present method are similar to those by the previous method. This clearly shows that the present method is natural extension of the previous method.

Table 5.1: The weights (%) of resonance structures, bond order, and atomic population of LiH. Mayer's bond order and Mulliken population are also showed.

No.		DZV	DZP	TZP
1	Li−H	46.8	48.4	44.0
2	Li^-H^+	14.1	16.9	10.7
3	Li^+H^-	39.1	34.7	45.3
Bond order	Present[a)]	0.937	0.969	0.879
	BOA	0.937	0.969	0.879
Li population	Present[a)]	2.750	2.822	2.654
	MPA	2.750	2.822	2.654
H population	Present[a)]	1.250	1.178	1.346
	MPA	1.250	1.178	1.346

a) The values are calculated by using Eqs. 5.1 and 5.2.

Table 5.2: The weights (%) of resonance structure in H_2O calculated by the previous and present methods.

No.		DZV		DZP		TZP	
		Previous	Present	Previous	Present	Previous	Present
1	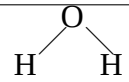	19.8	18.6	21.0	20.3	22.8	22.0
2	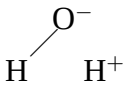	41.4	40.7	39.9	39.1	36.7	36.2
3	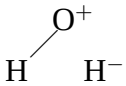	9.4	9.0	11.0	10.6	14.1	13.4
4	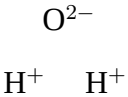	21.7	21.4	18.9	18.9	14.8	14.8
5	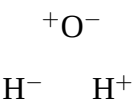	9.9	9.9	10.5	10.2	11.4	11.0
6	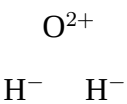	1.1	1.0	1.4	1.4	2.2	2.0

Table 5.3: The weights (%) of resonance structure in cis-butadiene calculated by Hiberty's method and the present method.

No.		Hiberty[a)]	The present method			
		STO-3G	STO-3G	DZV	DZP	TZP
1	C=C−C=C	22.1	23.2	23.5	23.1	22.9
2	$C^+-C^--C=C$	22.6	22.8	22.7	22.1	21.8
3	$C^--C^+-C=C$	23.2	23.7	24.3	24.1	24.0
4	$^{\odot}C-C=C-C^{\odot}$	1.0	1.8	2.2	1.8	2.0
5	$C^--C=C-C^+$	2.1	1.8	1.9	1.6	1.9
6	$^{\odot}C-C=C-C^{\odot}$	N/A	1.8	2.1	1.8	1.8
7	totally ionic structures	23.1	23.4	23.7	23.2	23.1

a) The results by Hiberty *et al*.

5.3.2 Resonance in Butadiene

In this section, we focus trans-butadiene, to which the previous method cannot be applied due to the conjugacy. Hiberty *et al.* calculated the weights of resonance structure of trans-butadiene by using their method, in which the MO wave function is expanded into VB type of wave functions, with minimal basis sets [2]. Their method is reliable but difficult to apply with extended basis sets, because VB type of wave functions should be defined by using hybrid orbitals. On the other hand, the present method is easy to apply with extended basis sets. We applied the present method to trans-butadiene with various basis set and compared the results with Hiberty's result. The orbital localization are employed to extract two π orbitals.

The weights of resonance structures are shown in Table 5.3. The present result are almost similar to Hiberty's result. The more important resonance structures are **1**, **2** and **3**, which contain double bonds C1=C2 and/or C3=C4. On the other hand, the weight of resonance structures **4**, **5** and **6**, which contain bonds C2=C3 and/or C1−C4 and are related to conjugacy of butadiene, are small. All basis set provide similar result and then the basis set dependency of the present method is very small in this molecule. In TZP basis sets, the weights of **4**, **5** and **6** are 2.0, 1.9 and 1.8 %, respectively.

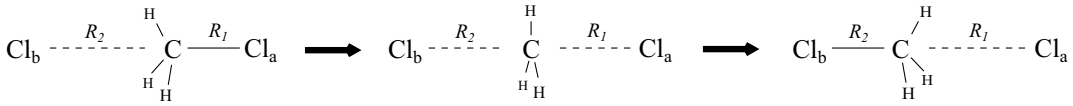

Figure 5.3: The reaction coordinate of $CH_3Cl + Cl^- \rightarrow Cl^- + CH_3Cl$.

Table 5.4: The weights (%) of resonance structure in transition state of the reaction $CH_3Cl + Cl^- \rightarrow Cl^- + CH_3Cl$.

No.		Weight
1	Cl_b^- CH_3-Cl_a	19.5
2	Cl_b^- CH_3^+ Cl_a^-	57.4
3	Cl_b-CH_3 Cl_a^-	19.5
4	$^{\odot}Cl_b$ CH_3^- $Cl_a^{\odot}$	3.3
5	Cl_b^- CH_3^- Cl_a^+	1.7
6	Cl_b^+ CH_3^- Cl_a^-	1.7
7	$Cl_b-CH_3^--Cl_a$	0.1

5.3.3 S_N2 reaction

Finally, we applied the present method to a typical S_N2 reaction, $CH_3Cl + Cl^- \rightarrow Cl^- + CH_3Cl$, with TZP basis sets. Because four electrons related to bonds breaking and formation are delocalized in the transition state, the previous method cannot be applied to this system. The reaction coordinate is selected as $R_1 - R_2$, where R_1 is the distance of C and Cl_a and R_2 is the distance of C and Cl_b, as shown in Figure 5.3. The other degrees of freedom are fully optimized. The orbital localization are employed to extract two valence orbitals participate in the reaction.

The weights of resonance structures in the transition state is shown in Table 5.4. The most important resonance structure is **2** which is the totally ionic., and the weight is 57.4 % The next is **1** and **3**, in which one Cl become an ion and the other Cl is covalently bonded to C, and those weights are exactly equal to each other (19.5 %). This is in agreement with our chemical intuitions. We focus those resonance structures **1**, **2** and **3**, and calculated the changes of the weights along reaction path.

Figure 5.4 shows the potential energy curve along the reaction path. This clearly shows that the reaction proceed via precursor complex and transition state. The changes in the weights

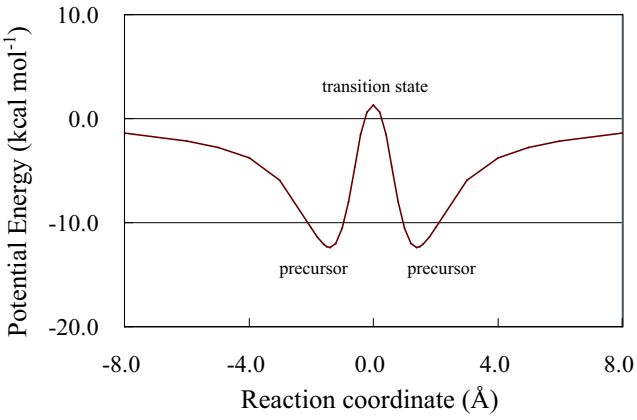

Figure 5.4: The potential energy curve of the reaction $CH_3Cl + Cl^- \rightarrow Cl^- + CH_3Cl$.

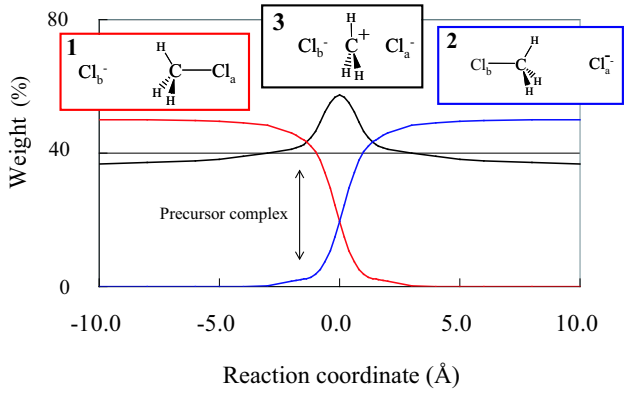

Figure 5.5: The weights of resonance structure in $CH_3Cl + Cl^- \rightarrow Cl^- + CH_3Cl$.

of resonance structures are shown in Figure 5.5. As the reaction proceeds, the weight of **1** decreases and the weight of **3** increases. This is corresponding the bond breaking and bond formation. The weight of **2** increases by the transition state and decreases from transition state. In the precursor complex, the weight of **2** is larger than it in the reactant. This means the bond between C and Cl_a is polarized by the electric field of Cl_b^- and the ion-dipole interaction stabilizes the precursor complex. Of course, these behaviours are consistent with MPA. In the reactant and precursor complex, the Mulliken charge of Cl_a is -0.15 and -0.30.

5.4 Conclusion

In this report, we presented a novel method to calculate the weights of resonance structures from HF wave function. The method is an extension of our previous method and consistent with MPA and BOA, and easy to apply. Only orbital localization and argebraic calculation of density matrices is the additional calculation except for HF method. The method is successfully applied to LiH, H_2O, butadiene and S_N2 reaction. In LiH and H_2O molecules, the consistency with MPA, BOA and the previous method is investigated numerically. Especially, atomic population and bond order calculated by the present method is exactly eqaul to MPA and BOA results. In trans-butadiene, the calculated result is almost similar to the results by Hiberty *et al.* It is noted that it is easy for our present method to apply with extended basis sets. In the case of S_N2 reaction, the change of the nature of chemical bond, bond breaking and bond formation become clear by the present method. In the precursor complex, a chemical bond between C and Cl is polarized by the electric field of Cl^-. In the transition state, the totally ionic resonance structure become very important and this is in agreement with our chemical intuitions.

Acknowledgements

We acknowledge financial support by grant-in Aid for Scientific Research on Priority Areas 'Water and biomolecule' (430-18031019) and 'Molecular Theory' (461) from the Ministry of Education, Science, Sports, and Culture (MONBU SHO) in Japan.

Bibliography

[1] Hiberty, P.C.; Leforestier, C. *J. Am. Chem. Soc.* **1978**, *100*, 2012.

[2] Glendening, E. D.; Weinhold, F. *J. Comput. Chem.* **1998**, *19*, 593.

[3] Karafiloglou, P. *J. Comput. Chem.* **2001**, *22*, 306.

[4] Reed, A. E.; Weinhold, F. *J. Chem. Phys.* **1985**, *83*, 1736.

[5] McDouall, J. J. W.; Robb, M. A. *Chem. Phys. Lett.* **1986**, *132*, 319.

[6] Hirao, K.; Nakano, H.; Nakayama, K.; Dupuis, M.; *J. Chem. Phys.* **1996**, *105*, 9227.

[7] (a) Mulliken, R. S. *J. Chem. Phys.* **1955**, *23*, 1833.(b) Mulliken, R. S. *J. Chem. Phys.* **1955**, *23*, 1841..

[8] (a) Mayer, I. *Chem. Phys. Lett.* **1983**, *97*, 270. (b) Mayer, I. *Int. J. Quantum Chem.* **1983**, *23*, 341.

[9] Wiberg, K. A. *Tetrahedron* **1966**, *24*, 1083.

[10] (a) Okada, T.; Fueno, T. *Bull. Chem. Soc. Jpn.* **1975**, *48*, 2025. (b) Okada, T.; Fueno, T. *Bull. Chem. Soc. Jpn.* **1976**, *49*, 1524.

[11] Löwdin, P. O. *J. Chem. Phys.* **1950**, *18*, 365.

[12] Jug, K. *J. Comput. Chem.* **1984**, *5*, 555.

[13] Pitanga, P.; Giambiagi, M.; Degiambiagi, M. S. *Chem. Phys. Lett.* **1986**, *128*, 411.

[14] Sannigrahi, A. B.; Kar, T. *Chem. Phys. Lett.* **1990**, *173*, 569.

[15] (a) Ikeda, A.; Nakao, Y.; Sato, H.; Sakaki, S. *J. Phys. Chem. A* **2006**, *110*, 9028.(b) Ikeda, A.; Yokogawa, D.; Sato, H.; Sakaki, S. *Chem. Phys. Lett.* **2006**, *424*, 499.(c) Ikeda, A.; Yokogawa, D.; Sato, H.; Sakaki, S. *Int. J. Quantum Chem.* **2007**, *107*, 3132.

[16] Pipek, J.; Mezey, P. G. *J. Chem. Phys.* **1989**, *90*, 4916.

[17] Schmidt, M. W.; Baldridge, K. K.; Boatz, J. A.; Elbert, S. T.; Gordon, M. S.; Jensen, J. H.; Koseki, S.; Matsunaga, N.; Nguyen, K. A.; Su, S. J.; Windus, T. L.; Dupuis, M.; Montgomery, J. A. *J. Comput. Chem.* **1993**, *14*, 1347.

[18] (a) Dunning, T. H. *J. Chem. Phys.* **1971**, *55*, 716.. (b) Huzinaga, S. *J. Chem. Phys.* **1965**, *42*, 1293.

Chapter 6

Solvation Effect on Resonance Structure: Extracting Valence Bond-like Character from Molecular Orbitals

6.1 Introduction

Imagine that a molecule is dissolved into solution. It is well established that the electronic structure of the solute molecule is changed due to the solvation effect such as electrostatic field and many other interactions. Rearrangement of electronic structure must change the strength and the nature of chemical bond building up the molecule. The questions arising here are whether chemical bond is strengthened by solvation or not, and if the solvation changes the nature of chemical bond or not. In the recent study, we have discussed the solvation effect on the strength of chemical bond using a new energy partitioning scheme [1]. However, how can we clarify the nature of chemical bond ?

Understanding of chemical bond has been one of the main subjects in physical chemistry from its foundation time. A very useful and popular concept to understand the bond is classification in terms of its polarization. A bond in which bond-making electrons are remarkably localized on one of the two atoms is called “ionic”, while a bond in which the electrons are shared by the two atoms is called “covalent”. The concept of electronegativity offers a heuristic explanation of such bonding. Nowadays, it is very easy for the modern quantum-chemical technique to compute bond energy or the detailed information of bonding wave functions. However, it is devilishly hard to bridge between the traditional concept and modern computational results directly. The wave function of a molecule is usually described in terms of

molecular orbital (MO). But it can be also represented based on the assembly of various types of chemical bonds, which are presumably described in the traditional concepts. The concept of the resonance structure is simple but useful tool to understand the electronic structure of a molecule.

How can we obtain the resonance structure by using modern computational method ? Except for valence bond studies that can directly provide such information, several attempts have been made to translate the results of MO calculations into the terms of the resonance structure. A monumental study was done by Hiberty, [2] in which MO is expanded into the set of atomic-orbital based determinant. NRT by Weinhold [3] and study by Karafiloglou [4] utilize characteristic of NBO to provide the weights of resonance structures. CASVB by Hirao and coworkers [5] and study by Robb *et al.* [6] are based on CASSCF-type wave function that can offer similar information on a molecule. Very recently, we have proposed a simple but promising procedure to compute the weights of resonance structure related to the set of localized molecular orbitals using the second quantization [7]. The results show excellent agreement with our chemical intuitions and previous works. The important issues that must be stressed are the present method requires only the one body density matrix obtained with the standard ab initio MO computation, and the additional calculations is just to localize the MOs.

In this letter, we wish to report the solvation effect on the weights of resonance structure of simple molecules. Our strategy is the combination of two methods, RISM-SCF and the new analysis method described above. Illustrative computational results are presented to demonstrate the superiority of the new method.

6.2 Method

In the present study, two types of methodologies are key to figure out the resonance structure in a solvated molecule. One is the RISM-SCF that treats solvation effect, and the other is the new procedure to compute the weight of resonance structure we have proposed very recently [7]. The RISM-SCF theory combines two major theoretical elements, the ab initio molecular orbital (MO) theory and the RISM integral equation method, that is a statistical mechanics

for molecular liquids. In the theory, electronic structure of a solute molecule in solution and solvent distribution around the solute are solved in a self-consistent manner. More detailed explanation of the theory can be found in the previous reviews [8, 9] and articles [10, 11] . By using our new analysis procedure on electronic wave functions of molecule, the weights of resonance structures can be computed from MOs utilizing localization of MOs and the second quantization. We found that the weights of resonance structures for BH_3 and H_3O^+, which are evaluated by Hiberty and coworkers [2], can be reproduced with our analysis method in a very simple procedure. In the consequence of the theory, the weights (probabilities) of resonance structure in a (localized) valence orbital ϕ_i between atoms A and B are expressed as follows $(\sigma_1 \neq \sigma_2)$,

$$\mathrm{A^-B^+} \;:\; \sum_{\mu\in A}\sum_{\nu\in A}\langle\phi_i|\chi_\nu^{\sigma_1+}\chi_\mu^{\sigma_2+}\varphi_\nu^{\sigma_2-}\varphi_\mu^{\sigma_1-}|\phi_i\rangle, \tag{6.1}$$

$$\mathrm{A-B} \;:\; 2\sum_{\mu\in A}\sum_{\nu\in B}\langle\phi_i|\chi_\nu^{\sigma_1+}\chi_\mu^{\sigma_2+}\varphi_\nu^{\sigma_2-}\varphi_\mu^{\sigma_1-}|\phi_i\rangle, \tag{6.2}$$

$$\mathrm{A^+B^-} \;:\; \sum_{\mu\in B}\sum_{\nu\in B}\langle\phi_i|\chi_\nu^{\sigma_1+}\chi_\mu^{\sigma_2+}\varphi_\nu^{\sigma_2-}\varphi_\mu^{\sigma_1-}|\phi_i\rangle, \tag{6.3}$$

where χ_μ^+ and φ_ν^- are, respectively, creation and annihilation operators related to biorthogonal atomic orbital basis functions, μ and ν. Since there is another contribution from essentially three (or higher)-body correlations, which are usually negligibly small, sum of these four components is exactly normalized to 1. The weights of resonance structures of a whole molecule can be obtained by multiplication of the weights of the valence LMOs ($w^i(A^-B^+), w^i(A-B), w^i(A^+B^-)$ and $w^i(\mathrm{other})$).

$$1 = \prod_i^{LMOs} \left\{w^i(A^-B^+) + w^i(A-B) + w^i(A^+B^-) + w^i(\mathrm{other})\right\}, \tag{6.4}$$

where $w^i(\mathrm{other})$ corresponds to the three (or higher)-body correlations. The choice of LMOs is related to the choice of valence bond configuration.

The electronic wave functions of solvated molecules were computed on the basis of the RHF method with DZP basis set [12]. LANL2DZ(d,p) [13] was used for iodine atom. After localization with Boys method, valence-type bonds that bridge two atoms (one for H–X and two for

Table 6.1: Lennard-Jones Potential Parameters for Solute-Water Interaction

atom	σ (Å)	ϵ (kcal/mol)
	HX	
F	2.72	1.364
Cl	3.62	0.364
Br	3.90	0.529
I	4.32	0.633
H	1.00	0.056
	Water[a]	
O	3.17	0.155
H	1.00	0.056

[a] The values -0.82 and $+0.41$ are assigned to q_O and q_H, respectively, as solvent molecule.

H–O) were selected to perform the analysis of the wave function. In the RISM theory, solute molecules were modeled with all atom-type interactions, whose Lennard- Jones parameters were taken from the literature [14] and summarized in Table 6.1. The SPC-like water [10] was employed to describe the solvent. All the van der Waals interactions between solute and solvent were determined by means of the standard combination rule. The density of water was assumed to be 0.033337 molecule/Å^3 at 298.15 K.

6.3 Results and discussion

6.3.1 Series of hydrogen halides

The acidity of hydrogen halides (HX, where X = F, Cl, Br, I) is one of those phenomena which have been most intensively studied by means of the quantum chemistry in its earlier history. From the earlier ages, the concept of electronegativity has been playing a significant role to classify the nature of H–X bond. An interesting question arising here is, how the concept is interpreted in terms of the ab initio electronic structure theory. In our previous study, this question has been already answered from the view point of solvation [14]. The subsequent question, especially from the quantum chemistry, is whether the concept can be related to the term of resonance structure or not. Furthermore, solvation effect on the weights of the resonance structure itself is of great interest.

Table 6.2: The weights of resonance structure in HX

	isolated molecule				aqueous solution			
	H^+X^-	H–X	H^-X^+	total	H^+X^-	H–X	H^-X^+	total
HF	0.497	0.416	0.087	1.000	0.545	0.390	0.069	1.000
HCl	0.342	0.486	0.172	1.000	0.399	0.465	0.136	1.000
HBr	0.337	0.487	0.176	1.000	0.384	0.471	0.145	1.000
HI	0.281	0.498	0.221	1.000	0.308	0.494	0.198	1.000

Table 6.2 lists the weights of resonance structure for the series of HX molecule both in vacuo and in aqueous solution. Since we treat diatomic molecules, there is no contributions from many-body ('other') term. The result is in good harmony with our chemical intuitions as follows:

(1) The halogen atoms strongly attract electrons and the contribution from the resonance structure of ionic character, H^+X^-, is much greater than that from the other ionic structure, H^-X^+.

(2) In the series of HXs, the weight of the ionic structure in HF is the greatest, suggesting that it has the most conspicuous ionic character in the electronic structure among the hydrogen halides. The weight decreases in the order HF $>$ HCl $>$ HBr $>$ HI.

(3) The ionic structure of H^+X^- is enhanced on transferring from the gas phase to aqueous solution. The enhancement tends to become smaller as the molecular size increases.

On the other hand, it is of great interests that the contribution from covalency is relatively great in all the molecules and it amounts to more than 40 % even for the most ionic HF molecule. Unfortunately, we could not find any other literatures describing the valence bond character of these molecules, so comparison is not available.

6.3.2 Water molecule

Probably, water is one of the most interesting molecule to analyze its resonance structure. Speculating from its auto-ionization character, the bond polarization of O–H should be enhanced in aqueous solution. In other words, the weights of resonance structure including these features should increase upon transferring from gas phase to solution phase.

Table 6.3: The weights of resonance structure in H_2O

No.		isolated molecule		aqueous solution	
		DZP	TZP	DZP	TZP
1	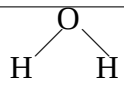	0.207	0.204	0.179	0.173
2	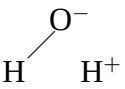	0.401	0.403	0.419	0.422
3	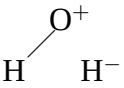	0.106	0.104	0.076	0.071
4	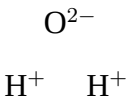	0.194	0.199	0.246	0.258
5	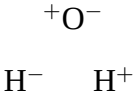	0.103	0.103	0.089	0.086
6	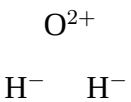	0.014	0.013	0.008	0.007
	other	-0.025	-0.026	-0.017	-0.017
	total	1.000	1.000	1.000	1.000
	$q_{\mathrm{O}}^{\mathrm{a}}$	8.6605	8.6826	8.7967	8.8351

[a] Mulliken Population on oxygen atom

Table 6.3 illustrates the weights of representative resonance structures both in gas and in aqueous solution phase. In both phases, the most important contribution arises from the structure **2**, in which one of O–H bonds is polarized and the other forms covalent bonding. The contributions from completely covalent character (**1**) and from the doubly ionized character (**4**) are comparable. Peterson *et al.* reported the valence bond study of water molecule [15], in which the structure **2** is predominant among various configurations. As expected, weights associated with ionic structures tend to increase in aqueous solution. The importance of **2** is furthermore enhanced and the contribution from **4** becomes greater than that from **1**. In summary, the weights related to ionic character tend to be grater. On the other hand, the weight of covalent character decreases in aqueous solution. This tendency was already suggested in

our previous study based on the energy partitioning technique [1]. In the Table, the weights computed by TZP [16] basis sets are also shown. It is very interesting that the basis-sets dependency is negligibly small, while the Mulliken populations on oxygen atom show greater dependency. In our experience, the present method gives relatively basis-set independent results.

We wish to mention that the contribution from 'other' term is minus value. It is known that Mulliken population and Mayer's covalent bond order index sometimes give minus value. Since the second quantized operators used in the present study are closely related to Mulliken population analysis, the minus value appeared here is considered to have the same origin. Actually, the Löwdin type operator does not give minus value of weight in our experience. These systematical studies will be reported in the forthcoming paper.

6.4 Conclusions

We have applied the new method to analyze the resonance structure in electronic structure for the solvated molecules, which are computed by RISM-SCF method. The new analysis offers a bridge between modern quantum computational results and chemical intuitions. As expected, the contribution from the ionic structure tends to be enhanced in aqueous solutions on the electronic structure polarization due to solvation. We believe that the present analysis method is promising tool to understand the nature of chemical bonds.

Bibliography

[1] H. Sato, S. Sakaki, *J.* Phys. Chem B, *submitted*

[2] P.C. Hiberty, C. Leforestier, *J. Am. Chem. Soc.* **100**, *2012*, 1978.

[3] E.D. Glendening, F. Weinhold, *J. Comput. Chem.* **19**, *593*, 1998.

[4] R.M. Parrondo, P. Karafiloglou, R.R. Pappalardo, E. Sanchez Marcos, *J. Phys. Chem.* **99**, *6461*, 1995.

[5] K. Hirao, H. Nakano, K. Nakayama, M. Dupuis, *J. Chem. Phys.* **105**, *9227*, 1996.

[6] J.J.W. McDouall, M.A. Robb, *Chem. Phys. Lett.* **132**, *319*, 1986.

[7] A. Ikeda, Y. Nakao, H. Sato, S. Sakaki, *to be submitted*

[8] F. Hirata, H. Sato, S. Ten-no, S. Kato, in: J. Gao and M.A. Thompson (Eds.), Combined Quantum Mechanical and Molecular Mechanical Methods, American Chemical Society, Washington DC, 1998.

[9] F. Hirata, H. Sato, S. Ten-no, S. Kato, in: M. O. Becker, D. A. MacKerell Jr., B. Roux, M. Watanabe (Eds.), Computational Biochemistry and Biophysics, Marcel Dekker Inc., New York, 2001.

[10] S. Ten-no, F. Hirata, S. Kato, *J. Chem. Phys.* **100**, *7443*, 1994.

[11] H. Sato, F. Hirata, S. Kato, *J. Chem. Phys.* **105**, *1546*, 1996.

[12] T.H. Dunning, Jr. *J. Chem. Phys.* **53**, *2823*, 1970.

[13] P.J. Hay, W.R. Wadt *J. Chem. Phys.* **82**, *284*, 1985.

[14] H. Sato, F. Hirata, *J. Am. Chem. Soc.* **121**, *3460*, 1999.

[15] C. Peterson, G.V. Pfeiffer, *Theor. Chim. Acta.* **26**, *321*, 1972.

[16] T.H. Dunning, Jr. *J. Chem. Phys.* **55**, *716*, 1971.

Chapter 7

Solvation Effect on the Interaction Between Sodium and Chloride Ions in Aqueous Solution. An Analysis Based on the New Resonance Theory

7.1 Introduction

What is the nature of the interaction between sodium and chloride in aqueous solution? It has been understood that sodium chloride is a typical electrolyte and the interaction between them is not covalent but ionic. However, when we wish to know the detail of interatomic interaction in solution, we may have the following straightforward questions: How different is the interaction in aqueous phase from it in gas phase? What is the relationship between the ionic character of the interaction and solvent distribution? These questions look very simple but difficult to answer. In fact, a clear and sufficient answer has not been provided from theoretical point of view.

How do we estimate the nature of interaction of solvated molecules? The covalent and ionic interactions were originally introduced as the intelligible concepts in resonance theory, which enable us to understand an electronic structure in terms of superposition of covalent and ionic bonding structures. There are two possible ways to obtain such information. One is calculating the electronic wave function by valence bond method, which is a direct realization of the original resonance theory. The other is to analyze the molecular orbital wave function based on the spirits of resonance theory [1–4]. In our time, molecular orbital computation becomes a standard tool in quantum chemistry and, in fact, most of quantum chemical calculations for solvated molecules, which are required in this study, have been developed based on molecular

orbital method [5–7]. The analysis based on resonance theory may be preferable, from a practical viewpoint.

In this study, we wish to give the clear answer to the questions using two theoretical methods. One is RISM-SCF theory, which allows us to calculate not only the molecular orbital wave function of a solvated molecule but also the statistical solvent distribution function [6, 7]. The other is our developed analysis of molecular orbital wave functions, which enables us to calculate the weight of ionic or covalent character from a molecular orbital wave function [4]. The combination of these method offers unified understandings of the nature of interaction between sodium and chloride in aqueous solution together with the statistical distribution of water molecules.

7.2 Method

The RISM-SCF theory is the combination of two major theoretical elements, the ab initio molecular orbital theory and the reference interaction site model (RISM) integral equation method, which is a statistical mechanical treatment of molecular liquid. In general, the total free energy $\mathcal{A}$ of the solvation system is defined as the sum of the electronic energy of the solute E_{solute} and the solvation free energy $\Delta\mu$.

$$\mathcal{A} = E_{solute} + \Delta\mu. \tag{7.1}$$

E_{solute} can be expressed by the electronic wave function of solvated molecule Ψ,

$$E_{solute} = \langle\Psi|\hat{H}|\Psi\rangle, \tag{7.2}$$

where $\hat{H}$ is the electronic Hamiltonian. In the RISM framework, the solvation free energy is expressed by using site-site total and direct correlation functions, $h_{\alpha s}$ and $c_{\alpha s}$ [8].

$$\Delta\mu = -\frac{\rho}{\beta}\sum_{\alpha s}\int d\mathbf{r}\left(c_{\alpha s} - \frac{1}{2}h_{\alpha s}^2 + \frac{1}{2}c_{\alpha s}h_{\alpha s}\right), \tag{7.3}$$

where α and s refer to interaction sites of solute and solvent molecules, respectively, $\beta = \frac{1}{k_B T}$, and k_B is Boltzmann constant. ρ is the number density of solvent. RISM-SCF equation was

derived by the variation principal of total free energy $\mathcal{A}$ [7]. Because the details of the theory have been discussed in various literatures, we would like to just emphasize here that, in RISM-SCF method, the electronic wave function of solute and spatial distribution of solvent are obtained in a self consistent manner.

The analysis of molecular orbital wave functions was developed by us very recently [4]. The method is based on second quantization of singlet coupling. Here, we will provide a simple overview of the method. Let us consider an orthonormalized molecular orbital ϕ_i^{local}, which is localized on two-atomic centers, A and B. This is, of course, related to chemical bond between A and B. We can define a density matrix $(\mathbf{P}^i\mathbf{S})_{\mu\nu}$ for the localized orbital ϕ_i^{local}, as follows,

$$(\mathbf{P}^i\mathbf{S})_{\mu\nu} = \langle\phi_i^{local}|\chi_\nu^+\varphi_\mu^-|\phi_i^{local}\rangle, \tag{7.4}$$

where χ_ν^+ and φ_μ^- are, respectively, creation and annihilation operators related to (nonorthogonal and biorthogonal) atomic orbital basis functions. $\mathbf{P}^i$ is a partially summed P-matrix ($P^i_{\mu\nu} = C_{i\mu}C_{i\nu}$) related to the localized orbital ϕ_i^{local}, $C_{i\mu}$ is the LCAO coefficient, and $\mathbf{S}$ is overlap matrix. The diagonal term of $(\mathbf{P}^i\mathbf{S})_{\mu\nu}$ corresponds to Mulliken atomic population of this orbital. By extending the operator in Eq. 7.4, we can define the probabilities of ionic and covalent bonds between atoms A and B as follows,

$$\mathrm{A^-B^+} \;:\; \sum_{\mu\in A}\sum_{\nu\in A}\langle\phi_i^{local}|\chi_\nu^{\sigma_1+}\chi_\mu^{\sigma_2+}\varphi_\nu^{\sigma_2-}\varphi_\mu^{\sigma_1-}|\phi_i^{local}\rangle, \tag{7.5}$$

$$\mathrm{A-B} \;:\; 2\sum_{\mu\in A}\sum_{\nu\in B}\langle\phi_i^{local}|\chi_\nu^{\sigma_1+}\chi_\mu^{\sigma_2+}\varphi_\nu^{\sigma_2-}\varphi_\mu^{\sigma_1-}|\phi_i^{local}\rangle, \tag{7.6}$$

$$\mathrm{A^+B^-} \;:\; \sum_{\mu\in B}\sum_{\nu\in B}\langle\phi_i^{local}|\chi_\nu^{\sigma_1+}\chi_\mu^{\sigma_2+}\varphi_\nu^{\sigma_2-}\varphi_\mu^{\sigma_1-}|\phi_i^{local}\rangle. \tag{7.7}$$

The operators in above equations provide the probability of the state in which two electrons are singlet-coupled between atomic orbital basis functions indexed by μ and ν. These quantities can be easily computed by using the density matrix in an analogous process to Mulliken population analysis.

$$\mathrm{A^-B^+} \;:\; \frac{1}{4}\sum_{\mu\in A}\sum_{\nu\in A}(\mathbf{P}^i\mathbf{S})_{\mu\nu}(\mathbf{P}^i\mathbf{S})_{\nu\mu}, \tag{7.8}$$

$$\mathrm{A-B} \;:\; \frac{1}{2}\sum_{\mu\in A}\sum_{\nu\in B}(\mathbf{P}^i\mathbf{S})_{\mu\nu}(\mathbf{P}^i\mathbf{S})_{\nu\mu}, \tag{7.9}$$

$$A^+B^- \quad : \quad \frac{1}{4}\sum_{\mu\in B}\sum_{\nu\in B}(\mathbf{P}^i\mathbf{S})_{\mu\nu}(\mathbf{P}^i\mathbf{S})_{\nu\mu}. \tag{7.10}$$

The weight of each bonding structure is obtained by multiplication of these probabilities of the participating bonds. The results obtained by the method show good agreement with our chemical intuitions [4].

The electronic wave functions of solvated molecules were computed on the basis of the RHF method with the 6-311G(d,p) basis set [9]. In RISM-SCF calculation, atomic charge of solute was computed under the electric field generated by solvents. Non-electrostatic interaction between solute and solvent molecules was modelled with Lennard-Jones type of potential, whose parameters were summarized in Table 7.1 [10]. The SPC/E-like water was employed to describe the solvent. All calculations were performed with program code GAMESS modified by us [11].

Table 7.1: Lennard-Jones potential parameters for solute-water interaction.

	σ (Å)	ϵ (kcal mol^{-1})
NaCl		
Na	2.350	0.130
Cl	4.400	0.100
H_2O		
O	3.166	0.155
H	1.000	0.056

7.3 Results and Discussion

We obtained eleven one-center and three two-center localized molecular orbitals of NaCl. Two-center ones consist of one σ bonding orbital and two π bonding orbitals (Fig. 7.1). At the equilibrium geometry, Mulliken populations of Na and Cl related to these localized orbitals are 0.202 and 1.798 for the σ bonding orbital, and 0.050 and 1.950 for the π bonding orbitals, respectively, in gas phase. Thus, we can see that NaCl has a relatively strong σ type interaction and weak π type interactions.

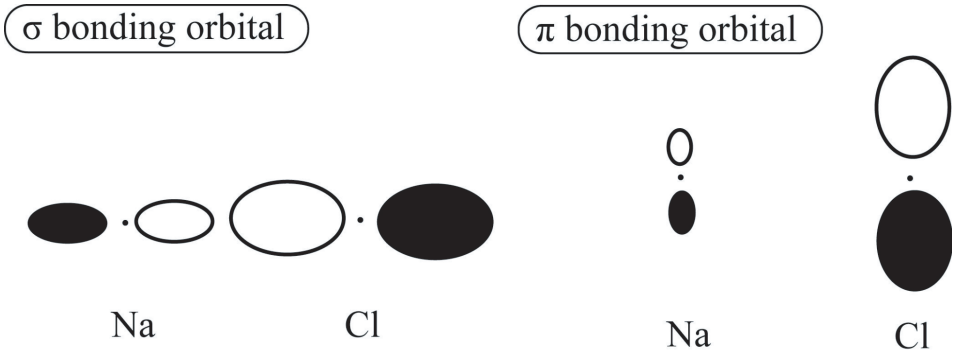

Figure 7.1: Two-center orbitals of NaCl

Using these two-center orbitals, we obtained the weights of resonance structures. The distance (R_{Na-Cl}) between Na and Cl is fixed at 2.40 Å, which is the equilibrium distance in gas phase. The most important resonance structure is Na^+Cl^-, and the weight in gas phase is 73.1 %. The weight of the covalent bonding resonance structure, Na−Cl, is 23.8 %. This result shows that the covalent bond is not negligible in gas phase, while the ionic character is dominant in the interaction. Other contributing resonance structures are Na^-Cl^+ and $Na^- =Cl^+$, whose weights are 1.0 % and 1.9 %, respectively. The latter has a double bond arising from above-described weak π type interactions. In aqueous phase, the resonance structure Na^+Cl^- is extremely enhanced; the weight becomes 91.3 %, while the covalent bonding resonance structure becomes less important. The weights of Na^-C^+ and $Na^- =Cl^+$ become negligibly small. Thus, the weight of Na^+Cl^- increases about 18 % by the solvation effect even if NaCl takes the same geometry in both phases.

The changes of the weights of resonance structures with respect to the distance between Na and Cl are plotted in Fig. 7.2. It is noted that the energy curve of NaCl in aqueous phase becomes double-well, unlike it in gas phase. This fact is widely known and the first and second minimums have been referred as contact ion pair (CIP) and solvent-separated ion pair (SSIP) minimums, respectively [10, 12]. Although the optimized distance in gas phase is 2.40 Å , the CIP and SSIP minimums are located at 2.77 and 4.26 Å, respectively. In both phases, the ionic character is enhanced with increase of R_{Na-Cl}, and the covalent character becomes important, as decreasing of R_{Na-Cl}. These results are consistent with the chemical intuition that a covalent

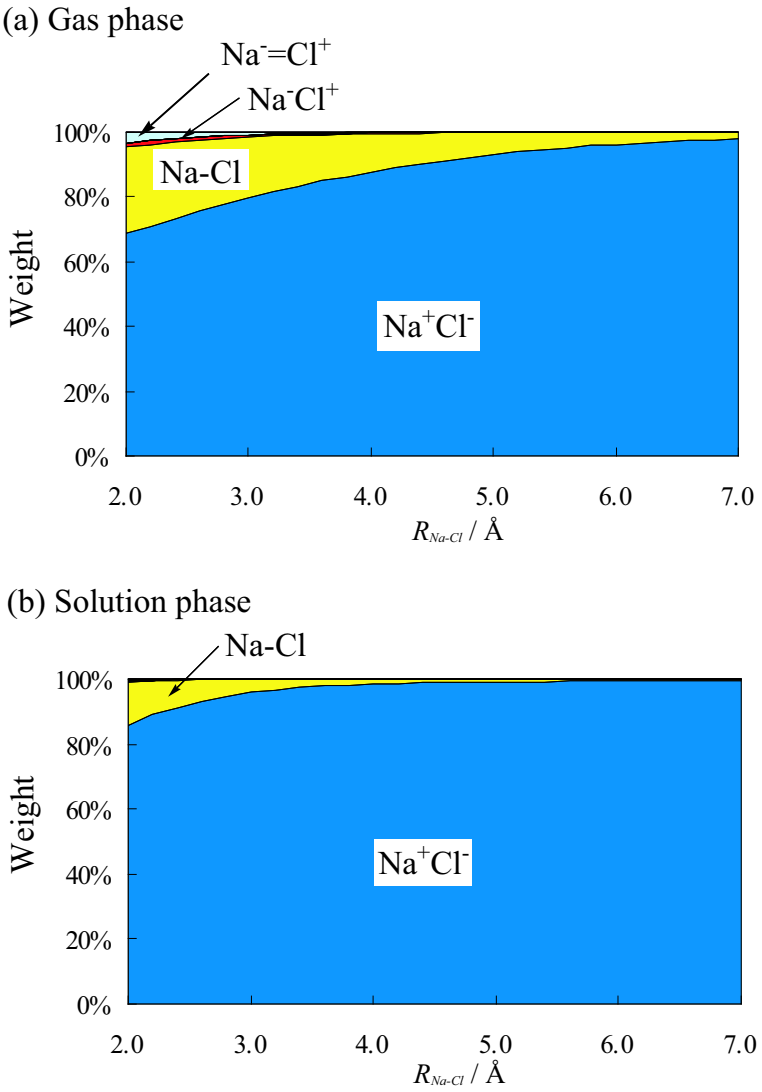

Figure 7.2: The weights of resonance structures of NaCl with respect to the distance between Na and Cl, in (a)gas and (b)solution phase.

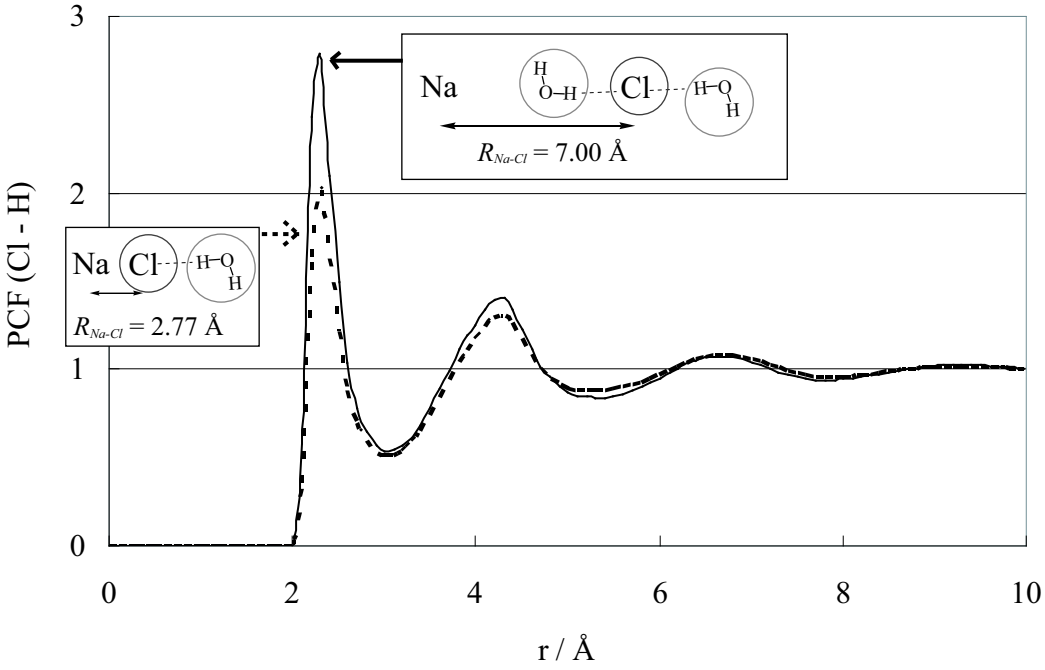

Figure 7.3: Solvation structure of sodium chloride at R_{Na-Cl} = 2.77 and 7.00 Å. Pair correlation function between H atoms of water and Cl atom of NaCl. The schematic picture of solvation is also depicted.

bond is a short-range interaction and an ionic bond is a long-range one [13]. In aqueous phase, with increase of R_{Na-Cl}, the weight of ionic bond increases rapidly compared to it in gas phase. At CIP and SSIP minimums, the weights of the ionic bonding resonance structure are 94.5 % and 98.7 %, respectively. Thus, in aqueous phase, the solvation effect enhances ionic character by up to 20 % at both minimums and NaCl can be completely regarded as an ion pair. These results indicate that the enhancement of ionic character by solvation effect plays crucial role on the dissolving process of NaCl.

In RISM-SCF theory, the information on the solvation structure is obtained in terms of pair correlation functions (PCFs) of solvent molecules. In Fig. 7.3, PCFs of hydrogen atoms of water around chloride atom of NaCl at R_{Na-Cl} = 2.77, and 7.00 Å are shown. A sharp peak located at r = 2.0 Å, at the respective distances of R_{Na-Cl}. On the other hand, in the PCF of oxygen atoms around chloride atom, a sharp peak was found at r = Å. These results mean

water molecule coordinate to chloride atom, corresponds to hydrogen bonding, which must enhance the ionic character of the interaction between Na and Cl. The peak height grows up with increasing R_{Na-Cl}, indicating the increase of the solvent coordination number. As R_{Na-Cl} becomes sufficiently large, solvent molecule can get into the space between the ions. Consequently, each ion is fully solvated with the solvent molecules. This picture is consistent with the result that the weight of ionic bond in aqueous solution rapidly increases with increasing R_{Na-Cl}.

7.4 Summary

The solvation effect on the interaction between sodium and chloride was investigated by RISM-SCF method and the analysis of molecular orbital wave function based on the new resonance theory. The strategy enabled us to evaluate the nature of interaction between sodium and chloride, and the statistical solvent distribution. The weight of ionic interaction was 73.1 % in gas phase, while the weight was 91.3 % in solution phase if NaCl taken the same geometry in both phases. The weight of covalent interaction decreased with increase the distance between sodium and chloride in both phase. It decreased more rapidly in solution phase and, at the same time, the coordination number of solvent increased.

Bibliography

[1] Hiberty, P. C.; Leforestier, C. *J. Am. Chem. Soc*. **1978**, *100*, 2012.

[2] Glendening, E. D.; Weinhold, F. *J. Comput. Chem.* **1998**, *19*, 593.

[3] Karafiloglou, P. *J. Comput. Chem.* **2001**, *22*, 306.

[4] a) Ikeda, A.; Nakao, Y.; Sato H.; Sakaki, S. *J. Phys. Chem. A* **2006**, *110*, 9028.b) Ikeda, A.; Yokogawa, D.; Sato H.; Sakaki, S. *Chem. Phys. Lett.* **2006**, *424*, 449.

[5] Tomasi, J.; Persico, M. *Chem. Rev.* **1994**, *94*, 2027.

[6] Ten-no, S.; Hirata, F.; Kato, S. *J. Chem. Phys.* **1994**, *100*, 7443.

[7] Sato, H.; Hirata, F.; Kato, S. *J. Chem. Phys.* **1996**, *105*, 1546.

[8] Singer, S. J.; Chandler, D. *Mol. Phys.* **1985**, *55*, 621.

[9] Hariharan, P. C.; Pople, J. A. *Theoret. Chim. Acta* **1973**, *28*, 213.

[10] a) Kovalenko, A.; Hirata, F. *J. Chem. Phys.* **2000**, *112*, 10391.b) Kovalenko, A.; Hirata, F. *J. Chem. Phys.* **2000**, *112*, 10403.

[11] Schmidt, M. W.; Baldridge, K. K.; Boatz, J. A.; Elbert, S. T.; Gordon, M. S.; Jensen, J. J.; Koseki, S.; Matsunaga, N.; Nguyen, K. A.; Su, S.; Windus, T. L.; Dupuis, M.; Montgomery J. A. *J. Comput. Chem.* **1993**, *14*, 1347.

[12] a) Berkowitz, M.; Karm, O. A.; McCammon, J. A.; Rossky, P. J. *Chem. Phys. Lett.* **1984**, *105*, 577.b) Smith, D. E.; Dang, L. X. *J. Chem. Phys.* **1994**, *100*, 3757.

[13] Lantz, M. A.; Hug, H. J.; Hoffmann, R.; van Schendel, P. J. A.; Kappenberger, P.; Martin, S.; Baratoff, A.; Guntherodt, H. -J. *Science* **2001**, *291*, 2580.

General Conclusion

In this thesis, the author discussed the nature and energy of chemical bond by using the method newly developed here and accurate ab-initio methods. The achievements in this thesis are summarized, as follows.

In Part I, the author investigated the binding energy and bonding nature of transition metal complexes of large π-conjugate molecule. In the investigation of the binding energy, the author compared the density functional theory (DFT) method with post-Hartree-Fock methods such as Møller-Plesset perturbation (MP) method and coupled cluster singles and doubles (CCSD) method. One of the most important results is that the DFT method underestimates the binding energies in these complexes by about 20 kcal/mol. Furthermore the nature of chemical bond was discussed in details by using the decomposition of total molecular orbitals (MOs) into fragment MOs.

In Chapter 1, the author systematically evaluated the binding energies of d^{10}, d^8, and d^6 transition-metal complexes of π-conjugate systems using the MP2 to MP4, CCSD(T), and DFT methods. The MP4(SDQ)-, CCSD- and CCSD(T)-calculated binding energies of Pt-$(PH_3)_2(C_2H_{4-n}(CH{=}CH_2)_n)$ change little as the size of the π-conjugate system increases, while the DFT-calculated binding energy considerably decreases. The difference between the DFT- and MP4(SDQ)-calculated binding energies reaches about 25 kcal/mol for n = 4. The DFT-calculated binding energies of such d^8 and d^6 metal complexes decreases similarly. Population analysis based on the fragment MOs and usual natural atomic population leads to conclusion that the bonding nature is quite different in these complexes; the π-back-donation mainly

participates in the coordinate bond of the Pt(0) complex, the σ-donation and π-back-donation comparably participate in the coordinate bond of the Pt(II) complex, and the σ-donation largely participates in the coordinate bond but the π-back-donation little in the Pt(IV) complex. Thus, it is concluded that the DFT method underestimates the binding energy independently of the coordinate bonding nature when the π-conjugate system is large. The reason for the underestimation is investigated with several model systems. We found that the DFT method underestimated the interaction between $Pt(PH_3)_2$ and two methane molecules to similar extent to that of the binding energy of $Pt(PH_3)_2$(trans-MeCH=CHMe). This result suggests that the poor description of dispersion interaction is one of the reasons for the underestimation of the binding energy by the DFT method. However, it is noted that the DFT-calculated binding energy between the bare Pt(0) atom and the π-conjugate system decreases with an increase of the size of the π-conjugate system but the MP4(SDQ)-calculated value changes little. It should be noted that the Hartree-Fock-calculated binding energy of $Pt(PH_3)_2(C_2H_{4-n}(CH{=}CH_2)_n)$ also decreases as the size of the π-conjugate system increases. These results indicate that not only the dispersion interaction between the substituents and the metal moiety but also another factor is responsible for the underestimation.

In Chapter 2, the MP2 to MP4(SDQ) and DFT methods were applied to $IrH(CO)(PH_3)_2(C_{60})$ (**1**), $IrCl(CO)(PH_3)_2(C_{60})$ (**2**), and $RhH(CO)(PH_3)_2(C_{60})$ (**3**), to estimate their binding energies and clarify the bonding nature. The DFT method presents much smaller binding energies than the MP2 method; for instance, the binding energy of **1** is evaluated to be 16.9 kcal/mol with the DFT method but 68.0 kcal/mol by the MP2 method. The binding energies of **1**, **2**, and **3** are evaluated to be 59.4, 43.5, and 48.2 kcal/mol, respectively, with the ONIOM(MP4(SDQ):UFF) method. This decreasing order is different from that of the E_{INT} value **1** $>$ **2** $>$ **3**, where the intrinsic binding energy (E_{INT}) is defined as stabilization energy by the interaction between C_{60} and $MX(CO)(PH_3)_2$ taking the distorted geometry in the total complex. The E_{INT} value is easily interpreted in terms of π-back donation and σ-donation; in **3**, both π-back donation and σ-donation are the weakest, which leads to the smallest E_{INT} value. The weakest π-back donation of **3** arises from the less expansion of the d orbital and the d_π orbital at low

energy. The weakest σ-donation is due to the d_σ orbital at high energy and the less expansion of the d orbital. The E_{INT} value of **2** is much larger than that of **3**, which arises from the larger expansion of the d orbital. However, the larger E_{DIST} value leads to the smaller binding energy value of **2** than that of **3**. The largest binding energy and E_{INT} value of **1** are interpreted in terms of the d_π orbital at the highest energy and the largest overlap $S(d_\pi\text{-}\pi^*)$ value. The smaller binding energy and E_{INT} value of $Pt(PH_3)_2(C_{60})$ than that of **1** is interpreted in terms of the presence of the doubly-occupied d_σ orbital in the Pt(0) center.

In Part II, the author developed new resonance theory, which is a method to analyze molecular orbital wave function with the resonance theory, in a spirit of the second quantized expression of Mulliken population analysis (MPA) and bond order analysis (BOA). The author applied the method to solvated molecules and discussed the solvation effect on the nature of chemical bond.

In Chapter 3, the author firstly presented a method to calculate the weights of resonance structures from the Hartree-Fock (HF) wave function. The method is formulated by using the second quantized operator corresponding to singlet coupling, in which only orbital localization and algebraic calculations of density matrices are necessary. Though the range of application of the present method is limited to the single Slater-type wave function in which each MO can be localized to either one- or two-center orbitals, the obtained results are in excellent agreement with the previous works and our chemical intuitions.

In Chapter 4, the author introduced the general formulation of the method described in Chapter 3. The author investigated the resonance structure of H_2, H_2O, NH_3 and H_2CO using the two density matrices, Mulliken and Löwdin types, and three orbital localization schemes, Boys-Foster (BF), Edmiston-Ruedenberg (ER), and Pipek-Mezey (PM) localizations, and various basis sets. The results are virtually independent on the choice of density matrices and basis sets. The results are also independent on localization schemes.

In Chepter 5, the author presented the new resonance theory, which is a novel method to calculate the weights of resonance structures from HF wave function. The method is natural

extension of the method presented in Chapter 3. The present method can be applied to the system in which electrons are delocalized. This method is consistent with MPA and BOA. The method was successfully applied to LiH, H_2O, butadiene and the S_N2 reaction of CH_3Cl with Cl^-. In LiH and H_2O molecules, we investigated numerically whether or not the present method is consistent with MPA, BOA, and the previously proposed method. Especially, atomic population and bond order calculated by the present method is exactly the same as MPA and BOA results. In the case of the S_N2 reaction, the change of the nature of chemical bond, bond breaking, and bond formation are clearly shown by the present method. In the precursor complex, a chemical bond between C and Cl is polarized by the electric field of Cl^-. In the transition state, the totally ionic resonance structure becomes very important, which is consistent with our chemical intuition.

In Chapter 6, the solvation effect on the nature of chemical bond was investigated by the combination of the new resonance theory and the RISM-SCF method, where the RISM-SCF method is the combination of statistical mechanics of molecular liquids and ab-initio MO method. The present method enables us to evaluate the nature of chemical bond of solute and statistical solvent distribution. The method was applied to the solvated H_2O and HX (X=F, Cl, Br, I). It is clearly shown that the contribution from the ionic structure tends to be enhanced in aqueous solution in all cases.

In Chapter 7, the combination of the new resonance theory and the RISM-SCF method was applied to sodium chloride in water and the solvation effect on the interaction between sodium and chloride was discussed in detail. The weight of ionic interaction is 73.1 % in gas phase, but increases to 91.3 % in solution phase, where the geometry of NaCl is taken to be the same in both phases. The weight of covalent interaction decreases with increase the distance between sodium and chloride in both phases. It decreases more rapidly in solution phase and, at the same time, the coordination number of solvent increases.

Nowadays, the electronic structure method is used as a black-box tool that everybody can use. However, this doesn't mean that the modern quantum chemistry is perfect for every-

body. There are many problems that remain to be solved. In Part I, a serious problem was newly pointed out and its origin was discussed in details. This result provides a hint for next-generation theory. The author believes that another important problem in the modern quantum chemistry is the lack of the method to understand well the computational results. In Part II, new resonance theory was presented, which provides us a new and fundamental analysis method of electronic structure. The theory bridges the gap between chemist's intuitions and tangled and specialized electronic structure theory.

List of Publications

Publications included in this thesis

Chapter 1

”Binding energy of transition metal complexes with large π-conjugate systems. DFT vs. Post Hartree-Fock methods”

Atsushi Ikeda, Yoshihide Nakao, Hirofumi Sato, Shigeyoshi Sakaki

J. Phys. Chem. A **2007**, *111*, 7124-7132.

Chapter 2

”Theoretical Study of $M(PH_3)_2$ Complexes of C_{60}, Corannulene ($C_{20}H_{10}$), and Sumanene ($C_{21}H_{12}$) (M = Pd or Pt). Unexpectedly Large Binding Energy of $M(PH_3)_2(C_{60})$”

Yuu Kameno, Atsushi Ikeda, Yoshihide Nakao, Hirofumi Sato, Shigeyoshi Sakaki

J. Phys. Chem. A **2005**, *109*, 8055-8063.

”Binding energies and bonding nature of $MX(CO)(PH_3)_2(C_{60})$ (M=Rh or Ir; X=H or Cl): Theoretical study”

Atsushi Ikeda, Yuu Kameno, Yoshihide Nakao, Hirofumi Sato, Shigeyoshi Sakaki

J. Organomet. Chem. **2007**, *692*, 299-306.

Chapter 3

”A New Analysis of Molecular Orbital Wave Function Based on Resonance Theory”

Atsushi Ikeda, Yoshihide Nakao, Hirofumi Sato, Shigeyoshi Sakaki

J. Phys. Chem. A **2006**, *110*, 9028-9030.

Chapter 4

”The Invariance of the Analysis Based on Resonance Theory. Dependence on Basis Set, Localization Scheme and Density Matrix”

Atsushi Ikeda, Hirofumi Sato, Shigeyoshi Sakaki

to be submitted

Chapter 5

”A New Resonance Theory Consistent with Mulliken Population Analysis”

Atsushi Ikeda, Hirofumi Sato, Shigeyoshi Sakaki

to be submitted

Chapter 6

”Solvation Effect on Resonance Structure. Extracting Valence Bond-like Character from Molecular Orbitals”

Atsushi Ikeda, Daisuke Yokogawa, Hirofumi Sato, Shigeyoshi Sakaki

Chem. Phys. Lett. **2006**, *424*, 449-452.

Chapter 7

”Solvation effect on the interaction between sodium and chloride ions in aqueous solution: An analysis based on the new resonance theory”

Atsushi Ikeda, Daisuke Yokogawa, Hirofumi Sato, Shigeyoshi Sakaki

Int. J. Quantum Chem. **2007**, *107*, 3132-3136.

Other publications

1. ”Hydrogen atom formation from the photodissociation of water ice at 193 nm”
   Akihiro Yabushita, Yuichi Hashikawa, Atsushi Ikeda, Masahiro Kawasaki, Hiroto Tachikawa
   J. Chem. Phys. **2004**, *120*, 5463-5468.

2. ”Discrete Sandwich Compounds of Monolayer Palladium Sheets”
   Tetsuro Murahashi, Mayu Fujimoto, Masa-aki Oka, Yasuhiro Hashimoto, Tomohito Uemura, Yasuki Tatsumi, Yoshihide Nakao, Atsushi Ikeda, Shigeyoshi Sakaki, Hideo Kurosawa
   Science **2006**, *313*, 1104-1107.

3. ”Photodissociation of OCS and CS_2 adsorbed on water ice films at 193 nm”
   Atsushi Ikeda, Noboru Kawanaka, Akihiro Yabishita, Masahiro Kawasaki
   J. Photochem. Photobiol. A in press

4. ”An experimental and theoretical study on temperature dependence of the reaction of NO_3 with CH_3I”
   Yukio Nakano, Hiromi Ukeguchi, Takashi Ishiwata, Yugo Kanaya, Hiroto Tachikawa, Atsushi Ikeda, Shigeyoshi Sakaki, Masahiro Kawasaki
   to be submitted